UNIVERSITY of LIVERPOOL

# ADVANCED CONTROL OF INDUCTION MOTORS

Thesis submitted in accordance with the
requirements of the University of Liverpool
for the degree of Doctor of Philosophy

in

Electrical Engineering and Electronics

by

Wei ZHANG , BSc(Eng.)

September 2013

**ADVANCED CONTROL OF INDUCTION MOTORS**

by

Wei ZHANG

## Acknowledgements

My first debt is to my supervisor Dr.Lin Jiang, both academically and personally, for providing me with an excellent working environment throughout the research. And invaluable support as well as intellectual guidance.

I am deeply grateful to Professor Q.H. Wu for his numerous insightful discussions and knowledgeable advice. I would like to also thank Dr.Wei Yao for his valuable guidance and encouragement during the preparation of this thesis. Thanks are also offered to the members of the Intelligence Engineering and Automation group for their counsel and guidance on various topics throughout my research.

I am grateful to the Department of Electrical Engineering and Electronics, the University of Liverpool, for providing the research facilities, which made my research possible.

Finally, I am deeply grateful to my girlfriend Mengyue He, for her encouragement, patience and understanding during the writing of this thesis, and to my parents and my sister, for their encouragement and love, throughout my postgraduate life.

**Abstract**

ADVANCED CONTROL OF INDUCTION MOTORS

by

Wei ZHANG

The current industrial standard for the control of the induction motor is the so-called vector control (VC) or field-orientated control (FOC) which transforms and controls the induction motor as a direct current (DC) motor. Besides its many advantages, such as fast and decoupled dynamics of speed and flux, it is well known that VC depends on the detailed system model and is very sensitive to parameter uncertainties and external disturbance (load torque). To clarify further the VC is a only a partial feedback linearising control which can achieve the decoupling of speed and flux asymptotically. The coupling still exists when flux is not kept in constant, i.e. when flux is weakened in order to operate the motor at a higher speed and keep the input voltage within saturation limits, or when flux is adjusted to maximize power efficiency of the motor with light load.

The thesis will summarise research of advanced control approaches of induction motors in Chapter One. The Chapter Two starts on building a fifth-order nonlinear dynamic model of an induction motor and then recalls the principal of traditional VC of induction motors.

The differential-geometric technique based nonlinear control has developed for induction motors, which can convert some intractable nonlinear problems into simpler problems by familiar linear system methods. The partial decoupled dynamic of the conventional VC has been investigated via feedback linearisation control (FLC) at first. Then input-output linearisation control is applied to design a fully decoupled control of the dynamics of speed and flux.

To remove the weak robustness and the requirement of an accurate model of the VC and FLC, a novel nonlinear adaptive control of induction motor is designed based on feedback linearisation control and perturbation estimation. The induction motor will be represented as a two coupled interconnected subsystems: rotor speed subsystem and rotor flux subsystem, respectively. System perturbation terms are defined to include the lumped term of system nonlinearities, uncertainties, and interactions between subsystems and are represented as a fictitious state in the state equations. Then perturbations are estimated by designing perturbation observers and the estimated perturbations are employed to cancel the real system perturbations, assumed all internal states are measured. The designed nonlinear adaptive control doesn't require the accurate model of the induction motor and has a simpler algorithm. It can fully decouple the regulation of rotor speed and rotor flux and handle time-varying uncertainties. The parameter estimations based on nonlinear adaptive controls can only deal with unknown constant parameters and are not suitable for handling fast time-varying and functional uncertainties.

Nonlinear adaptive control based on output measurements is addressed in Chapter Five, assuming that the rotor speed and the stator volatge/currents are measurable. A sliding mode rotor flux observer has been designed based on the stator voltage and current. Moreover, two third-order state and perturbation observers are designed to estimate the unmeasured states and perturbation, based on the rotor speed and the estimated rotor flux. Simulation studies have been carried out for verifying the effectiveness of the proposed advanced controllers and compared with the conventional VC and model based FLC.

# Contents

# List of Figures

# List of Tables

# Chapter 1

# Introduction

## 1.1 Background

Induction motors (IM) are widely used in industrial applications, such as elevators, industrial equipment and transport, because they are amongst the simplest construction, high reliability and least expensive high performance motors [1]. Induction motors are a quite important section of the electric load in all power system as they consume approximately 60% of the total electrical energy use around the world. For example, in South Africa (SA), the industrial and mining parts are the largest consumers of electricity. Motorized systems in these parts generate up to 60% of the total electricity consumption and about 57% of SA's peak power demand [3]. More than half of the total electrical energy is converted into mechanical energy by electric motors, at least 90% of industrial drive systems use induction motors. A lot of motors are uncontrolled. However, adjustable speed induction motor drives from power electronic converters are steadily increasing each year. It is estimated more than fifty billion dollars could be saved yearly by using induction motors with speed control.

An induction motor is motor which alternating current is supplied to the

stator directly and to the rotor by induction or transformer action from the stator [2]. The stator or stationary portion of an induction motor consists of a frame that packaged a magnetically active, the individual coils of this electrical winding are random-wound for smaller motors and form-wound for larger motors. The rotor or secondary part of an induction motor is made up of a shaft-mounted, magnetically active rotor winding. The rotor winding of an induction machine may be one of two types: wound-rotor or squirrel-cage. A wound rotor winding for an induction motor is similar in form to the stator winding. Typically, the winding is wye-connected with the three-phase line leads connected to rotor-mounted slip rings. Wound-rotor winding induction machines are relatively uncommon, they are only in a limited number of specialised applications, including wind power generation. On the other hand, the induction motor has a squirrel-cage rotor with a winding consisting of copper bars embedded in the rotor slots and shorted at both ends by copper end rings.

Most used induction machines have an induction motor with a squirrel-cage. This type of induction motor has the advantage of high power to weight ratio, lower inertia, cheap, available at all power ratings, and do not require too much maintenance. The DC motors and the synchronous motors require two excitation connections (doubly excited), but the induction motor has only one excitation connection (single excited) [1]. Currents that flow in the second winding of the induction motor are established by the process of magnetic induction through coupling with the singly excited winding, The name induction motor is derived from here. In induction machines, rotor currents are induced in the rotor winding by a combination of the stator currents and the motion of the rotor relative to the stator.

In the squirrel-cage induction motor, the rotor is inaccessible. So there is no moving contacts, like the commutator and brushes in DC machines. By using this arrangement it can increase reliability of induction motors greatly,

and eliminates the danger of sparking, It also enables the safe use of squirrel-cage machines in harsh environments. This rotor can run at high speeds and withstand heavy mechanical and electrical overloads. The other type, called wound-rotor induction motors, are rarer and used in special applications. An advantage of the wound-rotor involves the accessibility of the rotor winding. The wound-rotor motors is more expensive and less reliable than the squirrel-cage induction motors. Recently, the wound-rotor motors became popular in the wind power generation sector as they provide a solution to the variable speed operation of wind turbines. They are known as a doubly fed induction generator (DFIG). The accessibility of the rotor winding allows the usage of a power electronic converter at the rotor side to control the output power of the DFIG. This requires one-third of the power compared to a full-rate power electronic converter connected directly to the stator side.

Even though operating principles of induction motors have not changed, significant technological progress has been made over the years. In comparison with their previous construction, today's motors are now lighter, smaller, more reliable and more efficient. In applications where the power requirement is small and suited to single-phase distribution, the induction motor is available in single-phase versions. A lot of domestic appliances such as washing machines, dryers, fans, and air conditioning units use single-phase induction motors. However, industrial applications use the three-phase induction motor in integral-horsepower ratings with typical voltage ratings, for example, the ranging of United States is from 230 to 4160 V [1].

In the previous years, DC drives are traditionally considered as the preferable choice for high dynamic applications due to relatively simple control. Nowadays, with the use of advanced microprocessors and power electronics, an induction motor with control system, such as vector control (VC), has been applied to many high dynamic and large size applications to replace the DC motors.

However, due to its complex algorithm, the use of powerful microcomputers or dSpace hardware (DSP) is mandatory. This limits its applications to small and medium sized range motors due to its high cost, such as household appliances as refrigerators and washing machine as the market is very cost sensitive, due to pump and fans. Domestic refrigeration accounts for around 14% of the total UK electricity demand. UK households use one and a half billion pounds on electricity every year to cool or freeze food and drinks. Currently, refrigerators use the less efficient compressors based on constant speed drives. The more efficient, variable-speed vector controlled induction motor based compressors have so far achieved poor usage due to the price difference. One possible solution is to design an advanced high efficient motor using new material and techniques. This would include the use of permanent magnet material and a direct-drive linear motor compressor. However, despite the anticipated improvements in performance, the high cost sensitivity in the domestic refrigerator market remains a barrier to further development and commercial up-take of this technology. The improvement of the induction motor through the design of new control algorithms could be one solution for replacing the constant speed induction motor compressors in domestic refrigerators.

## 1.2 Induction Motor Control

The control system is an important part in a motor and drive system. However, the control system doesn't provide the required power for the load, they can regulate the dynamic performance of position and speed/torque of the induction motor. The control and estimation of induction motor drives constitute a large subject, it has attracted much attention in the last few decades, and the technology has further advanced in recent years. In References [4][5], they have provided an overview of the latest developments in control techniques for the induction motor. Those control methods can be summarised as three cate-

gories: scalar control (contact Voltage/Frequency ratio control), vector control and other advanced control methods.

### 1.2.1 Scalar Control: V/F

Scalar control is an open loop volts/Hz control of an induction motor which uses a feed forward approach to maintain the stator flux linkage constant up to rated speed [6]. It is the most popular method of constant speed operation of the induction motor because of its simplicity. As the name indicates, scalar control is due to control of the magnitude or frequency of the stator voltage feed to the induction motor only, while ignoring the coupling effect in the machine. With this type of control, the motor is fed with variable frequency voltage that is generated by the pulse-width modulation (PWM) controlled inverter. The V/Hz ratio is maintained constant in order to obtain the constant flux over the entire operating range. Generally speaking, the speed of an AC motor depends on the frequency of stator voltage and the developed torque is related to the stator voltage/current magnitude. So in the scalar-controlled drive systems, only the magnitudes of the input variables (frequency and stator voltage/current) are controlled [12].

The stator voltage of a machine can be controlled by controlling the flux, and frequency or slip can be controlled by controlling the torque. Note that flux and torque are also functions of voltage and frequency. Scalar-controlled drives are widely used for motors operating at low performance applications,such as compressors, fans, grinders, and adjustable speed pumps. In general, drives with this control method do not require any feedback devices. Thus this type of control only requires a little knowledge of the motor, and offers a low-cost, easily implemented solution.

The stability of an open loop induction machine drive has been discussed in [7]. [8] has taken a look at fault tolerant operation of scalar and vector methods.

[9] also proposed energy saving strategies for scalar control. An improvement of open loop volts/Hz control is the closed-loop speed control based on slip regulation, in which the speed control loop uses the speed regulation error to generate the slip command via a PI controller and limiter. The slip is added to the feedback speed signal in order to generate the frequency command, as the frequency command generates the voltage command through volts/Hz function generator. This incorporates the low-frequency stator drop compensation. As discussed above, the scalar control method needs to keep a constant ratio of V/Hz so as to maintain a constant stator flux linkage. This approach is problematic, due to low-speed operation, because of the voltage drop at the stator resistance. A necessary slip is needed to produce the torque. Thus some advanced methods which involve decoupling the control components, have been proposed in [10][11]. The volts/Hz control also has another drawback caused by the flux drift, as the result of torque sensitivity against the slip will vary. In addition, when the line voltage varies, the volts/Hz ratio would be incorrect.

### 1.2.2 Vector Control

Scalar control is simple to implement, but the inherent coupling effect gives a sluggish response and the system becomes instable due to internal coupled dynamic. To sort these problems out, VC can be used. The VC was invented at the beginning of 1970s [22]. It can be used with both induction and synchronous machines to transform the control of an AC machine into that of a separate excited DC motor. The vector control method has the advantage of fast torque response compared to other variable-speed control technique.

Vector control is an idea of regarding the machine torque as the product of two space vectors, the stator current vector and the rotor flux field vector. The controllers try to maintain a ninety degree phase angle between the two space vectors to achieve the maximum torque. The torque is proportional to

the cross product of stator current and rotor flux ($i_s \times \Psi_r$). Consequently, the decoupled control of torque and flux field excitation is quite similar to the DC motor control. This control is also known as the "field-oriented control", "flux oriented control", or the "indirect torque control" [12]. Eventually, the induction motor drive can achieve a four-quadrant operation with fast torque response and good performance. In order to implement vector control, it requires information regarding magnitude and position of rotor flux vector. This control action happens in a field-coordinate system by using the rotating rotor flux vector as a reference frame for stator currents and stator voltages.

The indirect vector control (IVC) without flux measurement was proposed by K. Hasse in 1968 [25]. By 1971, direct vector control (DVC) used direct flux measurement, to find the actual magnitude and position of the rotor flux, as developed by F. Blaschke (who worked for Siemens) [24]. These two methods are different essentially by how the unit vector ($\cos\theta_e$ and $\sin\theta_e$) is generated for the location of space vector [17][19]. It should be mentioned here that the orientation of $i_{ds}$ with the stator flux $\psi_s$, rotor flux $\psi_r$ and air gap flux $\psi_m$, are used with the VC [21].

Vector control theories have been advanced in recent years to solve the coupling problem in AC machines. The theories of vector control are dependent on the synchronously rotating d-q model [22] of the machine. Variables appear as the DC quantities are in a steady-state condition. In this model, the d-q component of the stator current are mutually decoupled. It can be controlled similarly to the flux component and torque components of the currents. In comparison with DVC and IVC, both control methods require complex coordinate transformation, complicated vector signal sensing the phase conversion, as well as signal processing. In the former method, the flux can be considered undesirable, and it is difficult to implement the control due to harmonics. In the latter method, the precision position encoder on the machine is not always desirable. The proposed control scheme, named scalar decoupled control of

induction motor [23], is expected to give a better performance than the conventional vector control methods. It describes a scalar control approach for an induction motor which is supplemented by a decoupled function to achieve static and dynamic decoupling at all conditions.

### Direct Vector Control and Indirect Vector Control

There are two general approaches of vector control. One called direct or feedback control method, which was invented by Blaschke [24]. The other method called indirect or feed forward control, which was invented by Hasse [25]. The two methods are different by how the unit vector is generated for the control.

The original approach of DVC included the flux measurement coils to accomplish the flux orientation. However, this will increase the hardware cost and the measurement is also not accurate. Therefore, this approach is not a good control technique in practice. The current DVCs usually use flux observers to estimate the flux vector in order to replace the flux measurement. For the direct vector control, the vector control parameters $i_{ds}^*$ and $i_{qs}^*$ used in the synchronous rotating frame, are transferred to the stationary frame, with the help of unit vector ($\cos\theta_e$ and $\sin\theta_e$), generated from rotor flux vector signals. The rotor flux signals $\Psi_{dr}^s$ and $\Psi_{qr}^s$ are generated from the machine terminal voltages and currents. A current $i_{ds}$ on $d^e$-axis and current $i_{qs}$ on $q^e$-axis have been given, at this condition, $\Psi_{qr} = 0$, $\Psi_{dr} = \hat{\Psi}_r$. The corresponding torque expression is given by $T_e = K_t\hat{\Psi}_r i_{qs}$, It is simple to control as demonstrated by the DC machine. The torque component of current $i_{qs}^*$ is generated from the speed control loop, when the $i_{qs}$ polarity is reversed by the speed loop, the current position also reverses, and gives a negative torque. To sum up, the generation of the unit vector signal from the feedback flux vectors becomes the "direct vector control."

The indirect vector control method is essentially the same as the direct

vector control, except the unit vector signals ($\cos\theta_e$ and $\sin\theta_e$) are generated in feed forward manner. The direct vector control is not a good control technique in practice. Consequently, the indirect vector control is more popular in industrial applications. In this method, the flux angle is not measured directly. However, it is estimated from the equivalent circuit model, from measurements of rotor speed, stator current and the voltage. The IVC provides asymptotic regulation of the rotor speed and flux modulus around constant references and does not need rotor flux sensor or estimators, as established in example [28]. A drawback of this method is that it relies on the assumption that the stator currents are available as control inputs. [35] represents an improved indirect vector controller for the induction motor. In this paper, the standard indirect field-oriented controller (IFOC) scheme is modified to achieve global exponential rotor velocity/rotor flux tracking. The modifications to the IFOC scheme involve the injection of additional nonlinear terms into the current control input and the so-called desired rotor flux angle dynamics.

Although VC is simple and better for high performance drive application, resulting in better speed and position control even at low speeds. However, there are still some disadvantages by using this approach. The major one is that the vector control is very sensitive to the rotor resistances which are changed during the operation of the motor and is estimated online [36].

### 1.2.3 Advanced Control of Induction Motors

The control of induction motors have been used as a test benchmark for nonlinear control design. This is because the induction motor is a complicated nonlinear dynamic system with some unmeasured variables [37]. This involves the equivalent rotor currents or fluxes, time-changing parameters (stator and rotor resistances) and external disturbances (load torque).

By the mid 1980s, numerous engineering researchers worked on how to

improve the basic method of VC. Few years later, M. Depenbrock presented the Direct Self Control (DSC) [38]. A new technique for the torque control of induction motors was also presented by I. Takahashi and T. Noguchi [62], called the direct torque control (DTC) [40]. By using DSC or DTC, it is possible to get a good dynamic control of the torque without any mechanical transducers on the machine shaft.

In comparison with FOC, DTC does not require any current regulator and PWM signal generator. Despite its simplicity, the DTC allows a good torque control in steady-state. Its major problem is to quantify how good torque control is with respect to VC, and the controller is aware of these parameters. On the other hand, the DTC finds it difficult to control the torque and flux at very low speed. Moreover, it has a high noise level during the low speed. [41] has given a fair comparison between both techniques (FOC and DTC). The other papers [42]-[52] introduced in previous years, confirmed research had been undertaken to solve the above mentioned problems by using the DTC method.

The control and estimation of AC drives in general are considered more complex than those of DC drives, and high performances are demanded if this complexity increases. The main reasons for this complexity are the need for variable-frequency, the complex dynamics of AC machines, machine parameter variations, and the difficulties of processing feedback signals in the presence of harmonics.

#### Feedback Linearisation Control

In the last two decades, it has witnessed a lot of progress in the design and application of feedback control of nonlinear systems [53]-[56]. The feedback linearisation control (FLC) method based on differential geometry has been proved to be an effective means of design and analysis of nonlinear control systems as was the case for the Laplace transform, complex variable theory and

linear algebra in relation to linear systems, as described in the comprehensive book of 'Isidori' [53] and references therein.

Feedback linearisation is an approach for nonlinear control design [31][32]. The central idea of the approach is to algebraically transform a nonlinear system dynamics into a fully or partly linear system, so that linear control techniques can be applied. Speed control of an induction motor using dynamic feedback linearisation was first considered in [57]. This methodology helps convert many previously intractable nonlinear problems into much more simpler problems solvable by familiar linear system methods. It consists of two kinds of approaches: input-state linearisation, developed by Gardner and Shadwick [60], where the full state equation is linearised and input-output linearisation [61], where the linearising of the input-output map from input to output is emphasised even if the state equation is only partially linearised [55]. A quite effective way to obtain the decoupling of flux and speed dynamics is the input-output linearising controller [63][51]. As the algorithm is very effective and reduces computational requirements.

During the 1970s and 1980s, feedback linearisation was a major topic of research [64]. In spite of many successful application every year, feedback linearisation has a few of drawbacks which hinder its use. One of them is that it is vulnerable to handle the presence of parameter uncertainty or external disturbances. This is because its effectiveness depends on an accurate system model to cancel the system nonlinearity. However, it is unrealistic to assume the perfect knowledge of system nonlinearities or that an exact mathematical representation of them is available due to exist model approximation, imprecision or uncertainty. Another drawback is complexity of the resulting nonlinear control law as it can not been implemented easily in practice. In fact, such a complex nonlinear controller may not always behave better than a simple linear controller. In recent years, the problem of controlling uncertain nonlinear dynamical systems has been a topic of considerable interest. Many works in this

field have been undertaken by employing robust or adaptive control method. We will review these results below.

### Nonlinear Adaptive Control

Adaptive control is another important approach to deal with uncertain and/or time-varying systems [44]-[47]. One of the reasons for the rapid growth and continuing popularity of the adaptive control is its clearly defined goals to control the plants with known structure, but unknown parameters or slowly time-varying parameters effect this [20]. Adaptive control has been most successful for the plant models in which the unknown parameters appear linearly. Systematic theories have been developed for the adaptive control of linear systems. The existing adaptive control techniques can also treat important classes of nonlinear systems with measurable states and linearly parameterizable dynamics [55].

Interests in adaptive control of nonlinear systems were stimulated by major advances in the differential-geometric theory of nonlinear feedback control in the mid 1980s. Nonlinear adaptive control is a research area that has been rapidly growing in the 1990s. A nonlinear state feedback control method shows the nonlinear motor dynamics can be linearized and decoupled by means of feedback-linearisation techniques [27]. The book by Kristić [65] gives a complete and pedagogical presentation of nonlinear adaptive control. A passivity-based approach is proposed for induction motor control [66]. This method uses energy dissipation property of the system to solve the advanced control problem. However, the motor parameters are assumed to be known. Recent developments in this area can be found in [67][68]. Further, more research has been proposed in the area of back-stepping based on Lyapunov's theory, see [65]. During each step, a Lyapunov Methodology identifies a stabilisation function for every virtual control and an associated Lyapunov Function that

is inductively increased to form a global Lyapunov Function for the complete system. The first adaptive back-stepping design was developed in [69]. Its over-parameterisation was removed by the tuning functions design [72]. Note that the back-stepping technique has been applied to the induction motor [65]. Assuming once again that the physical parameters are well known, the control law provides the global asymptotic stability of the system.

Amongst the early estimation based results are Sastry and Isidori [73], Pomet and Praly [74], etc. One of the first output-feedback design was proposed by Marino and Tomei for induction motor [75][76]. Kanellakopoulos, Kokotović and Morse [77] presented a solution to the partial state feedback problem. A tracking design where the regressor depends only on reference signals was given in [78]. Khalil [79] and Janković developed semi-global output feedback designs for a class which includes some systems not transformable into the output feedback form.

In adaptive output feedback control schemes, it is based on flux observers [18] and also can deal with additional parametric uncertainty (especially in rotor resistance) as represented in [80]-[83]. More recent efforts have focused on the speed-sensorless approaches. The load torque can be assumed be known, but the rotor speed is not available for the feedback, more examples can be found in [84][85]. By 2009, another new output feedback control scheme for the voltage-fed model of induction motor was developed [86]. This method uses measurements of stator current and rotor speed to achieve global asymptotic convergence of rotor speed and flux magnitude to achieve desired time-varying references. This proposed approach is based on the methodology in reference [87].

Observer-based methods [88]-[92] have offered a good performance in a large speed range. Observation algorithms are making use of the analytical model of the machine and allow the estimation of the rotor speed and flux from the motor terminal quantities (voltages/currents). In the last few decades,

research has been completed aimed at eliminating the speed sensor, such as developing speed-sensorless control methods [93]. In the adaptive observers, the speed or other unknown parameters are estimated by additional equations dependent on the adaptive control theory [94][88]. During these proposals, the sliding-mode observer represents an attractive choice due to robustness to disturbances, and system noise, as well as parameter deviations [95][92]. In 2000, [96] presented an adaptive speed-sensorless field-oriented control of an induction motor. It is based on a sliding-mode observer. The observer detects the rotor flux components in a two-phase stationary reference frame, using motor voltage equations. The speed of the motor is estimated by a further relation obtained by a Lyapunov function.

Note that most of the nonlinear adaptive work are dealing with unknown constant parameters of nonlinear systems [71]. This adaptive control paradigm is not suitable for handling fast time-varying and functional uncertainties. It is known that problems may arise from the influence of unknown disturbances and time-varying parameters. During the last twenty years, the sliding-mode control (SMC) [39] has gained wide attention because of its simple design, fast dynamic response, easy implementation and robustness to parameters variations and load disturbances [58][59]. This control method has been applied to the position and velocity control of induction motor drives [97]-[100]. Sliding mode control ideas [98], have been investigated for induction motor control, due to the fact that enforcing a sliding mode leads to a low sensitivity with respect to a type of disturbances and plant parameter variations. This methodology is described by [98] with regards to the design on a nonlinear switching manifold. In Reference [99], the authors proposed a sliding mode rotor flux observer with a non-linear sliding mode controller. In 1996, another new SMC method was proposed in [100] for induction motor speed control based on the model in the rotating reference frame with the vector of stator current. In 2001, a novel inner-loop sliding-mode current control scheme was proposed by L.G. Shiau

[101]. It is dependent on a nonlinear mathematical model of induction motor position drives. The parameters of the position and speed controllers are considered in the inner-loop sliding-mode current control. The overall system has exhibited robust stability and robust performance, despite the presence of motor parameters or load disturbances. [16] has been developed for the control of induction motor to achieve rotor angular speed and rotor flux amplitude tracking objectives by using the cascade sliding mode control method.

Classical control systems such as proportion-integration (PI) control is used together with vector control methods for the speed control of induction motor. However, the main disadvantages of the linear control approach are the sensitivity in performance to system parameters variations. In addition, inadequate rejection of external perturbations may change the load. To sort out these problems, variable-structure control based methods, like sliding-mode control [98], fuzzy logic based control (FLBC) [102][103], have been applied industrially to control of electrical drive system. There are some advantages using SMC, it has been shown to be an effective way for controlling electric systems. Its high-gain feedback control input can cancel nonlinearities, uncertainty parameters, and external disturbances due to its robust control. The experimental results that were obtained from implementing SMC on a DSP hardware platform, have shown the robust performance of this method [104]. In addition, a real-time comparison of 'vector control', 'feedback linearisation control', and the 'sliding-mode-based technique' has been undertaken in [105]. This paper has shown that in terms of rotor resistance variation, running at low speed, the sliding mode controller gave the best results. In [106], the backstepping approach was shown that it is an elegant method for the design of nonlinear sliding manifolds.

On the other hand, in comparison with permanent magnetic synchronous motors, induction motors are not able to be fully linearised [51]. To improve the methods mentioned, full linearising state feedback control based on differential

geometric theory has been proposed, and more details can be found in [107]-[110]. In order to improve this technique, the paper of [51] has been published. It added to the control algorithm on an adaptive law to estimate the rotor resistance and the load torque that are both assumed to be constant.

Robust control based on the estimation of perturbations from states derivative has been an interesting topic in the control of nonlinear systems with unmodelled dynamics, such as time-delay control [111][112] , sliding mode control with perturbation estimation [113][116] and robust adaptive control via perturbation observer [117]-[119]. Disturbance auto-rejection control proposed a similar idea based on nonlinear disturbance observer and has been applied to induction motor control [120]. However, the proposed nonlinear extended-state observer makes the stability analysis of the whole control /observer system is very difficult. In fact, linear observer or sliding mode observer can provide nearly similar performance as that of the nonlinear observer used in [119], but their structure is much simpler. This has been demonstrated by applications of robust adaptive control via perturbation observer and their applications for synchronous generator control and power electronics in power system [117]-[119].

## 1.3 Motivations and Objectives

The current industrial standard for control of induction motor is the so-called VC or FOC which transforms the control of the induction motor to that of a DC motor. However, the control of induction motor is more complex than DC motor. A challenging problem occurs due to the following three reasons: it is a highly nonlinear dynamic system, some electrical variables such as rotor flux and rotor currents are not easily measurable, and some physical parameters (rotor and stator resistance) vary considerably with a significant impact on the system dynamics.

VC is an example of an application before theory innovation. It was proposed in the 1970s. However, the stability issues were only established by the 1990s. Besides its many advantages, such as high dynamic and decoupled control of the speed and the flux, it is well known that VC depends on the detailed system model and is very sensitive to parameter uncertainties (stator and rotor parameters) and external disturbance (load torque). However, the rotor and stator resistance of a running motor will vary by up to 50% from their nominal values. The load torque is typically unknown and in some applications changes continuously, such as hybrid vehicle. It has already been clarified that VC has a partial feedback linearising control which establishes the decoupling of speed and flux asymptotically. The coupling still exists when flux is not kept be constant, i.e. when the flux is weakened to operate the motor at a higher speed and avoid the input voltage exceeding their limits, or when the flux is adjusted to maximise power efficiency of the motor running under light load condition.

The overall goal of this thesis is to develop an advanced controller for induction motors, based on nonlinear adaptive control method involving an input-output linearisation control and perturbation estimation and compensation, to improve the dynamic performance of the induction motor. To improve the VC, the input-output linearisation control (IOLC) will be investigated. Note that both VC and IOLC need all the parameters, and nonlinear dynamics of the system to be known exactly. All of them have relatively complicated nonlinear calculations in control algorithm. In order to develop the robustness of VC and IOLC, nonlinear adaptive input/output linearizing control of induction motor was introduced.

The induction motor has been represented as a two coupled interconnected subsystems, involving a rotor speed subsystem and a rotor flux subsystem. System perturbation terms are defined to include the lumped term of system nonlinearities, uncertainties, and interactions between subsystems, and represented as a fictitious state in the state equations. The perturbations are

estimated by designing perturbation observers and employed to cancel real system perturbations. The designed robust adaptive control doesn't require the accurate model of induction motor and has a simpler algorithm. It can fully decouple the regulation of rotor speed and rotor flux and can handle time-varying uncertainties. A fourth order model based flux observer is used to estimate the rotor flux.

The goal is to be achieved by realising the following objectives.

- modeling of a three-phase induction motor using controllers design and verification, including a stationary reference frame and synchronous rotating reference frame model. The basic concept of VC will be fully investigated as well, for comparison studies of the new control methods proposed;
- investigate the asymptotical regulation characteristic obtained by VC and design a fully decoupled controller for induction motor via feedback linearisation control theory;
- nonlinear adaptive control of induction motor based on state feedback and compensating perturbation obtained from with high gain perturbation observer will be investigated. The objective of this research work is to eliminate the requirement of detailed system model, and to improve the robustness against parameter uncertainties and unknown dynamic; and
- augmenting a sliding mode flux observer and assuming only the rotor speed is measured. Output feedback based on nonlinear adaptive control (NAC) is developed by designing two state and perturbation observers for the induction motor.

## 1.4 Major Contributions

The thesis reports the research work undertaken based on the review of current techniques for control of induction motor. The nonlinear adaptive control of nonlinear systems via state and perturbation observer has been studied for control of induction motor. Two types of controllers: state feedback nonlinear adaptive control and output feedback nonlinear control, have been investigated to obtain the estimate of states and perturbation.

The following results have been obtained:

- a fully decoupled nonlinear controller has been obtained for the regulation of speed and flux dynamic of induction motor, based on the input-output linearization control. The asymptotical regulation characteristic obtained by the conventional vector control has been analysed;

- nonlinear adaptive control via high gain perturbation observer has been developed for induction motor. The designed controller adopts the real-time estimates of perturbation to yield the adaptive control law. The real time estimate of system perturbation, which include nonlinearities, time-varying parameters and external disturbances, is a function estimation rather than a parameters estimation as in most nonlinear adaptive control. A simple adaptive control law is obtained. The system nonlinearities are included in the perturbation as an accurate system model is not required for the controller; and

- a sliding mode flux observer is designed for estimating the rotor flux. Assuming only speed as a measurement. This is based on the estimate of the rotor flux. Two state and perturbation observers are designed for estimating the other states and perturbation terms. Output feedback based upon nonlinear adaptive control via high gain state and perturbation observers have been studied for the induction motor.

## 1.5 Thesis Outline

The thesis is organized as follows.

**Chapter 2:** Modelling and Field-oriented Control of Three-phase Induction Motor

In this chapter, the model of three-phase induction machine has been investigated. The essential concepts of dynamical systems are given as well. Modeling of induction motors are developed based on two types of reference frames: stationary reference frame and synchronously rotating reference frame. Different types of VC, including DVC and IVC were discussed based on the method to obtain the rotor flux vector. Finally, the simulation results and analysis are given to demonstrate the operation dynamic of induction motor.

**Chapter 3:** Feedback Linearisation Control of Induction Motor

This chapter investigate control of induction motor via FLC. It represents a fully decoupled control of speed and flux dynamics by using FLC. The basic idea of the FLC technique are reviewed for single-input single-output (SISO) system and multi-input multi-output (MIMO) system respectively. The FLC technique is used to explain the asymptotical regulation characteristic of the speed and the flux dynamics achieved by conventional FOC. One type of FLC approach, called Input Output Linearisation Control (IOLC), is applied to design a fully decoupled controller for the speed and the flux dynamics. Simulation studies verify the effectiveness of the proposed IOLC, via comparison with the field-oriented control approach.

**Chapter 4:** Nonlinear Adaptive Control of Induction Motor: State Feedback

This chapter has investigated and discussed a novel robust adaptive control approaches of induction motors, based on perturbation estimation and input-output linearisation. Estimates of perturbation are employed to achieve robust and adaptive FLC. The detailed model of the induction motor is not required

and a simple control law is obtained. The simulation results have shown a better performance obtained by the proposed algorithm against uncertainties and time-varying unknown load torque disturbances, than the classical VC and FLC based on the accurate system model.

**Chapter 5:** Nonlinear Adaptive Control of Induction Motor: Output Feedback

This chapter has investigated an output feedback nonlinear adaptive control for induction motor. A sliding mode flux observer is designed for estimation of the rotor flux variables. A state and perturbation observer is designed for the flux subsystem to obtain the correspondent state variables and perturbation. Moreover, assuming only the rotor speed is measured, a state and perturbation observer is designed for estimating the derivative of the speed and the correspondent perturbation. Based on the estimated states and perturbation terms, output feedback NACs are designed for the speed and flux subsystems. The stability of the overall closed-loop system are investigated to include the flux observer, state and perturbation observer, NAC, and the induction motor. Simulation results verify the effectiveness of the proposed NACs.

**Chapter 6:** Conclusions

The thesis has concluded with a summary of the results and several suggestions for future work. The suggestions for future work will highlight the unsolved problems that remain.

# Chapter 2

# Modelling and Vector Control of the Three-phase Induction Motor

This chapter establishes the dynamic model of induction motor and investigates the basic principle of FOC of induction motor. Starting from the basic three-phase dynamic equations of the stator and rotor windings, coordination transformations from the original three-phase equations to stationary reference frame and synchronously rotating reference frame are discussed. An analysis of the FOC of induction motors are highlighted including the DVC and the IVC. The simulation results have been presented to show the characteristics of the three-phase induction motor and the dynamic response of FOC.

## 2.1 Introduction

AC machines are complicated systems which have multivariable, strong coupling, nonlinear, and time-variable characteristics. AC machines can be classified as induction machines, in conjunction with synchronous machines. A-

mongst all types of AC machines, the induction machine, especially the squirrel cage type machine, is most commonly used in industry. AC machines with a constant frequency sinusoidal power supply have been used in constant speed applications, whilst DC machines were preferred for variable speed drives.

One of the most fundamental principles of induction machines is the creation of a rotating and sinusoidally distributed magnetic field in the air gap. Three-phase induction machines are operating below synchronous speed when motoring and above synchronous speed when generating. The electrical machine converts electrical energy into mechanical energy, and vice versa. They are rugged and require very little maintenance. However, their speeds are not as easily controlled as with DC motors, as they draw on large starting currents. If the rotor is initially stationary, the interaction of air gap flux and rotor magnetic motive force (mmf) produces torque. When the rotor rotation is at speed, $\omega_r$ is equal to synchronous speed $\omega_e$, the rotor doesn't have any induction, and torque cannot be produced. At any other speed $\omega_r$, the speed differential $\omega_e - \omega_r$, called slip speed $\omega_{sl}$, induces rotor current and then torque is developed.

For power system studies, induction machine loads are often simulated on a system's synchronously rotating reference frame. For transient studies of adjustable speed drives, it is usually more convenient to simulate an induction machine and its converter on a stationary reference frame. Thus, this section presents a model of induction motor on a stationary and rotating reference frame. The mathematical model of induction machine is a high-order, strong coupling, multi-variable nonlinear system.

For a long time, DC motors dominated the major place in variable speed applications. Its flux and torque can be controlled easily by the field and armature currents. However, DC motors have certain disadvantages, which are due to the existence of the commutator and the brushes. They also have limited applications under high-speed conditions. AC motors have a simple mechanical

structure than DC motors and a cost advantage. AC machines are normally used as the constant speed machines due to their complex operating principle of rotating magnetic field. However, its easy-changing parameters, for instance rotor resistance, make it unsuitable for high performance applications. Both the machine designers and control engineers expect to combine the character of easy adjustable-speed control for DC machines with the simple mechanical structure for AC machines. VC can meet this requirement and the rapid development of the power electronics technology and microprocessor has turned this into a reality.

## 2.2 Model of Induction Motor

In this section, the control of induction motor will be briefly recalled by using Reference [22].

### 2.2.1 Coordinate Transformations

The control of vector transformation involves a three-phase stationary to two-phase stationary, two-phase stationary to two-phase rotating, and vice versa. The induction machine needs to be simplified through coordinate transformation. The voltage equations of stator and rotor circuits are:

$$\begin{aligned} v_{as} &= i_{as}R_s + \tfrac{d\Psi_{as}}{dt} \\ v_{bs} &= i_{bs}R_s + \tfrac{d\Psi_{bs}}{dt} \\ v_{cs} &= i_{cs}R_s + \tfrac{d\Psi_{cs}}{dt} \\ v_{ar} &= i_{ar}R_r + \tfrac{d\Psi_{ar}}{dt} \\ v_{br} &= i_{br}R_r + \tfrac{d\Psi_{br}}{dt} \\ v_{cr} &= i_{cr}R_r + \tfrac{d\Psi_{cr}}{dt} \end{aligned} \tag{2.2.1}$$

where $v_{as}, v_{bs}, v_{cs}$ are stator voltages, $v_{ar}, v_{br}, v_{cr}$ are rotor voltages. For the transient studies of drives, it's usually more convenient to model and simulate

an induction machine and its converter on a stationary reference frame. A

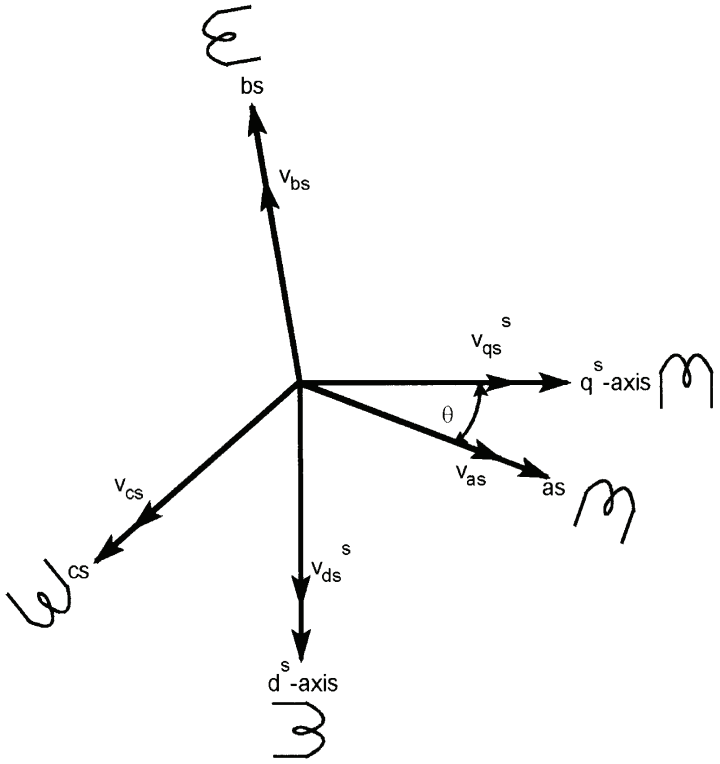


Figure 2.1: as-bs-cs to ds-qs axes transformation in stationary reference frame

three-phase machine can be represented by an equivalent two-phase machine, where the subscript $s$ in the $d_s - q_s$ corresponds to stator direct and quadrature axes, and the subscript $r$ in $d_r - q_r$ represents rotor direct and quadrature axes. Consider a symmetrical three-phase induction machine with stationary as-bs-cs axes at $2\pi/3$ angle apart. The objective is to transform the three-phase stationary reference frame a-b-c variables into two-phase stationary reference frame $d^s - q^s$ variables, where the superscript $s$ represents the stationary reference frame, and then transform them to the synchronously rotating reference frame $d^e - q^e$, where the superscript $e$ represents the rotating reference frame, and vice versa. As shown in Figure 2.1, the transformation from (as-bs-cs) $\Rightarrow$

$(d^s - q^s)$ is shown in form (2.2.3). The three-phase matrix form is:

$$\begin{bmatrix} v_{as} \\ v_{bs} \\ v_{cs} \end{bmatrix} = \begin{bmatrix} \cos\theta & \sin\theta & 1 \\ \cos(\theta - 120^\circ) & \sin(\theta - 120^\circ) & 1 \\ \cos(\theta + 120^\circ) & \sin(\theta + 120^\circ) & 1 \end{bmatrix} \begin{bmatrix} v_{qs}^s \\ v_{ds}^s \\ v_{os}^s \end{bmatrix} \tag{2.2.2}$$

From equation (2.2.2), the inverse relation can be rewritten as:

$$\begin{bmatrix} v_{qs}^s \\ v_{ds}^s \\ v_{os}^s \end{bmatrix} = \frac{2}{3} \begin{bmatrix} \cos\theta & \cos(\theta - 120^\circ) & \cos(\theta + 120^\circ) \\ \sin\theta & \sin(\theta - 120^\circ) & \sin(\theta + 120^\circ) \\ \frac{1}{2} & \frac{1}{2} & \frac{1}{2} \end{bmatrix} \begin{bmatrix} v_{as} \\ v_{bs} \\ v_{cs} \end{bmatrix} \tag{2.2.3}$$

where $v_{os}^s$ is the zero sequence component. Other variables such as current and flux linkages can be transferred by using the similar equations. The angle $\theta$ can be set as zero ($\theta = 0$), which means that $q^s$-axis is aligned with $as$-axis. The transformation relations can be simplified as:

$$v_{as} = v_{qs}^s \tag{2.2.4}$$

$$v_{bs} = -\frac{1}{2} v_{qs}^s - \frac{\sqrt{3}}{2} v_{ds}^s \tag{2.2.5}$$

$$v_{cs} = -\frac{1}{2} v_{qs}^s + \frac{\sqrt{3}}{2} v_{ds}^s \tag{2.2.6}$$

From the equations (2.2.3), the voltages on stationary $d-q$ axis can be represented as:

$$v_{ds}^s = -\frac{1}{\sqrt{3}} v_{bs} + \frac{1}{\sqrt{3}} v_{cs} \tag{2.2.7}$$

$$v_{qs}^s = v_{as} = \frac{2}{3} v_{as} - \frac{1}{3} v_{bs} - \frac{1}{3} v_{cs} \tag{2.2.8}$$

As shown in Figure 2.2, transformation model from two-phase stationary reference frame $d^s - q^s$ to two-phase synchronously rotating reference frame $d^e - q^e$, which rotates at synchronous speed $\omega_e$ with initial angle $\theta_e = \omega_e t$. Based on Figure 2.2, voltage equations can be converted from $d^s - q^s$ to $d^e - q^e$ as:

$$\begin{aligned} v_{ds}^e &= v_{qs}^s \sin\theta_e + v_{ds}^s \cos\theta_e \\ v_{qs}^e &= v_{qs}^s \cos\theta_e - v_{ds}^s \sin\theta_e \end{aligned} \tag{2.2.9}$$

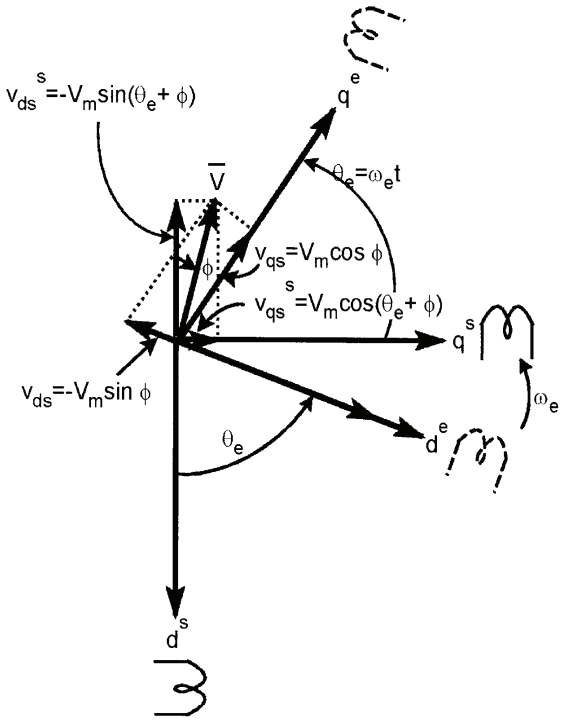


Figure 2.2: Transformation from $d^s - q^s$ stationary reference frame to $d^e - q^e$ synchronously rotating reference frame

and the inverse transformation from the rotating reference frame to a stationary reference frame as:

$$\begin{aligned} v_{ds}^s &= -v_{qs}^e \sin\theta_e + v_{ds}^e \cos\theta_e \\ v_{qs}^s &= v_{qs}^e \cos\theta_e + v_{ds}^e \sin\theta_e \end{aligned} \tag{2.2.10}$$

Note that the vector magnitudes of $V_m$ in the stationary reference frame and the rotating reference frame are equal, that is:

$$V_m = |\bar{V}| = \sqrt{(v_{ds}^s)^2 + (v_{qs}^s)^2} = \sqrt{(v_{ds}^e)^2 + (v_{qs}^e)^2} \tag{2.2.11}$$

### 2.2.2 Stationary Reference Frame

The dynamic machine model in the stationary frame can be derived simply by substituting $\omega_e = 0$. The corresponding stationary frame equations of a

symmetrical induction machine are given below, including stator and rotor voltages, torque equations:

$$v_{ds}^s = R_s i_{ds}^s + \frac{d}{dt}\Psi_{ds}^s \quad (2.2.12)$$

$$v_{qs}^s = R_s i_{qs}^s + \frac{d}{dt}\Psi_{qs}^s \quad (2.2.13)$$

$$v_{dr}^s = 0 = R_r i_{dr}^s + \frac{d}{dt}\Psi_{dr}^s + \omega_r \Psi_{qr}^s \quad (2.2.14)$$

$$v_{qr}^s = 0 = R_r i_{qr}^s + \frac{d}{dt}\Psi_{qr}^s - \omega_r \Psi_{dr}^s \quad (2.2.15)$$

where $\Psi_{ds}^s$ and $\Psi_{qs}^s$ are the stator flux linkages; $\Psi_{dr}^s$ and $\Psi_{qr}^s$ are the rotor flux linkages. The torque equations can also be written with the corresponding variables in stationary frame as:

$$T_{em} = \frac{3}{2}\frac{P}{2}(\Psi_{dr}^s i_{qr}^s - \Psi_{qr}^s i_{dr}^s) \quad (2.2.16)$$

$$T_{em} = \frac{3}{2}\frac{P}{2}(\Psi_{ds}^s i_{qs}^s - \Psi_{qs}^s i_{ds}^s) \quad (2.2.17)$$

$$T_{em} = \frac{3}{2}\frac{P}{2}L_m(i_{dr}^s i_{qs}^s - i_{qr}^s i_{ds}^s) \quad (2.2.18)$$

### 2.2.3 Synchronously Rotating Reference Frame

For a two-phase $d-q$ axes model, it is needed to represent both stator $d_s - q_s$ and rotor $d_r - q_r$ circuits and their variables in a synchronously rotating frame. The stator voltage equations in the stationary reference frame given in (2.2.12) and (2.2.13) can be converted to the $d^e - q^e$ rotating reference frame as:

$$v_{ds}^e = R_s i_{ds}^e + \frac{d}{dt}\Psi_{ds}^e - \omega_e \Psi_{qs}^e \quad (2.2.19)$$

$$v_{qs}^e = R_s i_{qs}^e + \frac{d}{dt}\Psi_{qs}^e + \omega_e \Psi_{ds}^e \quad (2.2.20)$$

Note that all the variables are in the rotating reference frame. The last term of above two equations ($\omega_e \Psi_{qs}^e$ and $\omega_e \Psi_{ds}^e$) can be defined as speed **emf** because of the rotation of the axes. When $\omega_e = 0$ is used, the above two equations change to the stationary reference frame.

If the rotor is not moving, that means $\omega_r = 0$. The rotor equation will be similar to the stator equations in the rotating reference frame, that is:

$$v_{dr}^e = R_r i_{dr}^e + \frac{d}{dt}\Psi_{dr}^e - \omega_e \Psi_{qr}^e \tag{2.2.21}$$

$$v_{qr}^e = R_r i_{qr}^e + \frac{d}{dt}\Psi_{qr}^e + \omega_e \Psi_{dr}^e \tag{2.2.22}$$

Note that all variables and parameters are referred to as the stator side. When the rotor actually moves at speed $\omega_r$, the d-axis fixed on the rotor moves at a speed $\omega_e - \omega_r$, relative to the synchronously rotating reference frame. Thus, the rotor equations should be modified as:

$$v_{dr}^e = R_r i_{dr}^e + \frac{d}{dt}\Psi_{dr}^e - (\omega_e - \omega_r)\Psi_{qr}^e \tag{2.2.23}$$

$$v_{qr}^e = R_r i_{qr}^e + \frac{d}{dt}\Psi_{qr}^e + (\omega_e - \omega_r)\Psi_{dr}^e \tag{2.2.24}$$

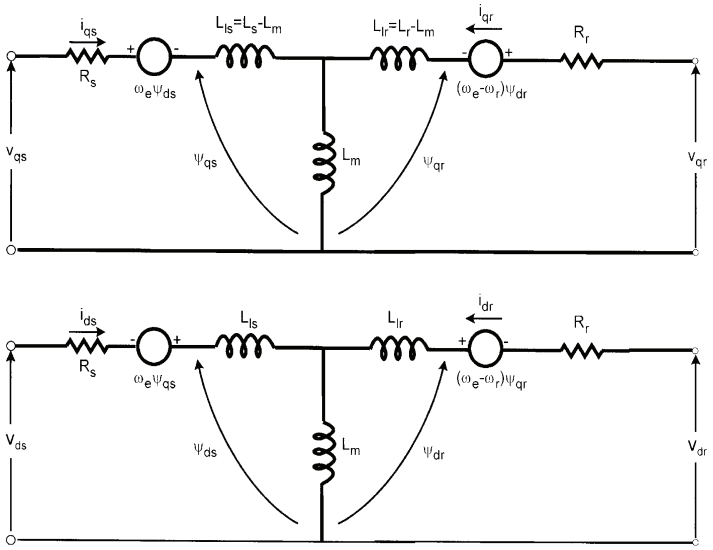


Figure 2.3: Dynamic $d^e - q^e$ equivalent circuits of machine

The dynamic model represented in equivalent circuit $d^e - q^e$ is shown in Figure 2.3. All flux linkage expressions used above can be written in terms of

currents as the following equations:

$$\Psi^e_{ds} = L_{ls} i^e_{ds} + L_m(i^e_{ds} + i^e_{dr}) \quad (2.2.25)$$

$$\Psi^e_{dr} = L_{lr} i^e_{dr} + L_m(i^e_{ds} + i^e_{dr}) \quad (2.2.26)$$

$$\Psi^e_{dm} = L_m(i^e_{ds} + i^e_{dr}) \quad (2.2.27)$$

$$\Psi^e_{qs} = L_{ls} i^e_{qs} + L_m(i^e_{qs} + i^e_{qr}) \quad (2.2.28)$$

$$\Psi^e_{qr} = L_{lr} i^e_{qr} + L_m(i^e_{qs} + i^e_{qr}) \quad (2.2.29)$$

$$\Psi^e_{qm} = L_m(i^e_{qs} + i^e_{qr}) \quad (2.2.30)$$

The motion equation related to speed $\omega_r$ and the torques is given by:

$$T_{em} = T_L + J\frac{d\omega_m}{dt} = T_L + \frac{2}{P}J\frac{d\omega_r}{dt} \quad (2.2.31)$$

where $T_L$ is load torque, J is rotor inertia, and $\omega_m$ is mechanical speed. Resolving the variables into $d^e - q^e$ components, the torque expression can be derived as:

$$T_{em} = \frac{3}{2}\frac{P}{2}(\Psi^e_{ds} i^e_{qs} - \Psi^e_{qs} i^e_{ds}) \quad (2.2.32)$$

$$T_{em} = \frac{3}{2}\frac{P}{2}L_m(i^e_{qs} i^e_{dr} - i^e_{ds} i^e_{qr}) \quad (2.2.33)$$

$$T_{em} = \frac{3}{2}\frac{P}{2}(\Psi^e_{dr} i^e_{qr} - \Psi^e_{qr} i^e_{dr}) \quad (2.2.34)$$

## 2.3 Vector Control of Induction Machine

In a DC machine, the axes of the field current and armature current are usually perpendicular to one another. If the saturation of iron was ignored, the orthogonal fields produce no net interaction effect on one another. The developed torque may be expressed as:

$$T_e = K_a I_a \phi(I_f) \quad (2.3.1)$$

where $K_a$ is a constant coefficient, $\phi(I_f)$ is the field flux, $I_a$ is armature current, and $I_f$ is field current. Here, the torque angle is naturally ninty degrees. It

is known that the flux of a DC machine may be controlled by adjusting the field current $I_f$, and torque may be controlled independently with the flux, by adjusting the armature current $I_a$. This means that when the control of torque and flux is not coupled, they can be controlled independently. In general, torque control of a three-phase induction machine is not as straightforward, compared to a DC machine. This is a result of the interactions between the stator and rotor fields, whose orientation are not held spatially at ninty degrees. This will also vary with operating condition [22].

A DC machine-like performance can be extended to an induction machine, if the machine control is considered in a synchronously rotating reference frame, where the AC variables appear as DC quantities in a steady state. If we were to select a synchronously rotating $d-q$ reference frame, whose d-axis is aligned with the rotor field, the q-axis component of the rotor field, $\Psi^e_{qr}$, in the chosen reference frame would be zero. With vector control, $i_{ds}$ is analogous to field current, and $i_{qs}$ is analogous to armature current of a DC machine. The torque can then be expressed as:

$$T_e = K_a^{'} I_{ds} I_{qs} \tag{2.3.2}$$

When this is compared to a DC machine space vector, the induction machine space vectors rotate synchronously at frequency $\omega_e$. To sum up, VC should maintain the correct orientation of variables such that and equality of command and actual currents.

### 2.3.1 Direct Vector Control

The VC schemes for the induction machine are referred to as a direct type, where the angle is being determined directly. This is the case with the direct air-gap flux measurement. On the contrary, the indirect type occurs when the rotor angle is determined from surrogate measurements, such as slip speed $\omega_{sl}$.

### Direct Vector Current Control

Direct vector control is necessary to estimate the rotor flux components $\Psi^s_{dr}$ and $\Psi^s_{qr}$. For field orientation, control of the stator current is more direct than that of the stator voltage. If the stator voltage is needed to be controlled, it must consider the additional transient dynamics of the stators. The direct stator current control can be achieved easily with help of a DC bus voltage and fast switching devices. The direct control method based on the sensing of airgap flux, by using specially fitted search coils or Hall-effect devices [124]. The angle $\theta_e$ is the desired angle for field orientation. Note that the flux which has measured in the airgap is the resultant or mutual flux. This is not the same as flux, which is connected to the rotor winding. Consequently, the measured stator current, with the value of $\theta_e$ in conjunction with the magnitude of rotor flux can be obtained.

After measuring the voltages and currents, flux variables are computed from the stationary frame variables. At first, the stator currents and voltages are transformed to the stationary reference frame $d^s - q^s$ using (2.3.3) and (2.3.4):

$$\begin{aligned} i^s_{ds} &= \frac{1}{\sqrt{3}}(i_{cs} - i_{bs}) \\ i^s_{qs} &= \frac{2}{3}i_{as} - \frac{1}{3}i_{bs} - \frac{1}{3}i_{cs} = i_{as} \end{aligned} \tag{2.3.3}$$

$$\begin{aligned} v^s_{ds} &= -\frac{1}{\sqrt{3}}v_{bs} + \frac{1}{\sqrt{3}}v_{cs} \\ v^s_{qs} &= \frac{2}{3}v_{as} - \frac{1}{3}v_{bs} - \frac{1}{3}v_{cs} \end{aligned} \tag{2.3.4}$$

Note that for the isolated neutral load, $i_{cs} = -(i_{as} + i_{bs})$ . Then, the $d^s - q^s$

stationary fluxes are obtained as follows:

$$\Psi^s_{ds} = \int (v^s_{ds} - R_s i^s_{ds})dt \tag{2.3.5}$$

$$\Psi^s_{qs} = \int (v^s_{qs} - R_s i^s_{qs})dt \tag{2.3.6}$$

$$\hat{\Psi}_s = \sqrt{(\Psi^s_{ds})^2 + (\Psi^s_{qs})^2} \tag{2.3.7}$$

$$\Psi^s_{dm} = \Psi^s_{ds} - L_{ls} i^s_{ds} = L_m(i^s_{ds} + i^s_{dr}) \tag{2.3.8}$$

$$\Psi^s_{qm} = \Psi^s_{qs} - L_{ls} i^s_{qs} = L_m(i^s_{qs} + i^s_{qr}) \tag{2.3.9}$$

$$\Psi^s_{dr} = L_m i^s_{ds} + L_r i^s_{dr} \tag{2.3.10}$$

$$\Psi^s_{qr} = L_m i^s_{qs} + L_r i^s_{qr} \tag{2.3.11}$$

Substituting the last term $i^s_{dr}$ and $i^s_{qr}$ from Equations (2.3.8) and (2.3.9) into Equations (2.3.10) and (2.3.11), we have the rotor flux in terms of stator variables as folllows:

$$\begin{aligned} \Psi^s_{dr} &= \frac{L_r}{L_m}\Psi^s_{dm} - L_{lr} i^s_{ds} \\ \Psi^s_{qr} &= \frac{L_r}{L_m}\Psi^s_{qm} - L_{lr} i^s_{qs} \end{aligned} \tag{2.3.12}$$

$$\begin{aligned} \Psi^s_{dr} &= \frac{L_r}{L_m}\Psi^s_{ds} - \sigma L_s i^s_{ds} \\ \Psi^s_{qr} &= \frac{L_r}{L_m}\Psi^s_{qs} - \sigma L_s i^s_{qs} \end{aligned} \tag{2.3.13}$$

where $\sigma = 1 - L^2_m / L_r L_s$.

The corresponding torque equation can be obtained from the substituting of equations (2.3.13) as:

$$T_{em} = \frac{3}{2}\frac{P}{2}\frac{L_m}{L_r}(\Psi^s_{dr} i^s_{qs} - \Psi^s_{qr} i^s_{ds}) \tag{2.3.14}$$

The transformation of the stationary frame rotor flux to synchronously rotating frame rotor flux is explained in Figure 2.4. The following equations

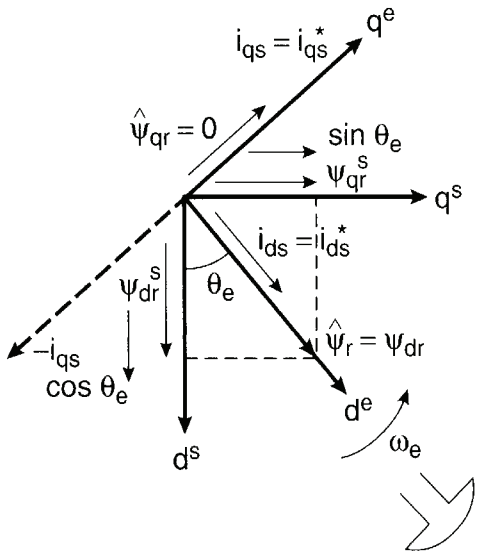


Figure 2.4: Transformation of rotor flux from *dqs* stationary frame to *dqe* rotating frame

can be written:

$$\begin{aligned} \Psi_{dr}^s &= \hat{\Psi}_r \cos\theta_e \\ \Psi_{qr}^s &= \hat{\Psi}_r \sin\theta_e \end{aligned} \tag{2.3.15}$$

by using the $\Psi_{dr}^s$ and $\Psi_{qr}^s$ computed from above equations (2.3.13), the sine and cosine of the angle $\theta$ are obtained as:

$$\cos\theta_e = \frac{\Psi_{dr}^s}{\hat{\Psi}_r} \tag{2.3.16}$$

$$\sin\theta_e = \frac{\Psi_{qr}^s}{\hat{\Psi}_r} \tag{2.3.17}$$

$$\hat{\Psi}_r = \sqrt{(\Psi_{dr}^s)^2 + (\Psi_{qr}^s)^2} \tag{2.3.18}$$

From equations (2.3.3) to (2.3.18), they are performed inside the field orientation block as demonstrated at the centre of Figure 2.5.

As shown in the Figure 2.5, the calculated value of $\hat{\Psi}_r'^e$ ($\hat{\Psi}_{dr}'^e$) is feed back to the input of the flux controller for regulating the airgap flux. Inside the

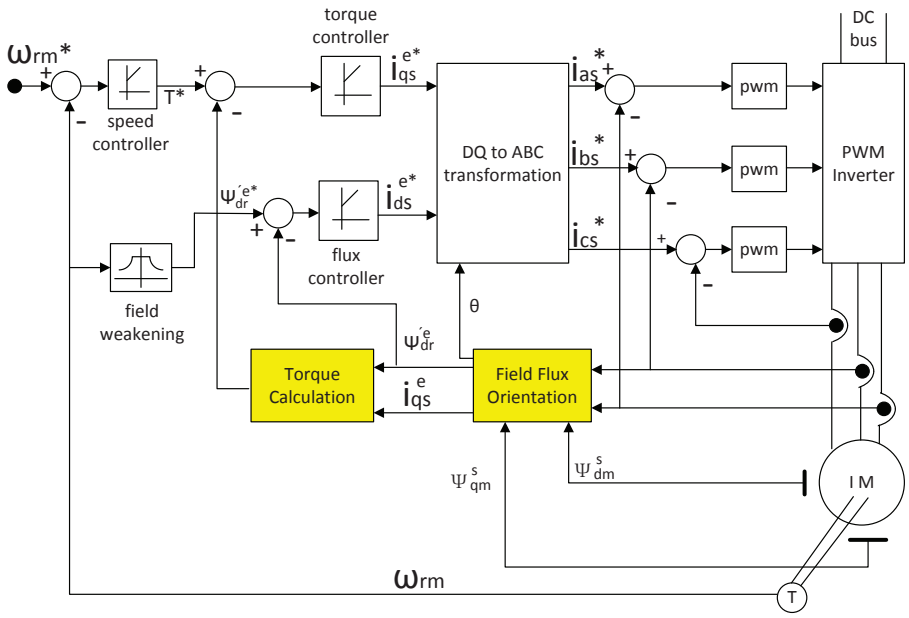


Figure 2.5: Direct vector control of a current-regulated PWM inverter for induction motor [124]

torque calculation block, the values $\Psi_r^{'e}$ ($\Psi_{dr}^{'e}$) and $i_{qs}^e$ are calculated based on (2.3.14). The outputs of the torque controller and flux controller are the current command values, $i_{qs}^{e*}$ and $i_{ds}^{e*}$ in the field-oriented rotating reference frame. Inside the d-q to a-b-c transformation block, are transformations from $d^e - q^e$ to $d^s - q^s$ (2.3.19), and then from $d^s - q^s$ to balanced $a - b - c$ (2.3.20), as follows:

$$\begin{aligned} i_{ds}^{s*} &= -i_{qs}^{e*}\sin\theta_e + i_{ds}^{e*}\cos\theta_e \\ i_{qs}^{s*} &= i_{qs}^{e*}\cos\theta_e + i_{ds}^{e*}\sin\theta_e \end{aligned} \tag{2.3.19}$$

$$\begin{aligned} i_{as}^{*} &= i_{qs}^{s*} \\ i_{bs}^{*} &= -\frac{1}{2}i_{qs}^{s*} - \frac{\sqrt{3}}{2}i_{ds}^{s*} \\ i_{cs}^{*} &= -\frac{1}{2}i_{qs}^{s*} + \frac{\sqrt{3}}{2}i_{ds}^{s*} \end{aligned} \tag{2.3.20}$$

The direct vector current control is feasible because the flux and the torque

are directly related to the currents. However, the direct vector current control is difficult to operate at a very low frequency. With regard to an industrial applications, the start-up of drives from zero speed is common. Therefore, the direct vector current control can not be used under these circumstance.

### Direct Vector Voltage Control

The field orientation of the stator currents can also be achieved by using the proper stator voltages, which is based on the usage of the transient model in conjunction with the properly-oriented $d-q$ stator currents. After the $d-q$ stator currents are determined by converting the measured $a-b-c$ currents to $d^s-q^s$ stationary frame by using (2.3.3), the value of $\theta_e$ can be determined using the following transformation:

$$\begin{aligned} i^e_{ds} &= i^s_{qs}\sin\theta_e + i^s_{ds}\cos\theta_e \\ i^e_{qs} &= i^s_{qs}\cos\theta_e - i^s_{ds}\sin\theta_e \end{aligned} \tag{2.3.21}$$

In a transient model of a three-phase induction motor, the machine can be represented by constant voltages behind the stator transient inductance. The response of the machine to stator side transients can be given as the following equations, where the following $d^e-q^e$ stator voltage stays in the rotating reference frame:

$$\begin{aligned} \frac{d\Psi^e_{ds}}{dt} &= v^e_{ds} - R_s i^e_{ds} + \Psi^e_{qs}\omega_e \\ \frac{d\Psi^e_{qs}}{dt} &= v^e_{qs} - R_s i^e_{qs} - \Psi^e_{ds}\omega_e \end{aligned} \tag{2.3.22}$$

It is defined the $d-q$ component voltages behind the stator transient inductance as:

$$\begin{aligned} E_{ds} &= -\omega_e(\Psi^e_{qs} - L_s i^e_{qs}) \\ &= -\omega_e(L_s i^e_{qs} + L_m i^e_{qr} - L_s i^e_{qs}) \\ &= -\omega_e\frac{L_m}{L_r}\Psi^e_{qr} \end{aligned} \tag{2.3.23}$$

$$\begin{aligned} E_{qs} &= \omega_e(\Psi^e_{ds} - L_s i^e_{ds}) \\ &= \omega_e(L_s i^e_{ds} + L_m i^e_{dr} - L_s i^e_{ds}) \\ &= \omega_e \frac{L_m}{L_r} \Psi^e_{dr} \end{aligned} \tag{2.3.24}$$

Based on the equations (2.3.23)(2.3.24), they are moved into the voltage terms on the right-hand side of equation (2.3.22). The desired set of stator voltage equations of simple transient model can be obtained. The rotor flux can be assumed to remain constant:

$$\begin{aligned} \frac{d\Psi^e_{ds}}{dt} &= v^e_{ds} - R_s i^e_{ds} - E_{ds} + L_s i^e_{qs} \omega_e \\ \frac{d\Psi^e_{qs}}{dt} &= v^e_{qs} - R_s i^e_{qs} - E_{qs} - L_s i^e_{ds} \omega_e \end{aligned} \tag{2.3.25}$$

where the d-q component voltages behind the stator transient inductance are proportional to the rotor flux linkage. The rotor flux linkages are constant and the newly defined voltages behind the transient inductance $E_{ds}$ and $E_{qs}$ will be constant as well. The stator flux linkages can be expressed only in terms of stator currents and rotor flux linkages, as below:

$$\Psi^e_{ds} = \frac{L_m}{L_r} \Psi^e_{dr} + L_s i^e_{ds} \tag{2.3.26}$$

$$\Psi^e_{qs} = \frac{L_m}{L_r} \Psi^e_{qr} + L_s i^e_{qs} \tag{2.3.27}$$

After substituting the above equations for stator flux linkages into the derivative term on the left side of transient model equations (2.3.25), as below:

$$L_s \frac{di^e_{ds}}{dt} + \frac{L_m}{L_r} \frac{d\Psi^e_{dr}}{dt} = v^e_{ds} - R_s i^e_{ds} - E_{ds} + L_s i^e_{qs} \omega_e \tag{2.3.28}$$

$$L_s \frac{di^e_{qs}}{dt} + \frac{L_m}{L_r} \frac{d\Psi^e_{qr}}{dt} = v^e_{qs} - R_s i^e_{qs} - E_{qs} - L_s i^e_{ds} \omega_e \tag{2.3.29}$$

Now setting the time derivative terms of rotor flux linkages to zero and by rearranging the equations, we obtain:

$$\begin{aligned} R_s i^e_{ds} + L_s \frac{di^e_{ds}}{dt} + E_{ds} &= v^e_{ds} + L_s i^e_{qs} \omega_e \\ R_s i^e_{qs} + L_s \frac{di^e_{qs}}{dt} + E_{qs} &= v^e_{qs} - L_s i^e_{ds} \omega_e \end{aligned} \tag{2.3.30}$$

From the equations given above, the two left-hand side values are assumed to be produced by the flux and torque controllers. The control process by using this method can be found in Figure 2.6.

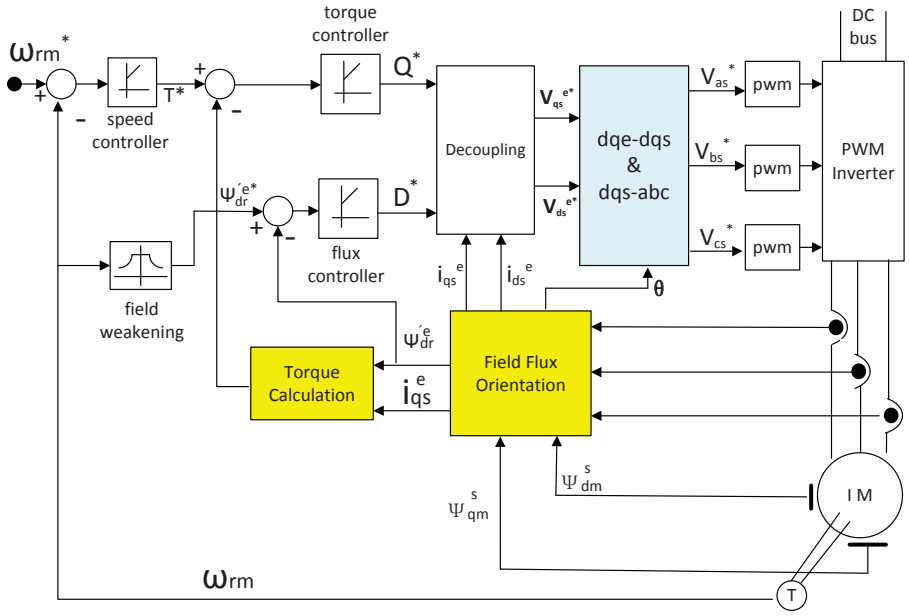


Figure 2.6: Direct vector control of a voltage-regulated PWM inverter for induction motor [124]

Adjusting outputs for current terms on the right-hand side of equation (2.3.30), the desired values for $v_{ds}^e$ and $v_{qs}^e$ will be obtained. The command values of $a-b-c$ stator voltages can be derived by the following methods (2.3.31):

$$\begin{aligned} v_{ds}^{s*} &= v_{ds}^e \cos\theta_e - v_{qs}^e \sin\theta_e \\ v_{qs}^{s*} &= v_{ds}^e \sin\theta_e + v_{qs}^e \cos\theta_e \end{aligned}$$

$$\begin{aligned} v_{as}^* &= v_{qs}^{s*} \\ v_{bs}^* &= -\frac{1}{2} v_{qs}^{s*} - \frac{\sqrt{3}}{2} v_{ds}^{s*} \\ v_{cs}^* &= -\frac{1}{2} v_{qs}^{s*} + \frac{\sqrt{3}}{2} v_{ds}^{s*} \end{aligned} \tag{2.3.31}$$

### 2.3.2 Indirect Vector Control (Current Method)

Another commonly used alternative is the indirect vector control, which is essentially the same as the direct vector control, except the unit vector signals ($\cos\theta_e$ and $\sin\theta_e$) are generated in a feed forward manner.

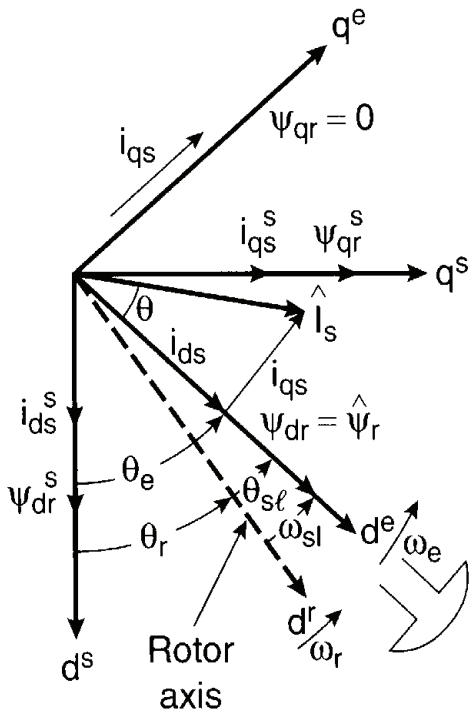


Figure 2.7: The fundamental principle of indirect vector control diagram

The fundamental principle of an indirect vector control can be illustrated with the help of Figure 2.7. The stator is aligned with $d^s - q^s$ axes, and the rotor is aligned with $d^r - q^r$ axes, it is moving at speed $\omega_r$ which is shown from the figure. During the Figure 2.7, the axes $d^e - q^e$ in rotating reference frame are rotating ahead of the $d^r - q^r$ axes by the slip angle $\theta_{sl}$. Thus, the relationship between $\theta_e$ and $\theta_{sl}$ can be written as:

$$\theta_e = \int \omega_e dt = \int (\omega_r + \omega_{sl})dt = \theta_r + \theta_{sl} \tag{2.3.32}$$

For a decoupling control, the stator flux component of current $i^e_{ds}$ should be aligned with the $d^e$ axis, and the torque component of current $i^e_{qs}$ should be aligned with the $q^e$ axis. Combining the rotor circuit equations and rotor flux linkage equations, it will obtain the following equations (2.3.34):

$$\frac{d\Psi^e_{dr}}{dt} + R^e_r i^e_{dr} - (\omega_e - \omega_r)\Psi^e_{qr} = 0 \quad (2.3.33)$$

$$\frac{d\Psi^e_{qr}}{dt} + R^e_r i^e_{qr} + (\omega_e - \omega_r)\Psi^e_{dr} = 0 \quad (2.3.34)$$

And the rotor flux linkage expressions can be given as:

$$\Psi^e_{dr} = L_r i^e_{dr} + L_m i^e_{ds} \quad (2.3.35)$$

$$\Psi^e_{qr} = L_r i^e_{qr} + L_m i^e_{qs} \quad (2.3.36)$$

From the above two equations, the rotor current form can be written as:

$$i^e_{dr} = \frac{1}{L_r}\Psi^e_{dr} - \frac{L_m}{L_r} i^e_{ds} \quad (2.3.37)$$

$$i^e_{qr} = \frac{1}{L_r}\Psi^e_{qr} - \frac{L_m}{L_r} i^e_{qs} \quad (2.3.38)$$

With the help of the above two rotor current equations, we put these equations into the rotor circuit equations and we have:

$$\begin{aligned} \frac{d\Psi^e_{dr}}{dt} + \frac{R_r}{L_r}\Psi^e_{dr} - \frac{L_m}{L_r} R_r i^e_{ds} - \omega_{sl}\Psi^e_{qr} &= 0 \\ \frac{d\Psi^e_{qr}}{dt} + \frac{R_r}{L_r}\Psi^e_{qr} - \frac{L_m}{L_r} R_r i^e_{qs} + \omega_{sl}\Psi^e_{dr} &= 0 \end{aligned} \quad (2.3.39)$$

where $\omega_{sl} = \omega_e - \omega_r$. The main idea is to put the rotor flux on the d-axis, thus it is desirable that: $\Psi^e_{qr} = 0$, will mean $\frac{d\Psi^e_{qr}}{dt} = 0$, so that the total rotor flux $\hat{\Psi}_r$ is directed on the $d^e$-axis. By substituting this into the rotor circuit equations (2.3.39), we get:

$$\frac{L_r}{R_r}\frac{d\hat{\Psi}_r}{dt} + \hat{\Psi}_r = L_m i^e_{ds} \quad (2.3.40)$$

$$\omega_{sl} = \frac{L_m R_r}{\hat{\Psi}_r L_r} i^e_{qs} \quad (2.3.41)$$

Assume rotor flux $\hat{\Psi}_r$ is constant, then from above equation, we have: $\hat{\Psi}_r = L_m i^e_{ds}$. That means the rotor flux is directly proportional to current $i^e_{ds}$ in a steady state.

To implement the indirect vector control strategy, the speed of the control loop generates the torque component of current $i^{e*}_{qs}$. The flux component of the current $i^{e*}_{ds}$ for desired rotor flux $\hat{\Psi}_r$ can be determined from equation $\hat{\Psi}_r = L_m i^e_{ds}$. The variation of magnetising inductance $L_m$ may cause some drift in the flux. The slip speed $\omega^*_{sl}$ is obtained from $i^{e*}_{qs}$ by using equation (2.3.41). The corresponding expression of slip gain $K_s$ is represented as:

$$K_s = \frac{\omega^*_{sl}}{i^{e*}_{qs}} = \frac{L_m R_r}{\hat{\Psi}_r L_r} \tag{2.3.42}$$

A DC machine-like electro-mechanical model of an ideal vector-controlled drive can be derived by using Equation (2.3.40). Furthermore, torque can be controlled by adjusting $i^e_{qs}$ and slip speed which is $\omega_e - \omega_r$. The rotor flux can be controlled by regulating $i^e_{ds}$. The desired value of $i^{e*}_{ds}$ can be obtained from equation (2.3.40). For the desired torque $T^*_e$ of rotor flux, the desired value of $i^{e*}_{qs}$ is given as follows:

$$T^*_{em} = \frac{3}{2}\frac{P}{2}\frac{L_m}{L_r}\hat{\Psi}_r i^{e*}_{qs} \tag{2.3.43}$$

The field orientation $\theta_e$ is the sum of the rotor angle from the position sensor $\theta_r$ and the slip angle $\theta_{sl}$. So the slip speed relation can be written as:

$$\omega^*_{sl} = \omega_e - \omega_r = \frac{R_r}{L_r}\frac{i^{e*}_{qs}}{i^{e*}_{ds}} \tag{2.3.44}$$

Figure 2.8 has shown an indirect vector control scheme for a current regulated PWM inverter for induction motor drive. From this figure, noted that the field orientation $\theta_e$ is the sum of rotor angle from the position sensor $\theta_r$ and slip angle $\theta_{sl}$ which from integrating the slip speed.

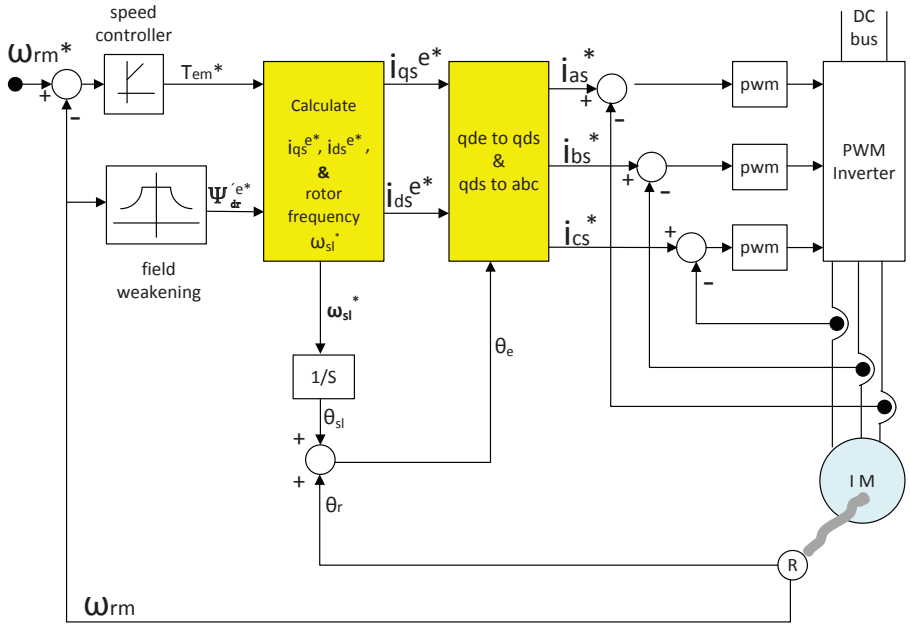


Figure 2.8: Indirect vector control of a current regulated PWM inverter for induction motor [124]

If perpendicular outputs of the form $\sin\theta_r$ and $\cos\theta_r$ are available from the shaft encoder, the values of $\sin\theta_e$ and $\cos\theta_e$ are generated from the following equations:

$$\begin{aligned} \sin\theta_e &= \sin(\theta_r + \theta_{sl}) = \sin\theta_r\cos\theta_{sl} + \cos\theta_r\sin\theta_{sl} \\ \cos\theta_e &= \cos(\theta_r + \theta_{sl}) = \cos\theta_r\cos\theta_{sl} - \sin\theta_r\sin\theta_{sl} \end{aligned} \tag{2.3.45}$$

Note that the indirect vector voltage control of induction motors is omitted in order to save space.

## 2.4 Simulation and Analysis

Parameters of machine used in the induction machine are given as in Table 2.1. Where $R_s$ is stator winding resistance; $L_{ls} = L_{lr}$ are stator and rotor leakage reactance, $(x_{ls}, x_{lr})$ respectively; $L_m$ is stator magnetizing reactance $(x_m)$; $R_r$

Table 2.1: Parameters of Induction Motor by using vector control

| | | |
|---|---|---|
| $R_s = 3.35\Omega$ | $L_s = 6.94mH$ | $R_r = 1.99\Omega$ |
| $L_m = 163.73mH$ | $J_{rotor} = 0.025kgm^2$ | $I_{rated} = S_b/(\sqrt{3} * V_{rated} * p.f.)$ |
| $S_b = 750VA$ | $P_{rated} = 750W$ | $H = J \cdot \omega_{bm} \cdot \omega_{bm}/2 \cdot S_b$ |
| $p.f. = 0.8$ | $f_{rated} = 60$ | $V_m = V_{rated} \times \sqrt{2/3}$ |
| $\omega_{bm} = \frac{2*\omega_b}{P}$ | $T_b = \frac{S_b}{\omega_{bm}}$ | $V_b = V_m$ |
| $\omega_b = 2\pi f_{rated}$ | $D_{omega} = 0$ | $T_{factor} = 3P/4\omega_b$ |
| $L_r = 6.94mH$ | $P = 4$ | $V_{rated} = 200V$ |
| $\omega_e = \omega_b$ | $x_M = 1/(\frac{1}{x_m} + \frac{1}{x_{ls}} + \frac{1}{x_{lr}})$ | |

is referred rotor winding resistance; $J_{rotor}$ is rotor inertia; $S_b$ is rating in VA; $P_{rated}$ is output power; $V_{rated}$ is rated line-to-line voltage; $p.f.$ is power factor; $I_{rated}$ is rated rms current; $P$ is number of poles; $f_{rated}$ is rated frequency; $\omega_b$ is base electrical frequency; $\omega_e$ is equal to $\omega_b$; $\omega_{bm}$ is base mechanical frequency; $T_b$ is base torque; $Z_b$ is base impedance in $\Omega$; $V_m$ is magnitude of phase voltage; $V_b = V_m$, which is base voltage; $T_{factor}$ is factor for torque expression; $x_M$ is mutual reactance; $H$ is rotor inertia constant in second; $D_{omega}$ is rotor damping coefficient.

### 2.4.1 Operating Characteristics

Firstly, this will be implemented as a simulation test of a three-phase induction motor based on a stationary reference $d-q$ model. The objectives of the simulation are examining the motoring and generating characteristics of a motor supplied with sinusoidal voltages. The simulation are used under ode15s method, and stop at two seconds, a minimum step size is $1e^{-4}$ second, a maximum step size is 0.01 second.

The characteristics testing are shown in Figure 2.9 and Figure 2.10. From these figures, after applying the sinusoidal voltages, the rotor speed of induction

motor can follow the reference speed quickly and smoothly by using indirect vector current control approach. The magnitude of rotor flux is maintained well by using this control method.

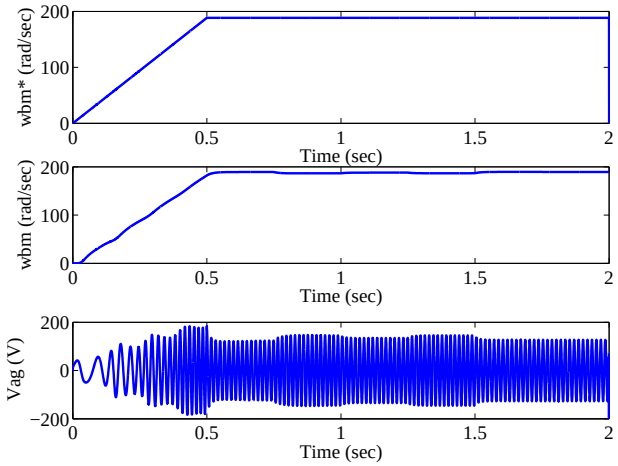


Figure 2.9: No-load startup and transient response of voltage and speed

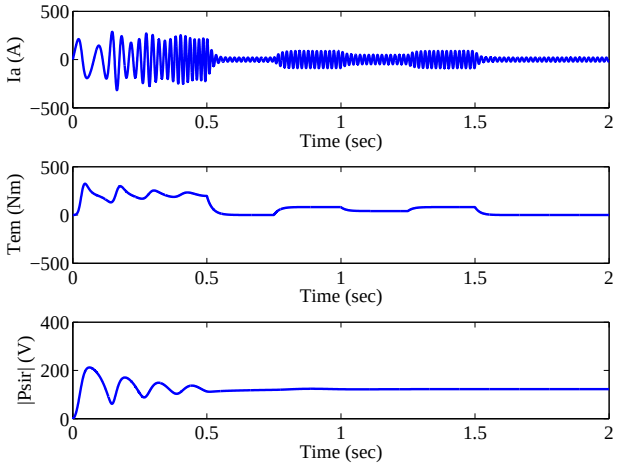


Figure 2.10: No-load startup and step load response of current, torque and $\Psi_r$

### 2.4.2 Vector Control

The simulation of a current regulated PWM induction motor with indirect vector control will be implemented. The objectives of the simulation are: to examine how well this control keeps rotor flux constant during changes in load torque, and afterwards, to observe the improvement in dynamic response with this method of vector control. To avoid long simulation time, the switchings of PWM converter are omitted. The proportional-integral (PI) torque controller converts the speed error to a reference torque $T_{em}^*$.

Inside of the field-oriented block, the equations (2.3.40)(2.3.41)(2.3.44) mentioned in the section concerning indirect vector control can be used to compute the values of $i_{ds}^{e*}$, $i_{qs}^{e*}$, and slip speed $\omega_{sl}^*$.

The angle $\theta_e$ is the sum of slip angle ($\theta_{sl}$) and rotor angle ($\theta_r$). For the field orientation block, there are reference torque, the d-axis rotor flux, and the angle $\theta_e$. In the SIMULINK simulation, from $d^e - q^e$ to the $a-b-c$ block, the transformations are used to generate the $a-b-c$ reference currents. Three large shunt resistors are used to generate the input terminal abc phase voltages to the stator windings of the induction motor.

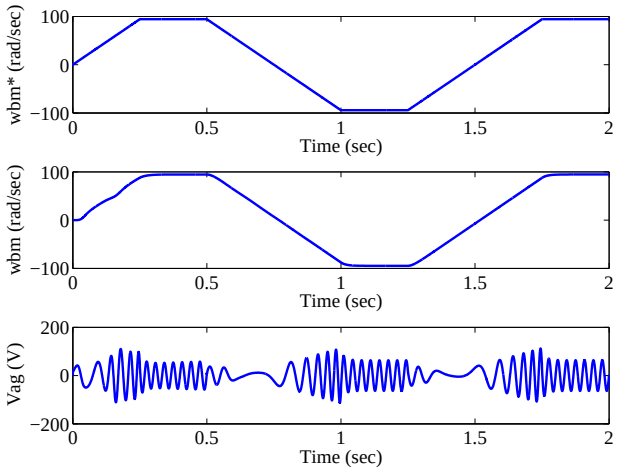


Figure 2.11: Startup and loading transients with vector control

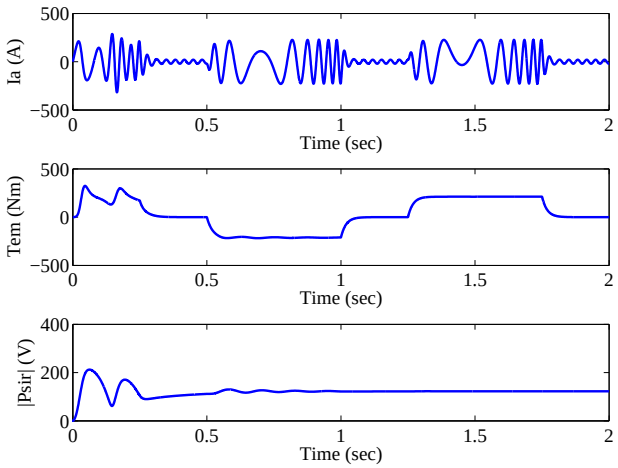


Figure 2.12: Response to changes in reference speed with no-load

Now, plot the values of the reference speed, $\omega_{ref}$; the rotor mechanical speed, $\omega_{rm}$; the stator a-phase voltage, $v_{ag}$; the stator a-phase current, $i_{as}$; the electromagnetic torque, $T_{em}$; and the magnitude of the rotor flux, $\hat{\Psi}_r$ ($\Psi_{dr}$). All the simulation results are recorded in Figures 2.11 and 2.12. These two figures have shown that after changing speed reference periodically, the rotor speed can also follow the reference value quickly, and the electromagnetic torque are also changed from positive to negative value.

## 2.5 Summary

This chapter studies the basic knowledge of modeling and controlling of induction motor. Coordinates transformation between the three-phase model to the stationary reference and rotating reference frame are presented. The dynamic model of the induction motor, including electrical equations, motion equations, and state variables are represented on a different reference frame. The VC based on the rotor flux and stator flux orientation are discussed extensively. Both the DVC and IVC of induction motor theory have been investigated.

# Chapter 3

# Feedback Linearisation Control of Induction Motor

This chapter investigates a fully decoupled control of speed and flux dynamics by using feedback linearisation control. The basic idea of the FLC technique are reviewed for the single-input single-output (SISO) system and the multi-input multi-output (MIMO) system. The FLC technique is used to explain the asymptotical regulation characteristic of the speed and the flux dynamics achieved by conventional FOC. One example of the FLC approach, called Input Output Linearisation Control (IOLC), is applied in order to design a fully decoupled controller for the speed and the flux dynamics. Simulation studies verify the effectiveness of the proposed IOLC by direct comparison with the FOC approach.

## 3.1 Introduction

The induction motor is a typical nonlinear system which has been used widely as a test benchmark for nonlinear control methods. It is used due to strong nonlinear interconnected dynamics (these are unmeasurable in some states,

such as rotor current and rotor flux). It should be noted that the parameters involving stator and rotor resistances change during the operation of the induction motor.

Feedback linearisation control transforms control of the original nonlinear system into that of a linear system via variable transformation and nonlinear feedback control. The basic idea is to transform a nonlinear system into a (fully or partially) linear system firstly, afterwards use the well-known and powerful linear design techniques to complete the control design. Not with standing, in its simplest form, feedback linearisation amounts to the cancelling of nonlinearities in a nonlinear system. Therefore, the closed-loop dynamics is in a linear form. In the last decade, particular feedback linearisation and input-output decoupling techniques have proved useful in applications and were applied even before the theory was fully developed. In fact, the VC of the induction motor is a typical example, in which the original motivation is to convert the control of an AC induction motor to that of a DC motor, from the complex and coupled dynamics to a decoupled one. FOC was proposed initially in the 1970s. However, nonlinear control theory has only been fully developed in 1990s.

This chapter will investigate the control of induction motor by using input-output linearisation. The induction motor will be modeled as a nonlinear dynamic system in fifth-order, a variable transformation will be found before, the nonlinear feedback control law can convert the original nonlinear system to a new linear system. By using a state feedback controller, the exact decoupling in the control of flux amplitude and speed is achieved.

## 3.2 Feedback Linearisation Control Method of Induction Motor

### 3.2.1 Single Input Single Output System

In this section, we review the basic results of nonlinear feedback linearisation control of a single-input single-output (SISO) nonlinear system. This method employs a transformation of coordinates and feedback control to transform a nonlinear system into a system which dynamic is linear (at least partial). It includes two kinds of approach: input-state linearisation (where the full state equation is linearised) and the input-output linearisation, (where the emphasis is on linearising the input-output map from input $u$ to output $y$ even if the state equation is only partially linearised).

We consider a SISO affine nonlinear system represented by:

$$\dot{x} = f(x) + g(x)u \tag{3.2.1}$$

$$y = h(x) \tag{3.2.2}$$

where $x \in \mathcal{R}^n$ is the state vector, $u \in \mathcal{R}$ the input, $y \in \mathcal{R}$ the output. $f(x)$, $g(x) : \mathcal{R}^n \to \mathcal{R}^n, h : \mathcal{R}^n \to \mathcal{R}$ smooth vector fields on the state space $\mathcal{R}^n$. We will assume $f(x_0) = 0$, $h(x_0) = 0$, i.e., $x_0 \in \mathcal{R}^n$ is an equilibrium point of the unforced system.

The point of departure of the whole analysis of the exact linearisation via feedback is the notion of *relative degree* of the system.

**Definiton 3.1.** *Nonlinear system (3.2.1) (3.2.2) is said to have a relative degree $r$, $r \leq n$, at point $x_0$ if*

- $\mathcal{L}_g\mathcal{L}_f^k(x)h(x) = 0$, $\forall$ *$x$ in a neighbourhood of $x_0$ and $k \leq r-2$;*
- $\mathcal{L}_g\mathcal{L}_f^{r-1}(x)h(x) \neq 0$.

*where* $x_0 \in \mathcal{R}^n$, $\mathcal{L}_f(\phi(x)) : \mathcal{R}^n \to R$ *and* $\mathcal{L}_g(\phi(x)) : \mathcal{R}^n \to R$ *represent for the Lie derivative of* $\phi(x)$ *with respect to* $f(x)$ *and* $g(x)$ *respectively, and*

$$\begin{aligned} \mathcal{L}_f^0(h(x)) &= h(x) \\ \mathcal{L}_f^k(h(x)) &= \left[\frac{\partial}{\partial x}\mathcal{L}_f^{k-1}(h(x))\right] f(x) \\ \mathcal{L}_g\left(\mathcal{L}_f^k(h(x))\right) &= \left[\frac{\partial}{\partial x}\mathcal{L}_f^k(h(x))\right] g(x). \end{aligned}$$

**Input-State Linearisation**

In this section, the state equation of input-state linearisation is given as:

$$\dot{x} = f(x) + g(x)u \tag{3.2.3}$$

where $f$ and $g$ are vector fields. System (3.2.1) and (3.2.2) is fully linearisable if there exists a diffeomorphism $\Psi : U \to R^n$ such that $D = \Psi(U) \in R^n$ and the state transformation $z = \Psi(x)$ transforms the system into the form:

$$\dot{z} = Az + B(\alpha(x) + \beta(x)u) \tag{3.2.4}$$

$$y = Cz \tag{3.2.5}$$

where $(A, B)$ is controllable and $\beta(z)$ is nonsingular $\forall z \in D$.

With the system in form (3.2.4) and (3.2.5), we can linearise it exactly by the state feedback control as:

$$u = (-\alpha(z) + v)/\beta(z) \tag{3.2.6}$$

to obtain the linear system

$$\dot{z} = Az + Bv \tag{3.2.7}$$

$$y = Cz, \tag{3.2.8}$$

where $v$ is the linear system control.

Consider the nonlinear system (3.2.1) and (3.2.2) having the relative degree $r = n$. This is exactly equal to the dimension of the state space, at the point $x_0$. In this case, the change of coordinates is required to construct the normal form is exactly given by

$$\Phi(x) = \begin{pmatrix} \phi_1(x) \\ \phi_2(x) \\ \vdots \\ \phi_n(x) \end{pmatrix} = \begin{pmatrix} h(x) \\ L_f h(x) \\ \vdots \\ L_f^{n-1} h(x) \end{pmatrix} \tag{3.2.9}$$

i.e. by the function $h(x)$ and its first $n-1$ derivatives along $f(x)$.

In the new coordinates

$$z_i = \phi_i(x) = L_f^{i-1} h(x), \qquad 1 \leq i \leq n, \tag{3.2.10}$$

the system (3.2.1) will be described in the following form:

$$\begin{cases} \dot{z}_1 &= z_2 \\ & \vdots \\ \dot{z}_{n-1} &= z_n \\ \dot{z}_n &= \alpha(z) + \beta(z) u \end{cases} \tag{3.2.11}$$

where $z = (z_1, ..., z_n)^T$, $\alpha(z) = L_f^n h(x)|_{x=\Psi^{-1}(z)}$, and $\beta(z) = L_g L_f^{n-1} h(x)|_{x=\Psi^{-1}(z)}$. It should be recalled at the point of $z^0 = \Phi(x_0)$, and in all further $z$ in a neighbourhood of $z_0$, the function $\beta(z)$ is nonzero. Now, if we choose the state feedback control law (3.2.6) which indeed exists and is well-defined in a neighbourhood of $z_0$. Imposing this feedback control yields a linear and controllable canonical system characterised by equations (3.2.7) and (3.2.8), where $A$,$B$ and

$C$ are given by:

$$A = \begin{bmatrix} 0 & 1 & 0 & \cdots & 0 \\ 0 & 0 & 1 & \cdots & 0 \\ \vdots & & & & \vdots \\ 0 & 0 & 0 & \cdots & 1 \\ 0 & 0 & 0 & \cdots & 0 \end{bmatrix}, \qquad B = \begin{bmatrix} 0 \\ 0 \\ \vdots \\ 0 \\ 1 \end{bmatrix}, \qquad C = \begin{bmatrix} 1 & 0 & \cdots & 0 & 0 \end{bmatrix} \tag{3.2.12}$$

The problem of finding an output function $\lambda(x)$ such that the relative degree of the system at $x_0$ is exactly $n$, namely a function such that

$$L_g\lambda(x) = L_gL_f\lambda(x) = \cdots = L_gL_f^{n-2}\lambda(x) = 0 \qquad \forall x \tag{3.2.13}$$

$$L_gL_f^{n-1}\lambda(x) \neq 0 \tag{3.2.14}$$

is apparently a problem of resolving partial differential equations of the system. It has been proven that above conditions are equivalent to

$$\begin{aligned} ad_f^{i-1}\lambda(x) &= 0,\ 1 \leq i \leq n-1 \\ ad_f^{n-1}\lambda(x_0) &\neq 0, \end{aligned} \tag{3.2.15}$$

where

$$\begin{aligned} ad_f^0 g(x) &= g(x) \\ ad_f^1 g(x) &= [f, g] \\ &= \frac{\partial g}{\partial x} f(x) - \frac{\partial f}{\partial x} g(x) \\ ad_f^k g(x) &= [f, ad_f^{k-1} g](x), \quad k = 0,\ 1,\ \cdots,\ n-1, \end{aligned} \tag{3.2.16}$$

are called Lie products.

Equation (3.2.15) can be written as:

$$\frac{\partial \lambda(x)}{\partial x} \left[ g(x)\ ad_f g(x)\ \cdots\ ad_f^{n-2} g(x) \right] = 0. \tag{3.2.17}$$

If equation (3.2.17) is solvable in a neighbourhood of $x_0$, there exists a function $\lambda(x)$ such that the system (3.2.1) has relative degree $n$ at $x_0$. The well-known

conditions (necessary and sufficient) for the solution of the state space exact linearisation problem are the following:

**A.1** Matrix $\left[g(x_0)\ ad_f^1 g(x_0)\ \cdots\ ad_f^{n-1} g(x_0)\right]$ has rank $n$.

**A.2** Distribution $D = \text{span}\left[g\ ad_f^1 g\ \cdots\ ad_f^{n-2} g\right]$ is involutive in a neighbourhood of $x_0$.

The above feedback linearisation is an exact input-state linearisation. The transformation of a nonlinear system into a linear one involves solving the first-order partial differential equation (3.2.17), which is normally quite difficult.

### Input-Output Linearisation

When certain output variables are of interest, as in tracking control problems, the system is described by state and output equations. If system (3.2.1) and (3.2.2) has relative degree $n$, then it is both input-state and input-output linearisable. In the input/output linearisation procedure, output $y$ is differentiated, with respect to time, $r$ times until the control input $u$ appears explicitly. The $r$-th derivative of $y$ with respect to time could be written as:

$$\frac{d^r y}{dt^r} = \alpha_r(x) + \beta_r(x)u \tag{3.2.18}$$

where $\alpha_r(x) = L_f^r h(x)$ and $\beta_r(x) = L_g L_f^{r-1} h(x)$. If $\beta(x) \neq 0$, the nonlinear feedback control law

$$u = \beta_r(x)^{-1}\left[-\alpha_r(x) + v\right] \tag{3.2.19}$$

yields a $r$th-order linear SISO system

$$v = \frac{d^r y}{dt^r} \tag{3.2.20}$$

where $v \in R$ is the control input of the linear system.

As system (3.2.1) and (3.2.2) has a relative degree $r,\ r < n$ at $x_0$. For this purpose there exists $n - r$ smooth functions $\psi_{r+1}(x),\cdots,\ \psi_n(x)$ such that

$$\xi \triangleq \begin{bmatrix} z \\ \varphi \end{bmatrix} \triangleq \begin{bmatrix} h(x) \\ \vdots \\ L_f^{r-1}h(x) \\ \psi_{r+1}(x) \\ \vdots \\ \psi_n(x) \end{bmatrix} \triangleq \Psi(x) \tag{3.2.21}$$

is a local diffeomorphism and satisfies

$$L_g\psi_i(x) = 0, \qquad i = r+1,\ \cdots,\ n, \tag{3.2.22}$$

and $\Psi(x_0) = 0$.

System (3.2.1) and (3.2.2) can be transferred into the following form:

$$\dot{z} = A_r z + B_r[\alpha_r(x) + \beta_r(x)u] \tag{3.2.23}$$

$$\dot{\varphi} = q(z, \varphi) \tag{3.2.24}$$

$$y = C_r z, \tag{3.2.25}$$

where $A_r \in R^{r\times r}$, $B \in R^{r\times 1}$, $C \in R^{1\times r}$ are given by

$$A_r = \begin{bmatrix} 0 & 1 & 0 & \cdots & 0 \\ 0 & 0 & 1 & \cdots & 0 \\ \vdots & & & & \vdots \\ 0 & 0 & 0 & \cdots & 1 \\ 0 & 0 & 0 & \cdots & 0 \end{bmatrix}, \qquad B_r = \begin{bmatrix} 0 \\ 0 \\ \vdots \\ 0 \\ 1 \end{bmatrix}, \qquad C = \begin{bmatrix} 1 & 0 & \cdots & 0 & 0 \end{bmatrix} \tag{3.2.26}$$

and

$$\begin{aligned} \alpha_r(\xi) &= L_g L_f^{r-1} h(\Psi^{-1}(\xi)) \\ \beta_r(\xi) &= L_f^r h(\Psi^{-1}(\xi)) \\ q_i(\xi) &= L_f \psi_i(\Psi^{-1}(\xi)), \qquad i = r+1, \cdots, n. \end{aligned}$$

If a nonlinear system is in minimum-phase, there always exists a smooth state-feedback control to make the whole system locally stable.

### Internal Dynamics and Zero-Dynamics of Linearized Systems

In general, it is very difficult to determine the stability of the internal dynamics directly due to its nonlinearity as it is coupled to the "external" closed-loop dynamics. Even though a Lyapunov analysis can be very useful for a few systems, it is difficult to find a Lyapunov function. Therefore, a part of the system dynamics has been rendered "unobservable" in the input-output linearisation. This part of the dynamics is called the internal dynamics, because it remains unseen from the external input-output relationship. It can be further illustrated by the following example:

$$\begin{aligned} \begin{bmatrix} \dot{x}_1 \\ \dot{x}_2 \end{bmatrix} &= \begin{bmatrix} x_2^3 + u \\ u \end{bmatrix} \\ y &= x_1 \end{aligned} \tag{3.2.27}$$

Assume that the control objective is to make y track $y_d(t)$. Differentiation of y simply leads to the first state equation which is $\dot{y} = \dot{x_1} = x_2^3 + u$. Choosing the control law:

$$u = -x_2^3 - e(t) + \dot{y}_d(t) \tag{3.2.28}$$

where $\dot{e} + e = 0$. The same control input is also applied to the second dynamic equation, and leading to the internal dynamics:

$$\dot{x}_2 + \dot{x}_2^3 = \dot{y}_d - e \tag{3.2.29}$$

where the internal dynamics is nonlinear. However, in view of the facts that e is guaranteed to be bounded by $\dot{e} + e = 0$ and $\dot{y}_d$ is assumed to be bounded, we have:

$$|\dot{y}_d(t) - e| \leq D \tag{3.2.30}$$

where D is a positive constant. Therefore, equation (3.2.28) does represent a satisfactory tracking control law for the system (3.2.27), given any trajectory

$y_d(t)$ whose derivative $\dot{y}_d(t)$ is bounded. Conversely, it's easy to show that if the second state equation in (3.2.27) is replaced by $\dot{x}_2 = -u$, then the resulting internal dynamics is unstable.

The stability of the internal dynamics for linear systems is simply determined by the locations of the zeros. It is interesting to see whether this relation can be extended to nonlinear systems. Firstly, it is necessary to extend the concept of zero to nonlinear systems, and then determine the relation of the internal dynamics stability to this extended concept of zero. Extending the notion of zero to nonlinear systems is not a trivial proposition. Hence, the transfer functions of linear system zeros which they are based on. This can not be defined for nonlinear systems. Zeros are intrinsic properties of a linear system. In contrast to nonlinear systems, where the stability of the internal dynamics may depend on the specific control input.

A way to approach these difficulties is to define the so-called zero-dynamics for a nonlinear system. The zero-dynamics is defined to be the internal dynamics of the system when the system output is kept at zero by the input. For example, for the system (3.2.27), the zero-dynamics is:

$$\dot{x}_2 + x_2^3 = 0 \tag{3.2.31}$$

It should be noted that the specification of maintaining the system output at zero uniquely defines the required input. We see that the zero-dynamics is an intrinsic property of a nonlinear system. Therefore, the reason to define and study the zero-dynamics is to discover a simpler way of determining the stability of the internal dynamics. For linear systems, the stability of the zero-dynamics implies the global stability of the internal dynamics. However, in nonlinear systems, the relation is not so clear.

Two useful remarks can be made about the zero-dynamics of nonlinear systems. First, the zero-dynamics is an intrinsic feature of a nonlinear system, which does not depend on the choice of control law or the desired trajectories.

Second, examining the stability of zero-dynamics is much easier than examining the stability of internal dynamics, because the zero-dynamics only involves the internal states.

### 3.2.2 Multi Input Multi Output Systems

The concepts concerning SISO systems, such as input-state linearisation, input-output linearisation, and zero-dynamics, can be extended to the multiple input multiple output systems (MIMO). In the MIMO systems, the system should be considered to have the same numbers of inputs and outputs, as follows:

$$\begin{aligned} \dot{x} &= f(x) + g_1(x)u_1 + \cdots + g_m(x)u_m \\ y_1 &= h_1(x) \\ \cdots & \\ y_m &= h_m(x) \end{aligned} \tag{3.2.32}$$

where the value of $x$ is the state vector, $u_m(s)$ are control inputs and $y_m(s)$ are system outputs, $f(x)$ and $g(x)$ are smooth vector fields, and $h(x)$ are smooth scalar functions. If we put the control inputs $u_i$ (i=1,...,m) into vector u, the corresponding vector $g(x)$ placed into matrix $G$, and then outputs $y_j$ (j=1,...,m) placed into a vector $y$. The new equations of the system can be compactly written as:

$$\begin{aligned} \dot{x} &= f(x) + G(x)u \\ y &= h(x) \end{aligned} \tag{3.2.33}$$

In order to obtain the input-output linearisation of the MIMO systems, it is required to differentiate the outputs $y_j$ of the system until the inputs appear. This step is similar to the SISO case. Now start with the following equation:

$$\dot{y}_j = L_f h_j + \sum_{i=1}^{m} (L_g h_j) u_i \tag{3.2.34}$$

If $L_g h_j = 0$ for all $i$, then the inputs cannot be seen from the outputs and we must repeat the differentiation. If the above procedure has been performed for each output $y_j$, the total equations in above form can be written compactly as follows:

$$\begin{bmatrix} y_1^{r1} \\ \cdots \\ \cdots \\ y_m^{rm} \end{bmatrix} = \begin{bmatrix} L_f^{r1} h_1(x) \\ \cdots \\ \cdots \\ L_f^{rm} h_m(x) \end{bmatrix} + E(x) \begin{bmatrix} u_1 \\ \cdots \\ \cdots \\ u_m \end{bmatrix} \tag{3.2.35}$$

where $r_j$ (j=1,...,m) is the smallest integer such that at least one of the inputs appear in $y_j^{rj}$. The $m \times m$ matrix E(x) can be defined as:

$$E(x) = \begin{bmatrix} L_g L_f^{r1-1} h_1 & \cdots & \cdots & L_g L_f^{r1-1} h_1 \\ \cdots & \cdots & \cdots & \cdots \\ \cdots & \cdots & \cdots & \cdots \\ L_g L_f^{rm-1} h_1 & \cdots & \cdots & L_g L_f^{rm-1} h_1 \end{bmatrix} \tag{3.2.36}$$

The matrix E(x) can be called as the decoupling matrix for MIMO system. The input transformation can be obtained from the following equation:

$$u = -E^{-1} \begin{bmatrix} L_f^{r1} h_1(x) \\ \cdots \\ \cdots \\ L_f^{rm} h_m(x) \end{bmatrix} + E^{-1} \begin{bmatrix} v_1 \\ \cdots \\ \cdots \\ v_m \end{bmatrix} \tag{3.2.37}$$

and a linear differential relation between the output $y$ and the new input $v$ is:

$$\begin{bmatrix} y_1^{r1} \\ \cdots \\ \cdots \\ y_m^{rm} \end{bmatrix} = \begin{bmatrix} v_1 \\ \cdots \\ \cdots \\ v_m \end{bmatrix} \tag{3.2.38}$$

From the above input-output equation (3.2.38), it is easy to see the relation is decoupled. Resulting in a linear system. The input $v_i$ only affects the

corresponding output $y_i$. The equation (3.2.37) is called a decoupling control law. After the decoupling, the equation can be used as SISO design on each y-v channel as demonstrated by decoupled dynamics (above) in order to build stabilisation controllers.

## 3.3 Modeling of Induction Motor

In Chapter Two, the detailed model of induction motors in stationary reference frame and rotating reference frame have discussed. However, in this chapter, the modeling of induction motor will be investigated in another simpler form, in order to design the following observers. Based on the general theory of electric machines, an induction motor consists of a three-phase stator and rotor windings. A two phase equivalent machine can be described as a two stator and two rotor windings [51]. Their equations are displayed as follows,

$$u_{as}^s = i_{as}^s R_s + \frac{d\psi_{as}^s}{dt} \tag{3.3.1}$$

$$u_{bs}^s = i_{bs}^s R_s + \frac{d\psi_{bs}^s}{dt} \tag{3.3.2}$$

$$0 = i_{dr}^e R_r + \frac{d\psi_{dr}^e}{dt} \tag{3.3.3}$$

$$0 = i_{qr}^e R_r + \frac{d\psi_{qr}^e}{dt} \tag{3.3.4}$$

where i is current, R is resistance, $\psi$ is flux linkage, and $u_s$ denote stator voltage. All of them are input into the machine. The subscripts s and r stand for stator and rotor, and the superscripts s denote the components of a vector with respect to a stator reference frame. Superscripts e denotes the components of a vector with respect to a frame rotating at speed $n_p\omega_r$, where $n_p$ denotes the number of pole pairs of the induction machine and $\omega_r$ is the rotor speed. If $\delta$ denotes an angle, we have:

$$\frac{d\delta}{dt} = n_p\omega_r \tag{3.3.5}$$

Rotor currents and rotor fluxes from the rotating reference frame to the stationary reference frame are as follows:

$$\begin{pmatrix} i^s_{ar} \\ i^s_{br} \end{pmatrix} = \begin{bmatrix} \cos\delta & -\sin\delta \\ \sin\delta & \cos\delta \end{bmatrix} \begin{pmatrix} i^e_{dr} \\ i^e_{qr} \end{pmatrix} \tag{3.3.6}$$

$$\begin{pmatrix} \psi^s_{ar} \\ \psi^s_{br} \end{pmatrix} = \begin{bmatrix} \cos\delta & -\sin\delta \\ \sin\delta & \cos\delta \end{bmatrix} \begin{pmatrix} \psi^e_{dr} \\ \psi^e_{qr} \end{pmatrix} \tag{3.3.7}$$

Applying the transformations from above equations (3.3.1) to (3.3.7) and we obtained

$$\begin{aligned} u^s_{as} &= i^s_{as}R_s + \frac{d\psi^s_{as}}{dt} \\ u^s_{bs} &= i^s_{bs}R_s + \frac{d\psi^s_{bs}}{dt} \\ 0 &= i^s_{ar}R_r + \frac{d\psi^s_{ar}}{dt} + n_p\omega_r\psi^s_{br} \\ 0 &= i^s_{br}R_r + \frac{d\psi^s_{br}}{dt} - n_p\omega_r\psi^s_{ar} \end{aligned} \tag{3.3.8}$$

Note that under the assumptions of linearity of the magnetic circuits, the equal mutual inductances in conjunction with the neglecting of the iron loss, the magnetic equations are shown as follows:

$$\begin{aligned} \psi^s_{as} &= L_s i^s_{as} + L_m i^s_{ar} \\ \psi^s_{bs} &= L_s i^s_{bs} + L_m i^s_{br} \\ \psi^s_{ar} &= L_r i^s_{ar} + L_m i^s_{as} \\ \psi^s_{br} &= L_r i^s_{br} + L_m i^s_{bs} \end{aligned} \tag{3.3.9}$$

where $L_s$ and $L_r$ are autoinductances, $L_m$ is the mutual inductance. In fact, fluxes and currents in equation (3.3.1) to the equation (3.3.4) are related by $\delta$-dependent auto and mutual inductances.

Now eliminating stator currents and flux linkages by using the above equations,

we obtain:

$$\begin{aligned} u_{as}^s &= i_{as}^s R_s + \frac{L_m}{L_r}\frac{d\psi_{ar}^s}{dt} + (L_s - \frac{L_m^2}{L_r})\frac{di_{as}^s}{dt} \\ u_{bs}^s &= i_{bs}^s R_s + \frac{L_m}{L_r}\frac{d\psi_{br}^s}{dt} + (L_s - \frac{L_m^2}{L_r})\frac{di_{bs}^s}{dt} \\ 0 &= \frac{R_r}{L_r}\psi_{ar}^s - \frac{R_r}{L_r}L_m i_{as}^s + \frac{d\psi_{ar}^s}{dt} + n_p\omega_r\psi_{br}^s \\ 0 &= \frac{R_r}{L_r}\psi_{br}^s - \frac{R_r}{L_r}L_m i_{bs}^s + \frac{d\psi_{br}^s}{dt} - n_p\omega_r\psi_{ar}^s \end{aligned} \tag{3.3.10}$$

The torque produced by the machine is expressed in terms of stator currents and rotor fluxes as:

$$T = \frac{n_p L_m}{L_r}(\psi_{ar}^s i_{bs}^s - \psi_{br}^s i_{as}^s) \tag{3.3.11}$$

Then the rotor dynamics are:

$$\frac{d\omega_r}{dt} = \frac{n_p L_m}{JL_r}(\psi_{ar}^s i_{bs}^s - \psi_{br}^s i_{as}^s) - \frac{T_L}{J} \tag{3.3.12}$$

where J is the moment of inertia of the rotor and $T_L$ is the load torque. By adding the rotor dynamics (3.3.12) to the electromagnetic dynamics equations (3.3.10) and then rearranging these equations in state space form. Finally, the overall dynamics of an induction motor under the assumptions of equal mutual inductances and linear magnetic circuit are given by the fifth-order model, which were given as follows:

$$\begin{aligned} \frac{d\omega_r}{dt} &= \frac{n_p L_m}{JL_r}(\psi_{ar}^s i_{bs}^s - \psi_{br}^s i_{as}^s) - \frac{T_L}{J} \\ \frac{d\psi_{ar}^s}{dt} &= -\frac{R_r}{L_r}\psi_{ar}^s - n_p\omega_r\psi_{br}^s + \frac{R_r}{L_r}L_m i_{as}^s \\ \frac{d\psi_{br}^s}{dt} &= -\frac{R_r}{L_r}\psi_{br}^s + n_p\omega_r\psi_{ar}^s + \frac{R_r}{L_r}L_m i_{bs}^s \\ \frac{di_{as}^s}{dt} &= \frac{L_m R_r}{\sigma L_s L_r^2}\psi_{ar}^s + \frac{n_p L_m}{\sigma L_s L_r}\omega_r\psi_{br}^s - (\frac{L_m^2 R_r + L_r^2 R_s}{\sigma L_s L_r^2})i_{as}^s + \frac{1}{\sigma L_s}u_{as}^s \\ \frac{di_{bs}^s}{dt} &= \frac{L_m R_r}{\sigma L_s L_r^2}\psi_{br}^s - \frac{n_p L_m}{\sigma L_s L_r}\omega_r\psi_{ar}^s - (\frac{L_m^2 R_r + L_r^2 R_s}{\sigma L_s L_r^2})i_{bs}^s + \frac{1}{\sigma L_s}u_{bs}^s \end{aligned} \tag{3.3.13}$$

where i, $u_s$, and $\psi$ denote current, stator voltage input to the machine, flux linkage. Note that the subscripts s and r stand for stator and rotor, and (a,

b) denote the components of a vector with respect to a fixed stator reference frame. We made $\sigma = 1 - (L_m^2/L_s L_r)$. Now, we are going to get rid of the subscripts s and r, we will only use stator currents and rotor fluxes as state variables.

Firstly, we use $x = (\omega_r, \psi_a, \psi_b, i_a, i_b)^T$ as the state variables, and get:

$$p = (p_1, p_2)^T = (T_L - T_{LN}, R_r - R_{rN})^T \tag{3.3.14}$$

where p is the unknown parameter deviations from the nominal values $T_{LN}$ and $R_{rN}$ of load torque $T_L$ and rotor resistance $R_r$.

Secondly, let $u = (u_a, u_b)^T$ be the control vector. We are using the following equations:

$$\alpha = \frac{R_r}{L_r} \tag{3.3.15}$$

$$\beta = \frac{L_m}{\sigma L_s L_r} \tag{3.3.16}$$

$$\gamma = \frac{L_m^2 R_r}{\sigma L_s L_r^2} + \frac{R_s}{\sigma L_s} \tag{3.3.17}$$

$$\mu = \frac{n_p L_m}{J L_r} \tag{3.3.18}$$

as a reparameterisation of the induction motor model, where $\alpha$, $\beta$, $\gamma$, $\mu$ are known parameters depending on the nominal value $R_{rN}$.

Finally, the fifth-order model system can be obtained as:

$$\dot{x} = f(x) + p_1 f_1(x) + p_2 f_2(x) + g_a u_a + g_b u_b \tag{3.3.19}$$

where the vector fields $f$, $f_1$, $f_2$, $g_a$, $g_b$ are written as:

$$f(x) = \begin{pmatrix} \mu(\psi_a i_b - \psi_b i_a) - \frac{T_{LN}}{J} \\ -\alpha\psi_a - n_p\omega_r\psi_b + \alpha L_m i_a \\ -\alpha\psi_b + n_p\omega_r\psi_a + \alpha L_m i_b \\ \alpha\beta\psi_a + n_p\beta\omega_r\psi_b - \gamma i_a \\ \alpha\beta\psi_b - n_p\beta\omega_r\psi_a - \gamma i_b \end{pmatrix} \tag{3.3.20}$$

$$f_1(x) = \begin{pmatrix} \frac{-1}{J} \\ 0 \\ 0 \\ 0 \\ 0 \end{pmatrix} \qquad f_2(x) = \begin{pmatrix} 0 \\ -\psi_a + L_m i_a \\ -\psi_b + L_m M i_b \\ \beta\psi_a - L_m \beta i_a \\ \beta\psi_b - L_m \beta i_b \end{pmatrix} \tag{3.3.21}$$

$$\begin{aligned} g_a &= \begin{pmatrix} 0 & 0 & 0 & \frac{1}{\sigma L_s} & 0 \end{pmatrix}^T \\ g_b &= \begin{pmatrix} 0 & 0 & 0 & 0 & \frac{1}{\sigma L_s} \end{pmatrix}^T \end{aligned} \tag{3.3.22}$$

where $x = (\omega_r, \psi_a, \psi_b, i_a, i_b)^T$ is state vector of the system. $(i_a, i_b)$ is stator current. $(\psi_a, \psi_b)$ is rotor flux. $\omega_r$ is rotor speed. Stator voltage consists of two control variables $(u_a, u_b)$.

## 3.4 Interpreting Vector Control as Partial Feedback Linearisation Control

There is a classical control technique for induction motors which is called the VC. As introduced by Blaschke in 1971. It includes the transformation of the stator current vector $(i_a, i_b)$ and rotor flux vector $(\psi_a, \psi_b)$ in the fixed stator stationary reference frame, into vector in the rotating reference frame which rotate along with the flux vector $(\psi_a, \psi_b)$. As stated before, let's define:

$$\rho = \arctan \frac{\psi_b^s}{\psi_a^s} \tag{3.4.1}$$

the transformations can be written as,

$$\begin{pmatrix} i_d^e \\ i_q^e \end{pmatrix} = \begin{bmatrix} \cos\rho & \sin\rho \\ -\sin\rho & \cos\rho \end{bmatrix} \begin{pmatrix} i_a^s \\ i_b^s \end{pmatrix} \tag{3.4.2}$$

$$\begin{pmatrix} \psi_d^e \\ \psi_q^e \end{pmatrix} = \begin{bmatrix} \cos\rho & \sin\rho \\ -\sin\rho & \cos\rho \end{bmatrix} \begin{pmatrix} \psi_a^s \\ \psi_b^s \end{pmatrix} \tag{3.4.3}$$

where $\cos\theta_e = \psi_a^s/|\psi|$, and $\sin\theta_e = \psi_b^s/|\psi|$, with $|\psi| = \sqrt{(\psi_a^s)^2 + (\psi_b^s)^2}$, from equation (3.4.2) and equation (3.4.3), we obtained

$$\begin{aligned} i_d^e &= \frac{\psi_a^s i_a^s + \psi_b^s i_b^s}{|\psi|} \\ i_q^e &= \frac{\psi_a^s i_b^s - \psi_b^s i_a^s}{|\psi|} \\ \psi_d^e &= \sqrt{(\psi_a^s)^2 + (\psi_a^s)^2} = |\psi| \\ \psi_q^e &= 0 \end{aligned} \tag{3.4.4}$$

It can be explained that vector control as a state feedback transformation into a control system of simpler structure. Now defining the state space change of coordinates:

$$\begin{aligned} i_d^e &= \frac{\psi_a^s i_a^s + \psi_b^s i_b^s}{|\psi|} \\ i_q^e &= \frac{\psi_a^s i_b^s - \psi_b^s i_a^s}{|\psi|} \\ \rho &= \arctan\frac{\psi_b^s}{\psi_a^s} \\ \psi_d^e &= \sqrt{\psi_a^2 + \psi_b^2} \\ \omega_r &= \omega_r \end{aligned} \tag{3.4.5}$$

And the state feedback can be represented as follows:

$$\begin{pmatrix} u_a^s \\ u_b^s \end{pmatrix} = |\psi| \begin{bmatrix} \psi_a^s & \psi_b^s \\ -\psi_b^s & \psi_a^s \end{bmatrix}^{-1} \begin{pmatrix} u_d^e \\ u_q^e \end{pmatrix} \tag{3.4.6}$$

The fifth-order system in Chapter two is applied to the following equations:

$$\begin{aligned} \frac{d\psi_d^e}{dt} &= -\alpha\psi_d^e + \alpha L_m i_d^e \\ \frac{d\rho}{dt} &= n_p\omega_r + \alpha L_m \frac{i_q^e}{\psi_d^e} \\ \frac{di_d^e}{dt} &= -\gamma i_d^e + \alpha\beta\psi_d^e + n_p\omega_r i_q^e + \alpha L_m \frac{(i_q^e)^2}{\psi_d^e} + \frac{1}{\sigma L_s}u_d^e \\ \frac{di_q^e}{dt} &= -\gamma i_q^e - \beta n_p\omega_r\psi_d^e - n_p\omega_r i_d^e - \alpha L_m \frac{i_d^e i_q^e}{\psi_d^e} + \frac{1}{\sigma L_s}u_q^e \\ \frac{d\omega_r}{dt} &= \mu\psi_d^e i_q^e - \frac{T_L}{J} \end{aligned} \tag{3.4.7}$$

The nonlinear state feedback control, is defined as:

$$\begin{pmatrix} u_d^e \\ u_q^e \end{pmatrix} = \sigma L_s \begin{pmatrix} -\alpha\beta\psi_d^e - n_p\omega_r i_q^e - \alpha L_m \frac{(i_q^e)^2}{\psi_d^e} + v_d^e \\ \beta\omega_r n_p \psi_d^e + n_p\omega_r i_d^e + \alpha L_m \frac{i_d^e i_q^e}{\psi_d^e} + v_q^e \end{pmatrix} \tag{3.4.8}$$

The equation is placed into the state feedback equation which is (3.4.6), it becomes:

$$\begin{pmatrix} u_a^s \\ u_b^s \end{pmatrix} = \sigma L_s |\psi| \begin{bmatrix} \psi_a^s & \psi_b^s \\ -\psi_b^s & \psi_a^s \end{bmatrix}^{-1} \begin{pmatrix} -\alpha\beta\psi_d^e - n_p\omega_r i_q^e - \alpha L_m \frac{(i_q^e)^2}{\psi_d^e} + v_d^e \\ \beta\omega_r n_p \psi_d^e + n_p\omega_r i_d^e + \alpha L_m \frac{i_d^e i_q^e}{\psi_d^e} + v_q^e \end{pmatrix} \tag{3.4.9}$$

When the fifth-order system equations have been transformed, we can obtain the following closed-loop system:

$$\begin{aligned} \frac{d\psi_d^e}{dt} &= -\alpha\psi_d^e + \alpha L_m i_d^e \\ \frac{di_d^e}{dt} &= -\gamma i_d^e + v_d \\ \frac{d\omega_r}{dt} &= \mu\psi_d^e i_q^e - \frac{T_L}{J} \\ \frac{di_q^e}{dt} &= -\gamma i_q^e + v_q \\ \frac{d\rho}{dt} &= n_p\omega_r + \alpha L_m \end{aligned} \tag{3.4.10}$$

From the closed-loop system (displayed in equations 3.4.10), there is a simpler structure for flux amplitude dynamics which are linear,

$$\begin{aligned} \frac{d\psi_d^e}{dt} &= -\alpha\psi_d^e + \alpha L_m i_d^e \\ \frac{di_d^e}{dt} &= -\gamma i_d^e + v_d \end{aligned} \tag{3.4.11}$$

where flux amplitude can be independently controlled by $v_d$ such as via a PI controller, and it is given as

$$v_d = -k_{d1}(\psi_d^e - \psi_{dref}^e) - k_{d2}\int_0^t (\psi_d^e(\tau) - \psi_{dref}^e)d\tau \tag{3.4.12}$$

When the flux amplitude $\psi_d^e$ was regulated to the constant reference value $\psi_{dref}^e$, rotor speed dynamics are linear as well,

$$\begin{aligned} \frac{d\omega_r}{dt} &= \mu\psi_{dref}^e i_q^e - \frac{T_L}{J} \\ \frac{di_q^e}{dt} &= -\gamma i_q^e + v_q \end{aligned} \tag{3.4.13}$$

where rotor speed can be controlled independently by $v_q$, for example, we can use two nested loops of PI controllers:

$$\begin{aligned} v_q &= -k_{q1}(T - T_{ref}) - k_{q2}\int_0^t (T(\tau) - T_{ref}(\tau))d\tau \\ T_{ref} &= -k_{q3}(\omega_r - \omega_{ref}) - k_{q4}\int_0^t (\omega_r(\tau) - \omega_{ref})d\tau \\ T &= \mu\psi_d^e i_q^e \end{aligned} \tag{3.4.14}$$

If rotor speed $\omega$ and flux amplitude $\psi_d$ are defined as outputs, field-oriented control achieves asymptotic input-output linearisation, and then decoupling via the nonlinear state feedback.

During flux transient the nonlinear term $\psi_d^e i_q^e$ in equations (3.4.10) makes four relatives equations in (3.4.10) also nonlinear and coupled. In the end, speed transients are difficult to evaluate and may be unsatisfactory. The next part will solve this problem.

## 3.5 Input-Output Feedback Linearization Control of Induction Motor

Vector control can be improved by achieving input-output decoupling and linearisation via a nonlinear state feedback control. This is not as complex as equation (3.4.9). This technique will be reviewed first, before investigating the adaptive control in Chapter Four.

Before proceeding, we need to review a few basic concepts from differential geometry. When dealing with stability in the sense of Lyapunov, the notion

of "time derivative of a scalar function V along the trajectories of a system $\dot{x} = f(x)$" is frequently used. As we know, given V: $D \to \mathbb{R}$ and $\dot{x} = f(x)$, we can have:

$$\dot{V} = \frac{\partial V}{\partial x}\dot{x} = \nabla V f(x) = L_f V(x) \tag{3.5.1}$$

Let's consider a scalar function $\phi$: $D \subset \mathbb{R}^n \to \mathbb{R}$ and a vector field f: $D \subset \mathbb{R}^n \to \mathbb{R}^n$. The Lie derivative of $\phi$, with respect to f which denotes as $L_f\phi$, is given by:

$$L_f\phi(x) = \frac{\partial \phi}{\partial x} f(x) \tag{3.5.2}$$

Thus, going back to Lyapunov functions, $\dot{V}$ is merely the Lie derivative of V with respect to f(x). The Lie derivative notation is usually more insightful by using at higher order derivatives. This needs to be calculated. It should be noted, two vector fields f and g: $D \subset \mathbb{R}^n \to \mathbb{R}^n$, so we have:

$$L_f\phi(x) = \frac{\partial \phi}{\partial x} f(x) \qquad\qquad L_g\phi(x) = \frac{\partial \phi}{\partial x} g(x)$$

and

$$L_g L_f\phi(x) = L_g[L_f\phi(x)] = \frac{\partial (L_f\phi)}{\partial x} g(x) \tag{3.5.3}$$

Further, when the special case has happened, that's $f = g$, the following equation can be obtained:

$$L_f L_f\phi(x) = L_f^2\phi(x) = \frac{\partial (L_f\phi)}{\partial x} f(x) \tag{3.5.4}$$

After understanding these concepts, We know the outputs to be controlled are $\omega_r$ and $\psi_d^e$ (also given as $(\psi_a^s)^2 + (\psi_b^s)^2$). Let's define the change of coordinates to assist the Lie derivative:

$$\begin{aligned}
y_1 &= \phi_1(x) = \omega_r \\
y_2 &= L_f\phi_1(x) = \mu(\psi_a^s i_b^s - \psi_b^s i_a^s) - \frac{T_L}{J} \\
y_3 &= \phi_2(x) = (\psi_a^s)^2 + (\psi_b^s)^2 \\
y_4 &= L_f\phi_2(x) = -2\alpha((\psi_a^s)^2 + (\psi_b^s)^2) + 2\alpha L_m(\psi_a^s i_a^s + \psi_b^s i_b^s) \\
y_5 &= \arctan(\frac{\psi_b^s}{\psi_a^s}) = \phi_3(x) = \rho
\end{aligned} \tag{3.5.5}$$

where the above equations must obey that $y_3 > 0$, $-90 \leq y_5 \leq 90$. Using the previous equations and the inverse transformation, we can obtain,

$$\begin{aligned}
\omega_r &= y_1 \\
\psi_a^s &= \sqrt{y_3}\cos y_5 \\
\psi_b^s &= \sqrt{y_3}\sin y_5 \\
i_a^s &= \frac{1}{\sqrt{y_3}}[-\frac{1}{\mu}\sin y_5(y_2 + \frac{T_{LN}}{J}) + \cos y_5(\frac{y_4 + 2\alpha y_3}{2\alpha M})] \\
i_b^s &= \frac{1}{\sqrt{y_3}}[\sin y_5(\frac{y_4 + 2\alpha y_3}{2\alpha M}) + \frac{1}{\mu}\cos y_5(y_2 + \frac{T_{LN}}{J})]
\end{aligned} \tag{3.5.6}$$

The dynamics of the induction motor, with nominal parameters, are given new coordinates by the following equations:

$$\begin{aligned}
\dot{y_1} &= y_2 \\
\dot{y_2} &= L_f^2\phi_1 + L_{g_a}L_f\phi_1 u_a^s + L_{g_b}L_f\phi_1 u_b^s \\
\dot{y_3} &= y_4 \\
\dot{y_4} &= L_f^2\phi_2 + L_{g_a}L_f\phi_2 u_a^s + L_{g_b}L_f\phi_2 u_b^s \\
\dot{y_5} &= L_f\phi_3
\end{aligned} \tag{3.5.7}$$

The first four equations in (3.5.7) can be rewritten as:

$$\begin{pmatrix} \ddot{y_1} \\ \ddot{y_3} \end{pmatrix} = \begin{pmatrix} L_f^2\phi_1 \\ L_f^2\phi_2 \end{pmatrix} + D(x)\begin{pmatrix} u_a^s \\ u_b^s \end{pmatrix} \tag{3.5.8}$$

where $L_f^2\phi_1$ and $L_f^2\phi_2$ are given as following:

$$L_f^2\phi_1 = -\mu\beta n_p\omega_r[(\psi_a^s)^2 + (\psi_b^s)^2] - \mu(\alpha+\gamma)(\psi_a^s i_b^s - \psi_b^s i_a^s) - \mu n_p\omega_r(\psi_a^s i_a^s + \psi_b^s i_b^s)$$

$$\begin{aligned}
L_f^2\phi_2 = \quad & (4\alpha^2 + 2\alpha^2\beta L_m)[(\psi_a^s)^2 + (\psi_b^s)^2] + 2\alpha L_m n_p\omega_r \\
& (\psi_a^s i_b^s - \psi_b^s i_a^s) - (6\alpha^2 L_m + 2\alpha\gamma L_m)(\psi_a^s i_a^s + \psi_b^s i_b^s) \\
& +2\alpha^2 L_m^2[(i_a^s)^2 + (i_b^s)^2]
\end{aligned} \tag{3.5.9}$$

where $D(x)$ in equation (3.5.8) is the decoupling matrix. It can be defined as:

$$D(x) = \begin{bmatrix} L_{g_a}L_f\phi_1 & L_{g_b}L_f\phi_1 \\ L_{g_a}L_f\phi_2 & L_{g_b}L_f\phi_2 \end{bmatrix} = \begin{bmatrix} -\frac{\mu}{\sigma L_s}\psi_b^s & \frac{\mu}{\sigma L_s}\psi_a^s \\ \frac{2\alpha L_m}{\sigma L_s}\psi_a^s & \frac{2\alpha L_m}{\sigma L_s}\psi_b^s \end{bmatrix} \tag{3.5.10}$$

And then

$$Det[D] = -2\frac{\alpha\mu L_m}{(\sigma L_s)^2}[(\psi_a^s)^2 + (\psi_b^s)^2] \neq 0 \tag{3.5.11}$$

$D(x)$ is nonsingular for $(\psi_a^s)^2 + (\psi_b^s)^2 \neq 0$.

The dynamics of the flux angle $y_5$ are:

$$\frac{dy_5}{dt} = \frac{d\phi_3}{dt} = n_p\omega_r + \frac{\alpha L_m}{(\psi_a^s)^2 + (\psi_b^s)^2}(\psi_a^s i_b^s - \psi_b^s i_a^s) = n_p y_1 + \frac{R_{rN}}{n_p y_3}(Jy_2 + T_{LN}) \tag{3.5.12}$$

The input-output linearisation feedback for system (3.5.7) if given by the following

$$\begin{pmatrix} u_a^s \\ u_b^s \end{pmatrix} = D^{-1}(x)\left[\begin{pmatrix} L_f^2\phi_1 \\ L_f^2\phi_2 \end{pmatrix} + \begin{pmatrix} v_a^s \\ v_b^s \end{pmatrix}\right] \tag{3.5.13}$$

Note that $v = (v_a, v_b)^T$ is the new input vector. It is now possible to make some transformations and substitutions (3.5.13) into the equations (3.5.7). The closed-loop dynamics become the y-coordinates:

$$\begin{aligned} \dot{y_1} &= y_2 \\ \dot{y_2} &= v_a \\ \dot{y_3} &= y_4 \\ \dot{y_4} &= v_b \\ \dot{y_5} &= n_p y_1 + \frac{R_{rN}}{n_p}\frac{1}{y_3}(Jy_2 + T_{LN}) \end{aligned} \tag{3.5.14}$$

In order to track the desired reference signals of $\omega_{ref}$ and $\psi_{ref}^2$ for the speed ($y_1 = \omega_r$) and the square of flux modulus ($y_3 = \psi_a^2 + \psi_b^2$), the input signals of $v_a$ and $v_b$ in the equation (3.5.13) can be designed as follows:

$$
\begin{aligned}
v_a &= -k_{a1}(y_1 - \omega_{ref}(t)) - k_{a2}(y_2 - \dot{\omega}_{ref}(t)) + \ddot{\omega}_{ref}(t) \\
&= -k_{a1}(\omega_r - \omega_{ref}(t)) - k_{a2}[\mu(\psi_a^s i_b^s - \psi_b^s i_a^s) \\
&\quad -\frac{T_{LN}}{J} - \dot{\omega}_{ref}(t)] + \ddot{\omega}_{ref}(t) \qquad (3.5.15) \\
v_b &= -k_{b1}(y_3 - |\psi|_{ref}^2) - k_{b2}(y_4 - |\dot{\psi}|_{ref}^2) + |\ddot{\omega}|_{ref}^2 \\
&= -k_{b1}((\psi_a^s)^2 + (\psi_b^s)^2 - |\psi|_{ref}^2) - k_{b2}[2\alpha(L_m(\psi_a^s i_a^s + \psi_b^s i_b^s) \\
&\quad -(\psi_a^s)^2 + (\psi_b^s)^2) - |\dot{\psi}|_{ref}^2] + |\ddot{\psi}|_{ref}^2 \qquad (3.5.16)
\end{aligned}
$$

where the constant design parameters $(k_{a1}, k_{a2})$, and $(k_{b1}, k_{b2})$ are to be determined to make the decoupled linear second-order systems asymptotically stable, which is:

$$
\begin{aligned}
\frac{d^2}{dt^2}(\omega_r - \omega_{ref}) &= -k_{a1}(\omega_r - \omega_{ref}) - k_{a2}\frac{d}{dt}(\omega_r - \omega_{ref}) \\
\frac{d^2}{dt^2}(|\psi|^2 - |\psi|_{ref}^2) &= -k_{b1}(|\psi|^2 - |\psi|_{ref}^2) - k_{b2}\frac{d}{dt}(|\psi|^2 \\
&\quad -|\psi|_{ref}^2) \qquad (3.5.17)
\end{aligned}
$$

The construction diagram by using feedback linearisation controller is shown in Figure 3.1.

## 3.6 Simulation and Analysis

Simulation studies are carried out based on Matlab/Simulink. Parameters of a induction motor in [51] were used and listed in the Table 3.1 as shown below.

The simulation test includes the following two scenarios: 1) start-up of the unloaded motor to reach the rated speed and rated rotor flux amplitude, and then speed regulation under rated flux magnitude. 2) speed regulation under a load torque which is unknown to the controller.

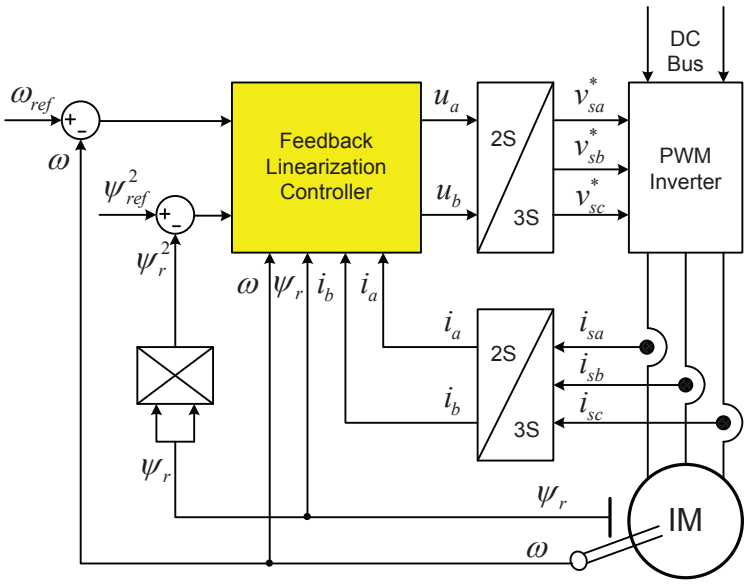


Figure 3.1: Diagram of the induction motor by using feedback linearisation controller

Table 3.1: Parameter of Induction Motor

| | | |
|---|---|---|
| $R_s = 0.18\Omega$ | $L_s = 0.0699H$ | $R_r = 0.15\Omega$ |
| $M = 0.068$H | $J_{rotor} = 0.0586Kgm^2$ | $T_r = \frac{L_r}{R_r} = 0.466$ |
| $L_r = 0.0699H$ | $\Gamma = \frac{M^2 R_r}{\Delta L_s L_r^2 + R_s/(\Delta L_s)}$ | $N_p = 1$ |
| $\alpha = \frac{R_r}{L_r} = 2.14592$ | $\beta = \frac{M}{\Delta L_s L_r} = 259.53223$ | $\mu = \frac{N_p M}{J L_r}$ |

### 3.6.1 Decoupled Dynamics Without External Disturbances

The speed regulation response are shown in Figure 3.2 and Figure 3.3, respectively. The flux is regulated to achieve a rated level $1.2Wb$ at 1s, the step change of the speed happens at 2s from 0 to $200rad/s$. At 5s, the speed reference rises from $200rad/s$ to a high speed range of $300rad/s$ at the same time the flux reference is reduced from $1.2Wb$ to $0.8Wb$ to avoid the high voltage based on the flux-weaken principle. The result show that both controllers can provide a satisfactory response. While the IOLC has a much smaller overshoot

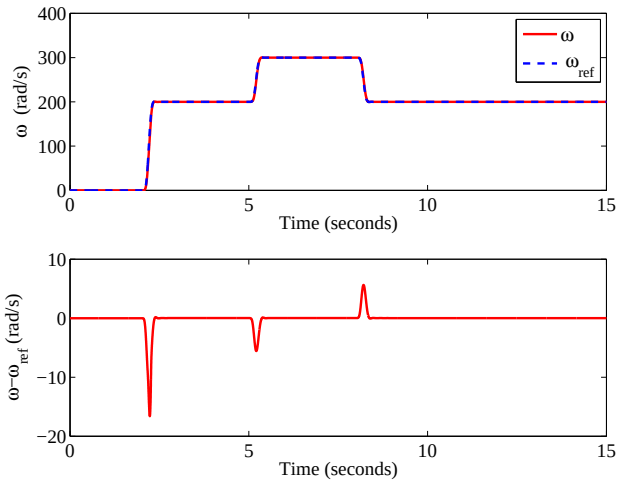


Figure 3.2: Speed regulation response without load by using FOC

of the speed response which is within the range of $\pm 5 rad/s$. In contrast to the FOC which is within the range of $\pm 20 rad/s$. Similarly, as shown in Figure 3.4 and Figure 3.5, the range of flux error in the FOC is larger than the IOLC. The control input signals $u_a$ and $u_b$ of the FOC and the IOLC are similar, as represented in Figure 3.6 and Figure 3.7.

### 3.6.2 Performance Under Unknown Load Torque

The unknown load torque is simulated to test performance of both the FOC and IOLC as represented by Figure 3.8. The load torque $T_L(t) = 50 + 5sin(2t)$ is simulated from 10s. Speed responses under unknown load conditions, are shown in Figures 3.9 and 3.10. This demonstrates that the FOC can not maintain the regulation of speed under an unknown load torque, whilst the IOLC can still maintain the zero regulation error. The response of flux for both controllers are not affected by the load variation, as shown in Figures 3.11 and 3.12. It should also be noted that the control input of both controllers are almost same.

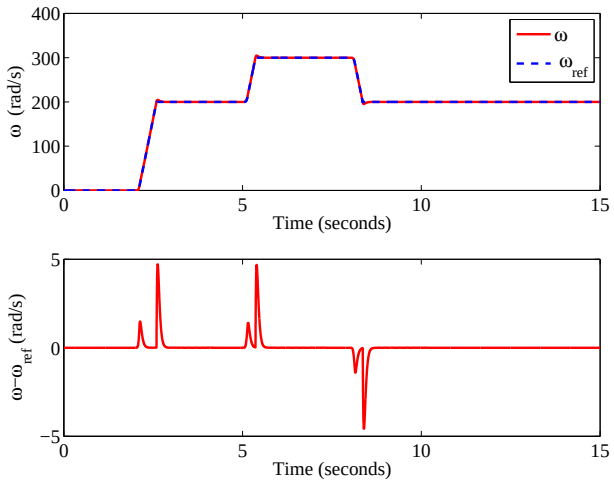


Figure 3.3: Speed regulation response without load by using IOLC

## 3.7 Summary

In this chapter, the feedback linearisation control has been applied to the control induction motor. After representing the induction motor in a convenient state space form, FOC has been re-investigated as a partial feedback linearisation control which can only achieve the partial decoupling of the dynamics of speed and flux. The input-output linearisation has been applied for control of induction motor, in which the dynamic of speed and flux can be fully decoupled. According to simulated results it can be found, that without external disturbances, the feedback linearisation control approach can provide an improved decoupled dynamic in comparison with VC. It should pointed out that both methods have a weak robustness against parameter uncertainties and un-modeled dynamics, which will be addressed in the following chapters.

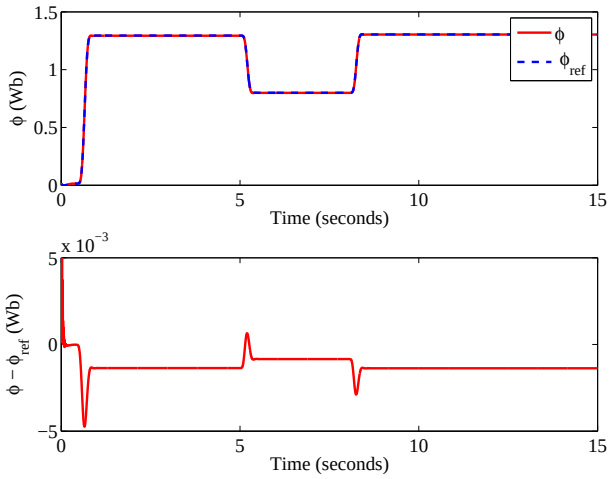


Figure 3.4: Flux response by using FOC

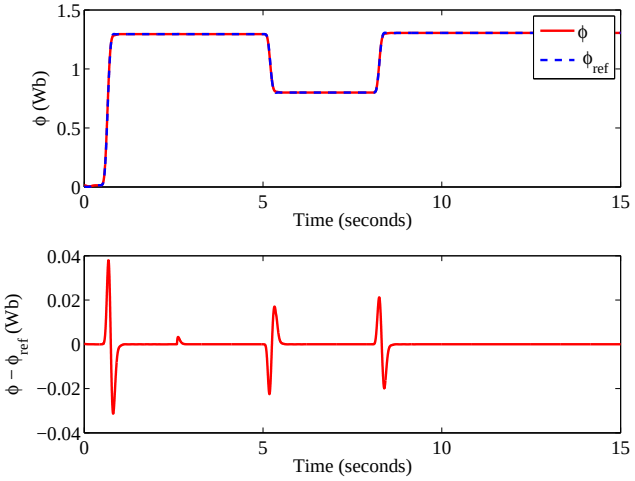


Figure 3.5: Flux response by using IOLC

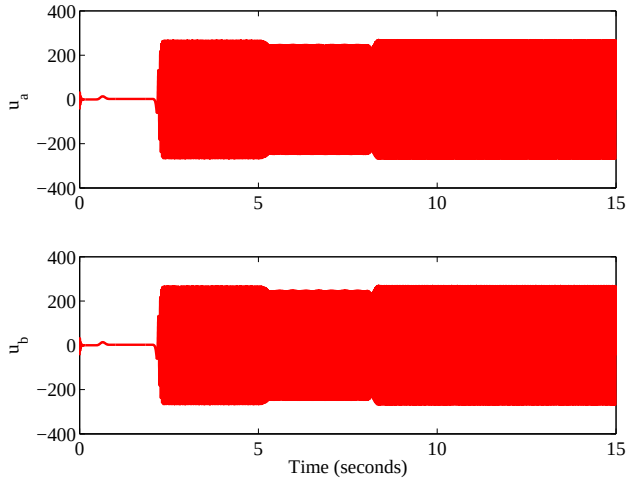


Figure 3.6: Control output of field-oriented control

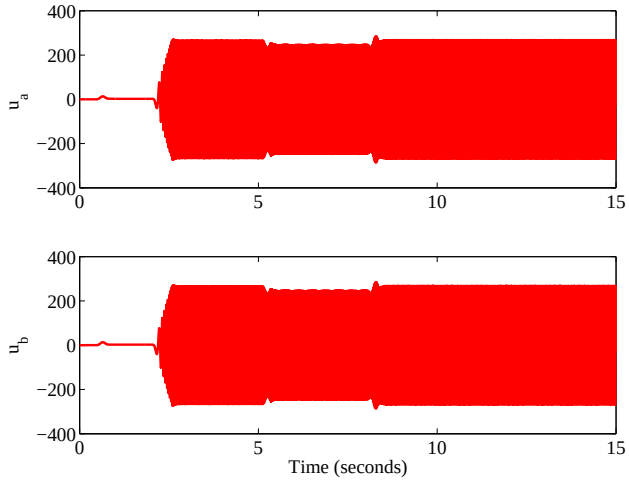


Figure 3.7: Control output of input-output linearisation control

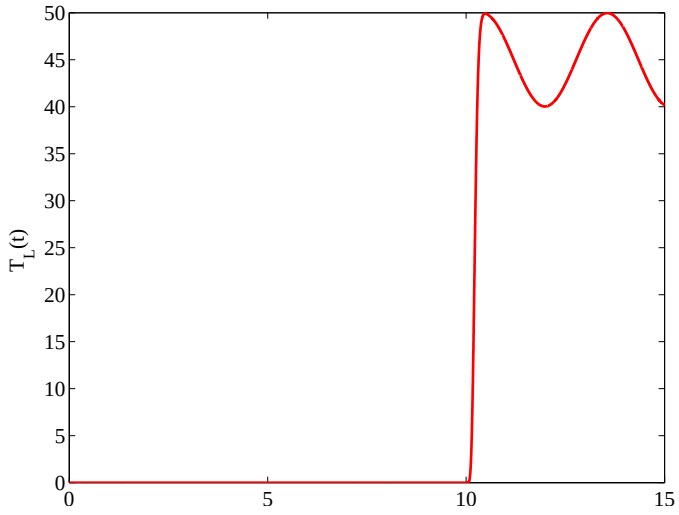


Figure 3.8: Unknown load torque from 10s

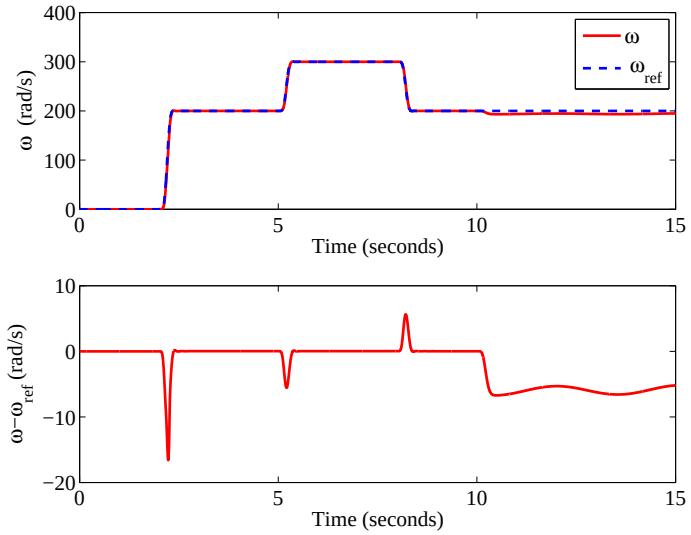


Figure 3.9: Speed response of FOC under load variation

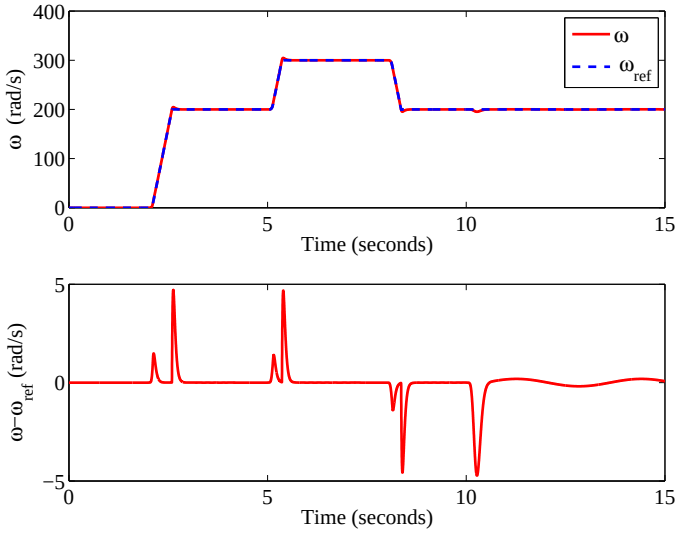


Figure 3.10: Speed response of IOLC under load variation

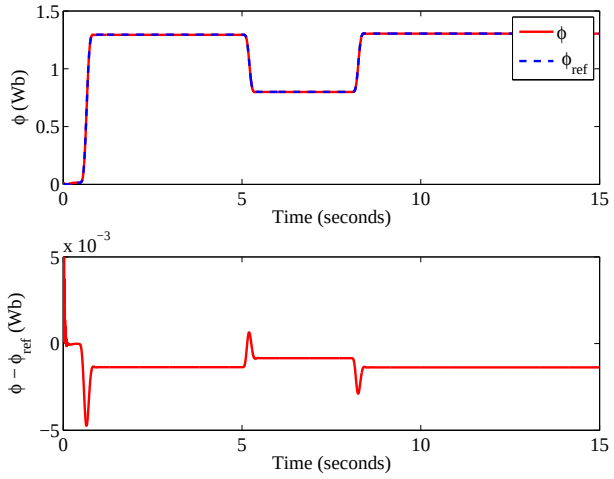


Figure 3.11: Flux response with load torque by using FOC

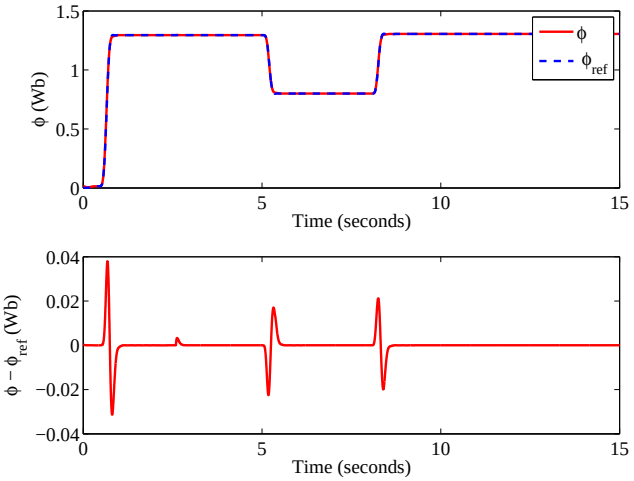


Figure 3.12: Flux response with load torque by using IOLC

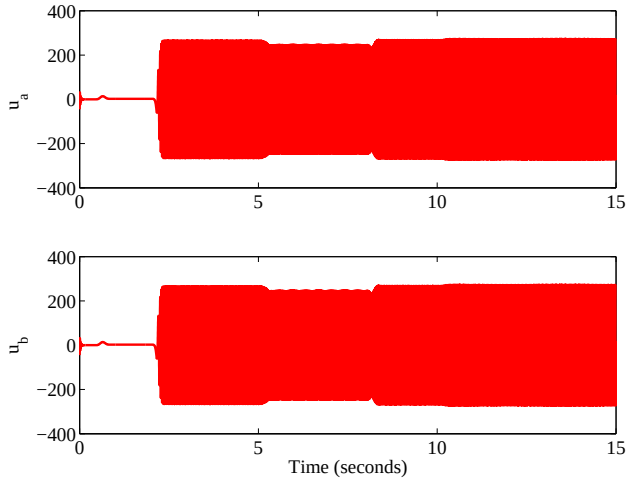


Figure 3.13: Input voltage signals $u_a$ & $u_b$ of FOC with load torque

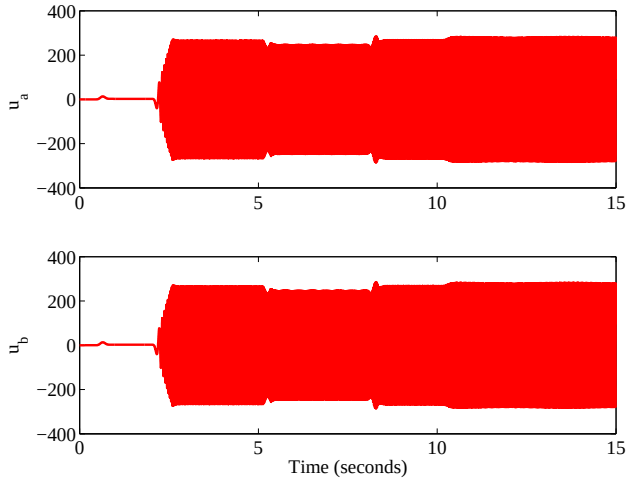


Figure 3.14: Input voltage signals $u_a$ & $u_b$ of IOLC with load torque

# Chapter 4

# Nonlinear Adaptive Control of Induction Motor: State Feedback

This chapter investigates a nonlinear adaptive control of an induction motor based on adaptive feedback linearisation and perturbation estimation. The induction motor is represented by two subsystems: a speed subsystem and a flux subsystem, in an input/output linearisation format at first. Two second-order high-gain perturbation observers are designed to estimate the real time perturbation term. Subsequently, a state feedback control has been derived by cancelling the real perturbation with the estimated one. Bounded and asymptotical tracking results are then obtained. A simulation based on MATLAB/Simulink is presented.

## 4.1 Introduction

The induction motor is a nonlinear system with unmeasured states (rotor currents and rotor flux) and time varying parameters (rotor resistance and load

torque). Further, over the past few decades, a number of nonlinear control techniques have been applied to the induction motor control [37][4]. One of the most significant techniques in this area is the VC which uses partial feedback linearisation and PI control. To improve VC, the input/output linearisation control based on differential geometric was proposed [37]. Both VC and IOLC require that all parameters and system nonlinear dynamics are known exactly. For this purpose, they have relatively complicated nonlinear calculation in the control algorithm.

To improve the robustness of VC and IOLC, nonlinear adaptive input/ouput linearising control of induction motor was investigated based on parameters updated by law and state feedback [51][37][4]. Those designs always treat uncertain parameters, including load torque, as unknown constants. This assumption works well for rotor resistance $R_r$ as it is a slow time-varying parameter. Even so it is not suitable for load torque $T_L$ which varies rapidly in some high performance applications. With good robustness to a class of disturbances, parameters uncertainties, sliding mode control ideas have been applied to induction motor with time-varying uncertainties [104][113].

A robust adaptive control based on perturbation observer was proposed and applied to the power systems [117][118][119]. The original idea of the perturbation estimation stems from the Time Delay Control [125][112], which involved the time-delay values of control input and the derivatives of state variables. In addition, the previous time steps are used to cancel the nominal nonlinear dynamics and uncertainties. The disturbance auto-rejection control proposed a similar idea based on nonlinear disturbance observer [120] and has been applied to the induction motor control [127]. However, the proposed nonlinear extended-state-observer make the stability analysis of the closed-loop controller/observer system be very difficult.

In this chapter, a novel nonlinear adaptive control of the induction motor is designed based on the decentralised control via high gain perturbation observer

(HGPO) [119]. The induction motor is represented as two coupled subsystems, a rotor speed subsystem and a rotor flux subsystem, respectively. The lumped term of system nonlinearities, uncertainties, and interactions between subsystems, are defined as system perturbation terms and represented as a *fictitious state* in the extended-order state equations. Those perturbations are estimated by designing two second-order high-gain perturbation observers and two third-order state and perturbation observers. Robust adaptive feedback linearising control are obtained based on the cancelation of perturbation. The proposed control does not require the accurate model of the induction motor and can deal with all kinds of time-varying uncertainties. Simulation studies are given with the comparison against input/ouput linearising control.

## 4.2 Nonlinear State Feedback Adaptive Control Methodology

This section briefly review the nonlinear adaptive control (NAC) proposed in [118] and [119]. The NAC includes three steps: input-output linearisation representation of nonlinear system, defining of perturbation terms; designing perturbation observer; and the design of linearising control using the estimated perturbation to compensate the real perturbation.

A nonlinear system in a controllable canonical form is represented as follows:

$$\begin{cases} \dot{x} &= Ax + B\left(a(x) + b(x)u\right) \\ y &= x_n, \end{cases} \tag{4.2.1}$$

where $x_i$, $i = 1, 2, \cdots, n$ are the state variables, and $x = [x_1, x_2, \cdots, x_n]^T \in \mathcal{R}^n$ is the state vector; $u \in \mathcal{R}$ the control input; $y \in \mathcal{R}$ the system output; $a(x) : \mathcal{R}^n \to \mathcal{R}$ and $b(x) : \mathcal{R}^n \to \mathcal{R}$ are $C^\infty$ unknown smooth functions, defined on

$\mathcal{R}^n$. The $n \times n$ matrix $A$ and the $n \times 1$ matrix $B$ are given by

$$A = \begin{bmatrix} 0 & 1 & 0 & \cdots & 0 \\ 0 & 0 & 1 & \cdots & 0 \\ \vdots & & & & \vdots \\ 0 & 0 & 0 & \cdots & 1 \\ 0 & 0 & 0 & \cdots & 0 \end{bmatrix}, \qquad B = \begin{bmatrix} 0 \\ 0 \\ \vdots \\ 0 \\ 1 \end{bmatrix}. \tag{4.2.2}$$

The main source of the system (4.2.1) is the normal form of a fully linearisable nonlinear system which has a relative degree $r = n$. In the design of a nonlinear controller using the feedback linearisation technique, the most commonly used control structure is

$$u = [-a(x) + v]/b(x), \tag{4.2.3}$$

where $v$ is a new control variable for the equivalent linear system. Such a controller works based on an exact cancellation of nonlinear terms $a(x)$ and $b(x)$. However, the exact cancellation is almost impossible for several reasons, such as model simplification, parameter uncertainties and computational errors. When nonlinear functions $a(x)$ and $b(x)$ are unknown or with uncertainties, many adaptive control schemes or robust control schemes have been developed.

### 4.2.1 Definition of Perturbation

With the help of system (4.2.1), after assuming the known part of nonlinear functions $a(x)$ and $b(x)$ are zero for the simplification of formulations, the system perturbation is defined as:

$$\Psi(x, u, t) = a(x) + (b(x) - b_0)u, \tag{4.2.4}$$

then the last equation of system (4.2.1) can be rewritten as

$$\dot{x}_n = \Psi(x, u, t) + b_0 u, \tag{4.2.5}$$

where $b_0$ is a constant control gain which will be decided later.

If $\dot{x}_n$ can be estimated, then the perturbation can be obtained by

$$\Psi(x, u, t) = \dot{x}_n - b_0 u. \tag{4.2.6}$$

The original idea of this kind of perturbation estimation stems from the time delay control [111][112], in which the time-delayed values of control input and the derivatives of state variables, at the previous time steps, are used to cancel the nominal nonlinear dynamics and uncertainties. A similar method has also been proposed for disturbance auto-rejected control [120]. In the control scheme, the perturbation is estimated by an extended-order nonlinear observer based on the track-differentiator.

In the time delay control, the derivatives of state variables are always calculated by the numerical differential method, such as the backward difference algorithm. It is well known that the numerical differentiator will magnify the measurement noise. In the past years, high gain observers have played an important role in the design of a nonlinear output feedback controller for nonlinear systems. They are mainly used to estimate the derivatives of the output. In this section, an extended-order high gain observer is designed to estimate the system states and perturbation.

Define a *fictitious state* to represent the system perturbation, that is, $x_{n+1} = \Psi(x, u, t)$, the state equation of system (4.2.1) may be represented as

$$\begin{cases} \dot{x}_1 &= x_2 \\ & \cdots \\ \dot{x}_n &= x_{n+1} + b_0 u \\ \dot{x}_{n+1} &= \dot{\Psi}(\cdot) \\ y &= x_{n+1}, \end{cases} \tag{4.2.7}$$

where $\dot{\Psi}(\cdot)$ is the derivative of $\Psi(\cdot)$.

Then system (4.2.7) can be rewritten in a matrix form:

$$\begin{cases} \dot{x}_e &= A_1 x_e + B_3 u + B_1 \dot{\Psi}(\cdot) \\ y &= C_1 x_e, \end{cases} \tag{4.2.8}$$

where

$$x_e = \begin{bmatrix} x_1 \\ x_2 \\ \vdots \\ x_n \\ x_{n+1} \end{bmatrix}, \quad A_1 = \begin{bmatrix} 0 & 1 & \cdots & \cdots & 0 \\ 0 & 0 & 1 & \cdots & 0 \\ \vdots & & & & \vdots \\ 0 & 0 & 0 & \cdots & 1 \\ 0 & 0 & 0 & \cdots & 0 \end{bmatrix}_{(n+1)\times(n+1)},$$

$$B_3 = \begin{bmatrix} 0 \\ 0 \\ \vdots \\ 1 \\ 0 \end{bmatrix}_{(n+1)\times 1}, \quad B_1 = \begin{bmatrix} 0 \\ 0 \\ \vdots \\ 0 \\ 1 \end{bmatrix}_{(n+1)\times 1}, \text{ and } C_1 = \begin{bmatrix} 1 \\ 0 \\ \vdots \\ 0 \\ 0 \end{bmatrix}^T_{(n+1)\times 1}.$$

The following assumptions are made on system (4.2.1).

**A4.1** $b_0$ is chosen to satisfy: $|b(x)/b_0 - 1| \leq \theta < 1$, where $\theta$ is a positive constant.

**A4.2** The function $\Psi(x,u,t) : \mathcal{R}^n \times \mathcal{R} \times \mathcal{R}^+ \to \mathcal{R}$ and $\dot{\Psi}(x,u,t) : \mathcal{R}^n \times \mathcal{R} \times \mathcal{R}^+ \to \mathcal{R}$ are locally Lipschitz in their arguments over the domain of interest and are globally bounded in $x$:

$$|\Psi(x,u,t)| \leq \gamma_1, \quad |\dot{\Psi}(x,u,t)| \leq \gamma_2,$$

where $\gamma_1$ and $\gamma_2$ are positive constants. In addition, $\Psi(0,0,0) = 0$ and $\dot{\Psi}(0,0,0) = 0$.

The assumptions of $A4.2$ guarantees that the origin is an equilibrium point of the open-loop system. The control problem is described as follows. Under

assumptions $A4.1 \sim A4.2$, $a(x)$ and $b(x)$ are unknown continuous functions, and all state variables are available, find the state feedback control $u$, such that the origin of system (4.2.1) is stable.

In this chapter, all the system states are assumed to be available and a high gain perturbation observer is designed to track the last system state and estimate the perturbation. The output feedback case is investigated in the next chapter. Only one state is available a high gain state. Further, the perturbation observer is investigated to obtain the estimate of the system states. Consequently, the perturbation and another observer is designed for flux estimation.

### 4.2.2 High Gain Perturbation Observer (HGPO)

Assuming that all states $x_n$, $i = 1, \cdots, n$ are available and taking $x_n$ as a measurement, a high gain perturbation observer (also called track differentiator) is designed as

$$\begin{cases} \dot{\hat{x}}_n &= \hat{x}_{n+1} + h_1(x_n - \hat{x}_n) + b_0 u \\ \dot{\hat{x}}_{n+1} &= h_2(x_n - \hat{x}_n), \end{cases} \tag{4.2.9}$$

where $h_1$ and $h_2$ are gains of the high gain observer. Throughout this section, $\tilde{x}_i = x_i - \hat{x}_i$ refers to the estimation error of $x_i$ whereas $\hat{x}_i$ symbolises the estimated quantity of $x_i$. The estimation error $\tilde{x}_i = x_i - \hat{x}_i$, $i = n, n+1$, satisfies the equation:

$$\begin{cases} \dot{\tilde{x}}_n &= -h_1\tilde{x}_n + \tilde{x}_{n+1} \\ \dot{\tilde{x}}_{n+1} &= -h_2\tilde{x}_n + \dot{\Psi}(\cdot). \end{cases} \tag{4.2.10}$$

The above error dynamics can be represented in a matrix form as:

$$\dot{\tilde{x}}_{\text{po}} = A_{\text{po}}x_{\text{po}} + B_{\text{po}}\dot{\Psi}(\cdot), \tag{4.2.11}$$

where $\tilde{x}_{\text{po}} = [\tilde{x}_n,\ \tilde{x}_{n+1}]^T$, and

$$A_{\text{po}} = \begin{bmatrix} -h_1 & 1 \\ -h_2 & 0 \end{bmatrix}, B_{\text{po}} = \begin{bmatrix} 0 \\ 1 \end{bmatrix},$$

where $A_{\text{po}}$ is a Hurwitz matrix.

### Analysis of estimation error

As in any asymptotic observer, the observer gain $H_{\text{po}} = [h_1, h_2]^T$ should be chosen to achieve the asymptotical error convergence, that is:

$$\lim_{t\to\infty} \tilde{x}_{\text{po}} = 0.$$

In the absence of the perturbation $\dot{\Psi}(\cdot)$, the asymptotic error convergence is achieved by choosing the observer gain such that the matrix $A_{\text{po}}$ is a Hurwitz matrix, e.g., its eigenvalues have negative real parts. For this second-order system, $A_{\text{po}}$ is Hurwitzian for any positive constants $h_1$ and $h_2$.

In the presence of $\Psi(\cdot)$, the observer gain needeeds to be determined with the additional goal of rejecting the effect of the perturbation $\dot{\Psi}(\cdot)$ on the estimation error $\tilde{x}_{\text{po}}$. This could ideally be achieved, for any perturbation $\dot{\Psi}(\cdot)$, if the transfer function from $\dot{\Psi}(\cdot)$ to $\tilde{x}_{\text{po}}$

$$H_{\text{po}}(s) = \frac{1}{s^2 + h_1 s + h_2} \begin{bmatrix} 1 \\ s + h_1 \end{bmatrix}$$

is identically zero.

By calculating the $\|H_{\text{po}}\|_\infty$, it can be seen that the norm can be arbitrarily small by choosing $h_2 \gg h_1 \gg 1$. In particular, taking

$$h_1 = \frac{\alpha_1}{\epsilon}, \quad h_2 = \frac{\alpha_2}{\epsilon^2} \tag{4.2.12}$$

for some positive constants $\alpha_1$, $\alpha_2$, and $\epsilon$, $\epsilon \ll 1$. It can be shown that

$$H_{\text{po}}(s) = \frac{\epsilon}{(\epsilon s)^2 + \alpha_1 \epsilon s + \alpha_2} \begin{bmatrix} \epsilon \\ \epsilon s + \alpha_1 \end{bmatrix}.$$

Hence, $\lim_{\epsilon\to 0} H_{\text{po}}(s) = 0$. While an infinite gain is not possible in practice, the observer gain can be determined such that the estimation error $\tilde{x}_{\text{po}}$ will converge exponentially to a small neighbourhood which is arbitrarily close to origin.

**Perturbation observer represented in singular perturbation form**

The perturbation rejection property of the high gain observer (4.2.12) can also be seen in the time domain by representing the error equation (4.2.10) in the singularly perturbed form. To that end, the scaled estimation errors are defined as:

$$\eta_1 = \frac{\tilde{x}_n}{\epsilon}, \quad \eta_2 = \tilde{x}_{n+1}. \tag{4.2.13}$$

The newly defined variables satisfy the singularly perturbed equation

$$\epsilon\dot{\eta} = A_2\eta + \epsilon B_2\dot{\Psi}(\cdot), \tag{4.2.14}$$

where

$$A_2 = \begin{bmatrix} -\alpha_1 & 1 \\ -\alpha_2 & 0 \end{bmatrix}, \qquad B_2 = \begin{bmatrix} 0 \\ 1 \end{bmatrix},$$

and the positive constants $\alpha_1$ and $\alpha_2$ are chosen such that $A_2$ is a Hurwitz matrix.

This equation shows clearly that reducing $\epsilon$ diminishes the effect of the perturbation $\dot{\Psi}(\cdot)$. It also shows that, for small $\epsilon$, the dynamics of the estimation error will be much faster than that of $x$. However, the change of variables (4.2.13) may cause the initial condition $\eta_1(0)$ to be of order $O(1/\epsilon)$, even when $\tilde{x}_n(0)$ is of order of $O(1)$. With the initial condition, the equation in (4.2.14) will contain a term of the form $(1/\epsilon)e^{-at/\epsilon}$ for the constant $a > 0$. While this exponential mode decays rapidly, it exhibits an impulse-like behaviour where the transient peaks to $O(1/\epsilon)$ value before it decays rapidly towards zero. In fact, the function $(1/\epsilon)e^{-at/\epsilon}$ approaches an impulse function as $\epsilon$ tends to zero. This behaviour is known as the " *peaking phenomenon*". It is important to realise that the peaking phenomenon is not a consequence of using the change of variables (4.2.13) to represent the error dynamics in the singularly perturbed form. It is an intrinsic feature for any high gain observer design that it rejects the effect of the perturbation $\dot{\Psi}$ in (4.2.10). This includes any design with $h_2 \gg h_1 \gg 1$.

System (4.2.9) is basically an approximate differentiator. This can be easily seen in the special case when the perturbation $\dot{\Psi}(\cdot)$ and control $u$ are chosen to be zero. Thus, the observer is linear. For system (4.2.9) the transfer function from $y = x_n$ to $\hat{x}_{\text{po}}$ is given by:

$$\frac{\alpha_2}{(\epsilon s)^2 + \alpha_1 \epsilon s + \alpha_2} \begin{bmatrix} 1 + (\epsilon\alpha_1/\alpha_2)s \\ s \end{bmatrix} \rightarrow \begin{bmatrix} 1 \\ s \end{bmatrix} \quad \text{as} \quad \epsilon \rightarrow 0.$$

Thus, on a compact frequency internal, the high gain observer approximates $x_{n+1} = \dot{x}_n$ for the sufficiently small $\epsilon$.

### 4.2.3 Nonlinear Adaptive Control Law

The estimate of perturbation $\hat{x}_{n+1}$ is used to realise the feedback linearisation of the nonlinear system (4.2.1). After the unknown system nonlinearities and uncertainties are cancelled by the perturbation estimate, a linear state feedback controller is designed for the equivalent linear system. The complete control is designed as follows:

$$u = \frac{v - \hat{x}_{n+1}}{b_0} \tag{4.2.15}$$

$$v = -Kx \tag{4.2.16}$$

where $K = [k_1, k_2, \cdots, k_n]^T$ is the linear feedback controller gains, which make the matrix $A_0 = A - BK$ be Hurwitzian.

The analysis of the closed-loop system under the perturbation observer and the controller is given as follows. The system is represented in the singularly perturbed form:

$$\dot{x} = A_0 x + B\eta_2, \tag{4.2.17}$$

$$\epsilon\dot{\eta} = A_2\eta + \epsilon B_2 \dot{\Psi}(\cdot). \tag{4.2.18}$$

The system represented by equations (4.2.17) and (4.2.18) is a standard singular perturbed system, and $\eta = 0$ is the unique solution of equation (4.2.18)

when $\epsilon = 0$. The reduced system, obtained by substituting $\eta = 0$ in equation (4.2.17), is as:

$$\dot{x} = A_0 x. \tag{4.2.19}$$

The boundary-layer system, obtained by applying the change of time variable $\tau = t/\epsilon$ to equation (4.2.18) and setting $\epsilon = 0$, is given by

$$\frac{d\eta}{d\tau} = A_2 \eta. \tag{4.2.20}$$

## 4.3 Nonlinear State Feedback Adaptive Controller of Induction Motor

### 4.3.1 Input/Output Representation and Perturbation Definition

The derivation process presented in the following is based on the model given in Chapter Three. The outputs to be controlled are rotor speed $y_1 = \phi_1(x) = \omega_r$ and square of the rotor flux modulus $y_2 = \phi_2(x) = (\psi_a^s)^2 + (\psi_b^s)^2$, where functions $\phi_1(x)$ and $\phi_2(x)$ are smooth function of states. Let $z_{11} = y_1$, $z_{12} = \dot{y}_1$, $z_{21} = y_2$, and $z_{22} = \dot{y}_2$ be state variables of two interconnected system. Considering the system model (3.3.19) with time-varying parameters $T_L(t)$ and $\alpha(t)(R_r(t))$ (i. e. $p_1 \neq 0$ and $p_2 \neq 0$), the input/ouput decoupling of (3.3.19) is obtained as follows:

$$\begin{aligned}
\dot{z}_{11} &= L_f\phi_1 + p_1 L_{f_1}\phi_1 \\
\dot{z}_{12} &= L_f^2\phi_1 + p_2 L_{f_2} L_f \phi_1 + \tfrac{dp_1}{dt} L_{f_1}\phi_1 \\
&\quad + L_{g_a} L_f \phi_1 u_a + L_{g_b} L_f \phi_1 u_b \\
\dot{z}_{21} &= L_f\phi_2 + p_2 L_{f_2}\phi_2 \\
\dot{z}_{22} &= L_f^2\phi_2 + p_2 L_{f_2} L_f \phi_2 + \tfrac{dp_2}{dt} L_{f_2}\phi_2 \\
&\quad + p_2^2 L_{f_2}^2 \phi_2 + (L_{g_a} L_f \phi_2 + p_2 L_{g_a} L_{f_2}\phi_2) u_a \\
&\quad + p_2 L_f L_{f_2}\phi_2 + (L_{g_b} L_f \phi_2 + p_2 L_{g_b} L_{f_2}\phi_2) u_b
\end{aligned} \tag{4.3.1}$$

where:

$$\begin{aligned}
L_f\phi_1 &= \mu(\psi_a i_b - \psi_b i_a) - \tfrac{T_{LN}}{J} \\
L_f^2\phi_1 &= -\mu\beta n_p\omega_r(\psi_a^2+\psi_b^2) - \mu n_p\omega_r(\psi_a i_a + \psi_b i_b) \\
&\quad -\mu(\alpha_N+\gamma_N)(\psi_a i_b - \psi_b i_a) \\
L_f\phi_2 &= -2\alpha_N(\psi_a^2+\psi_b^2) + 2\alpha_N L_m(\psi_a i_a + \psi_b i_b) \\
L_f^2\phi_2 &= (4\alpha_N^2 + 2\alpha_N^2\beta L_m)(\psi_a^2+\psi_b^2) + 2\alpha_N^2 L_m^2(i_a^2+i_b^2) \\
&\quad -(6\alpha_N^2 L_m + 2\alpha_N\gamma_N L_m)(\psi_a i_a + \psi_b i_b) \\
&\quad +2\alpha_N L_m n_p\omega_r(\psi_a i_b - \psi_b i_a). \\
L_{f_1}\phi_1 &= -\tfrac{1}{J} \\
L_{f_2}L_f\phi_1 &= -\mu(1+L_m\beta)(\psi_a i_b - \psi_b i_a) \\
L_{f_2}\phi_2 &= 2L_m(\psi_a i_a + \psi_b i_b) - 2(\psi_a^2+\psi_b^2) \\
L_f L_{f_2}\phi_2 &= 2\alpha_N(2+L_m\beta)(\psi_a^2+\psi_b^2) + 2\alpha_N L_m^2(i_a^2+i_b^2) \\
&\quad -2L_m(\gamma_N+3\alpha_N)(\psi_a i_a + \psi_b i_b) \\
&\quad +2N_p L_m\omega_r(\psi_a i_b - \psi_b i_a) \\
L_{f_2}^2\phi_2 &= (4+2L_m\beta)(\psi_a^2+\psi_b^2) + 2L_m^2(i_a^2+i_b^2) \\
&\quad -2L_m(3+L_m\beta)(\psi_a i_a + \psi_b i_b) \\
L_{f_2}L_f\phi_2 &= R_{rN}L_{f_2}^2\phi_2 \\
&= 2\alpha_N(2+L_m\beta)(\psi_a^2+\psi_b^2) + 2\alpha_N L_m^2(i_a^2+i_b^2) \\
&\quad -2\alpha_N L_m(3+L_m\beta)(\psi_a i_a + \psi_b i_b) \\
L_{g_a}L_{f_2}\phi_2 &= 2\beta L_r\psi_a \\
L_{g_b}L_{f_2}\phi_2 &= 2\beta L_r\psi_b
\end{aligned} \tag{4.3.2}$$

and the Lie derivatives are used in the Reference book of [128].

The second and fourth equation in system (4.3.1) can be rewritten as:

$$\begin{pmatrix} \dot{z}_{12} \\ \dot{z}_{22} \end{pmatrix} = \begin{pmatrix} L_f^2\phi_1 \\ L_f^2\phi_2 \end{pmatrix} + D(x)\begin{pmatrix} u_a \\ u_b \end{pmatrix} + \begin{pmatrix} \triangle_1 \\ \triangle_2 \end{pmatrix} \tag{4.3.3}$$

$$\begin{pmatrix} \triangle_1 \\ \triangle_2 \end{pmatrix} = \begin{pmatrix} p_2 L_{f_2}L_f\phi_1 + \frac{dp_1}{dt}L_{f_1}\phi_1 \\ p_2 L_{f_2}L_f\phi_2 + p_2 L_f L_{f_2}\phi_2 + p_2^2 L_{f_2}^2\phi_2 + \frac{dp_2}{dt}L_{f_2}\phi_2 \end{pmatrix} + \triangle D(x)\begin{pmatrix} u_a \\ u_b \end{pmatrix} \tag{4.3.4}$$

$$D(x) = \begin{bmatrix} L_{g_a}L_{f_1}\phi_1 & L_{g_b}L_{f_1}\phi_1 \\ L_{g_a}L_{f_2}\phi_2 & L_{g_b}L_{f_2}\phi_2 \end{bmatrix}, \tag{4.3.5}$$

$$\triangle D(x) = p_2 \begin{bmatrix} 0 & 0 \\ L_{g_a}L_{f_2}\phi_2 & L_{g_b}L_{f_2}\phi_2 \end{bmatrix} \tag{4.3.6}$$

where $D(x)$ and $\triangle D(x)$ are the constant and uncertain control gain matrix. $\triangle_1$ and $\triangle_2$ are combined uncertainties which include both the parameters derivation $(p_1, p_2)$ and their time dynamics $(\frac{dp_1}{dt}, \frac{dp_2}{dt})$. $D(x)$ is nonsingular for $\psi_a^2 + \psi_b^2 > 0$.

All system nonlinearities are assumed to be unknown and included in the perturbation term. As a result, the proposed control algorithm does not require the detailed model of the induction motor and the complex calculation as in FOC and IOLC. Let

$$\Psi_i(x, p_1, p_2, t) = \triangle_i + L_f^2\phi_i \tag{4.3.7}$$

and introduce a *fictitious state* to represent perturbation term: $z_{i3} = \Psi_i$. The extended-order model of the induction motor is given as follows:

$$\begin{cases} \dot{z}_{i1} = z_{i2} \\ \dot{z}_{i2} = z_{i3} + D_{i1}u_a + D_{i2}u_b \\ \dot{z}_{i3} = \dot{\Psi}_i \end{cases} \tag{4.3.8}$$

where $i = 1, 2$, $D_{ij}$ is known control gain as (4.3.5), $\dot{\Psi}_i$ is derivative of perturbation.

**Remark 1.** *From assumption A2, equations (4.3.4 and equations (4.3.7), and with a continuous control law, we know that all of their components are $c^\infty$ functions with bounded derivatives, thus the perturbation term $\Psi_i(\cdot)$ and its derivative $\dot{\Psi}_i(\cdot)$ are bounded over the domain of interest. In addition, $\Psi_i(0) = 0$ and $\dot{\Psi}_i(0) = 0$, i=1,2.*

### 4.3.2 Input/Output Linearising Control

Under the assumption that $T_L$ and $\alpha$ are known nominal value $T_{LN}$ and $\alpha_N$, i. e. $\triangle_1 = 0$ and $\triangle_2 = 0$, and all nonlinearities are exact known, the IOLC for system (4.3.1) is given by:

$$\begin{pmatrix} u_a \\ u_b \end{pmatrix} = D^{-1}(x) \left[ \begin{pmatrix} -L_f^2\phi_1 \\ -L_f^2\phi_2 \end{pmatrix} + \begin{pmatrix} v_a \\ v_b \end{pmatrix} \right] \tag{4.3.9}$$

$$\begin{aligned} v_a &= -k_{11}z_{11} - k_{12}z_{12} + v_{a_{ref}} \\ v_b &= -k_{21}z_{21} - k_{22}z_{22} + v_{b_{ref}} \end{aligned} \tag{4.3.10}$$

where $v_a$ and $v_b$ are the controls for two linearised sub-systems, $v_{a_{ref}}$ and $v_{b_{ref}}$ are the control for the reference model

$$\begin{aligned} v_{a_{\mathrm{ref}}} &= k_{11}y_{1_{\mathrm{ref}}}(t) + k_{12}\dot{y}_{1_{\mathrm{ref}}}(t) + \ddot{y}_{1_{\mathrm{ref}}}(t) \\ v_{b_{\mathrm{ref}}} &= k_{21}y_{2_{\mathrm{ref}}}(t) + k_{22}\dot{y}_{2_{\mathrm{ref}}}(t) + \ddot{y}_{2_{\mathrm{ref}}}(t) \end{aligned} \tag{4.3.11}$$

and control parameters $k_{ij}$, $i, j = 1, 2$, are chosen to make

$$A_{i0} = \begin{bmatrix} 0 & 1 \\ -k_{i1} & -k_{i2} \end{bmatrix}, \qquad i = 1, 2 \tag{4.3.12}$$

be a Hurwitzian matrix.

Let $e_{i1} = z_{i1} - y_{iref}$, $e_{i2} = z_{i2} - \dot{y}_{iref}$, and $e_i = [e_{i1} \quad e_{i2}]^T$ be the state variables of the track error system, then from system (4.3.1) and control law of (4.3.9), (4.3.10), and (4.3.11), the track error dynamic is given by:

$$\dot{e}_i = A_{i0}e_i + B_{i0}\triangle_i, \quad i = 1, 2. \tag{4.3.13}$$

where $B_{i0} = [0 \quad 1]^T$. With the stable matrixes $A_{i0}$, it is reported that system (4.3.13) can handle a certain format of uncertainties [128].

### 4.3.3 State Feedback with High Gain Perturbation Observer

This section will design two second-order perturbation observers under the assumption that all sub-system states are available. Taking the second state

$z_{i2}$ as input. Two high gain perturbation observers (HGPOs) are designed as:

$$\begin{cases} \dot{\hat{z}}_{i2} &= \hat{z}_{i3} + h_{i1}(z_{i2} - \hat{z}_{i2}) + D_{i1}u_a + D_{i2}u_b \\ \dot{\hat{z}}_{i3} &= h_{i2}(z_{i2} - \hat{z}_{i2}), \end{cases} \tag{4.3.14}$$

where $i = 1, 2$ for two HGPOs, $h_{ij}$, $i, j = 1, 2$ are gains of the high gain observers. Throughout this Chapter, $\tilde{z}_i = z_i - \hat{z}_i$ refers to the estimate error of $z_i$ whereas $\hat{z}_i$ represents the estimate of $z_i$.

From system (4.3.8) and (4.3.14), the error dynamics of (4.3.14) becomes:

$$\begin{cases} \dot{\tilde{z}}_{i2} &= \tilde{z}_{i3} - h_{i1}\tilde{z}_{i2} \\ \dot{\tilde{z}}_{i3} &= -h_{i2}\tilde{z}_{i2} + \dot{\Psi}_i, \end{cases} \tag{4.3.15}$$

Let $h_{i1} = \frac{\alpha_{i1}}{\epsilon_i}$,$h_{i2} = \frac{\alpha_{i2}}{\epsilon_i^2}$ observer gain, and $\eta_{i1} = \frac{\tilde{z}_{i2}}{\epsilon_i}$,$\eta_{i2} = \tilde{z}_{i3}$ be the scaled estimation errors, system (4.3.15) can be represented in a singularly perturbed form as:

$$\epsilon_i \dot{\eta}_i = A_i \eta_i + \epsilon_i B_i \dot{\Psi}_i, \tag{4.3.16}$$

where $\eta_i = [\eta_{i1}\ \eta_{i2}]^T$,

$$A_i = \begin{bmatrix} -\alpha_{i1} & 1 \\ -\alpha_{i2} & 0 \end{bmatrix}, \qquad B_i = \begin{bmatrix} 0 \\ 1 \end{bmatrix}.$$

The positive constants $\alpha_{i1}$ and $\alpha_{i2}$ are chosen such that $A_i$ is a Hurwitzian matrix, and $\epsilon_i$, $0 < \epsilon_i \leq 1$, is a small positive parameter to be specified.

By using the estimate of perturbation $\hat{z}_{13}$ and $\hat{z}_{23}$ to cancel the nonlinearities and uncertainties, a robust adaptive control law is obtained as:

$$\begin{pmatrix} u_a \\ u_b \end{pmatrix} = D^{-1}(x) \left[ \begin{pmatrix} -\hat{z}_{13} \\ -\hat{z}_{23} \end{pmatrix} + \begin{pmatrix} v_a \\ v_b \end{pmatrix} \right] \tag{4.3.17}$$

where $D(x)$ is defined in (4.3.5) and based on nominal value of $R_{rN}$ and measurement of states $(\psi_a, \psi_b)$, and $(v_a, v_b)$ are controls defined in (4.3.10). To prevent the peak phenomena caused by the high gain observer, we should saturate both observer outputs $(\hat{z}_{13}, \hat{z}_{13})$ and control $(u_a, u_b)$ outside their operation range [128].

Substitute the control law in (4.3.17) and (4.3.10) into the system model of (4.3.8), the track error dynamic is given by:

$$\dot{e}_i = A_{i0}e_i + B_{i0}\tilde{z}_{i3} \tag{4.3.18}$$

with $A_{i0}$ and $B_{i0}$ as defined in (4.3.12) and (4.3.13). To compare the system in (4.3.13) with (4.3.18), let define $\Psi_i = \triangle_i$ and include nonlinearities, it can find that the driving uncertain term of track error dynamics is reduced from perturbation term $\Psi_i$ to its estimate error $\tilde{\Psi}_i$. This achieves an improved track performance with same controller gain in $(v_a, v_b)$ in (4.3.10) after designing the observer to make $|\tilde{\Psi}_i|_{sup} < |\Psi_i|_{sup}$.

The diagram of nonlinear adaptive control of induction motor by using state feedback method are represented in Figure 4.1.

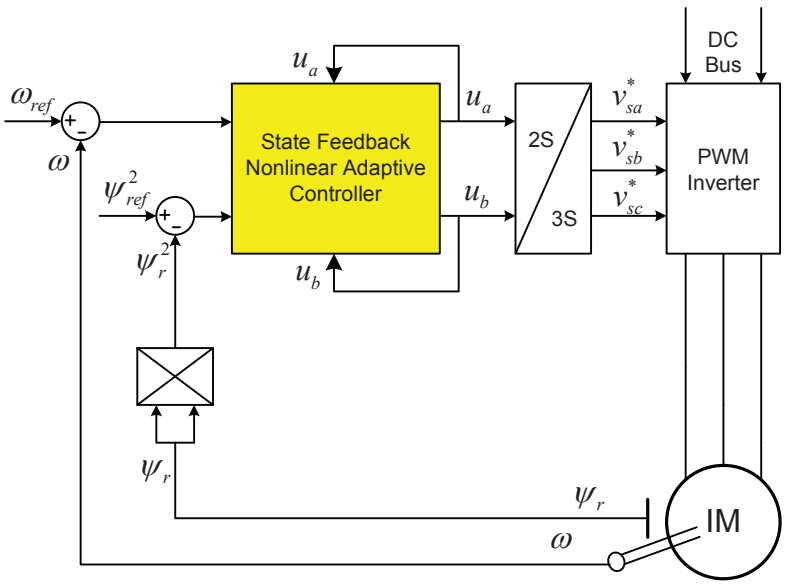


Figure 4.1: Diagram of the proposed state feedback nonlinear adaptive control of induction motor

And the detailed block diagram of the proposed control algorithm is shown in Figure 4.2, in which the general notation of an induction motor is used.

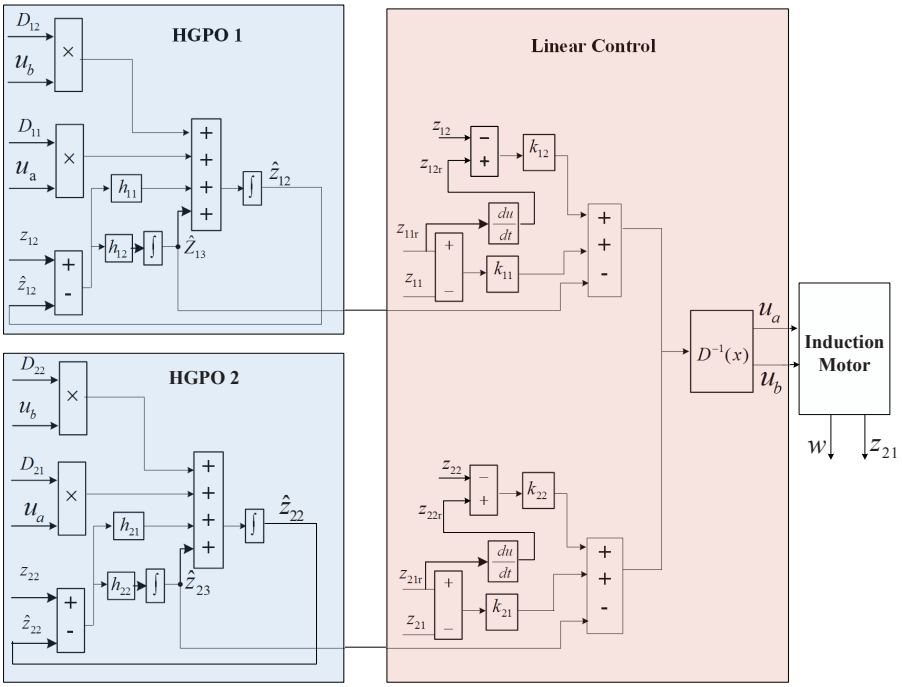


Figure 4.2: Detailed diagram of the state feedback nonlinear adaptive controller

**Remark 2.** *The proposed perturbation estimation method is one kind of function estimation method, rather than a parameters estimation method [51]. It can estimate time-varying dynamics which include nonlinearities, uncertainties, and unmodelled dynamics. Moreover, as the perturbation is compensated for by its real-time estimate, the controller gain can be chosen a less conservative than that used in the conventional robust design and high gain feedback design. The designed controller will result in a reasonably smaller control output under most operating conditions.*

**Remark 3.** *It is known that the high gain observer with very small $\epsilon$ is sensitive to measurement noise. This will also trigger unmodelled high-frequency dynamics. This limits its real application. The proposed controller is tested with noise measurement in simulation studies and as the results demonstrate that performance does not deteriorate very much. Moreover, for the purpose of improving the robustness of the IOLC only, the design only needs to design the*

*observer to make* $|\tilde{\Psi}(\cdot)|_{sup} < |\Psi(\cdot)|_{sup}$, $\epsilon$ *is not needed to be very small.*

## 4.4 Simulation and Analysis

Simulation studies are based on the same parameters of the induction motor used in Chapter Three. Due to the extensive comparisons between IOLC and FOC which have been established Chapter Three and in [4][51]. This chapter only provides simulation studies between IOLC and NAC. The time varying uncertainties are simulated as follows: the load torque $T_L = 40Nm$ is added at $t = 3.5s$, and a time varying term $5 + 5sin(2.5t)$ is added at $t = 10s$. A time-varying term $0.007t + 0.01 + 0.01sin(2t), t > 5$ is added to the rotor resistance at $t = 5s$. The response of time varying parameters $R_r$ and $T_L$ was given in the Figure 4.3.

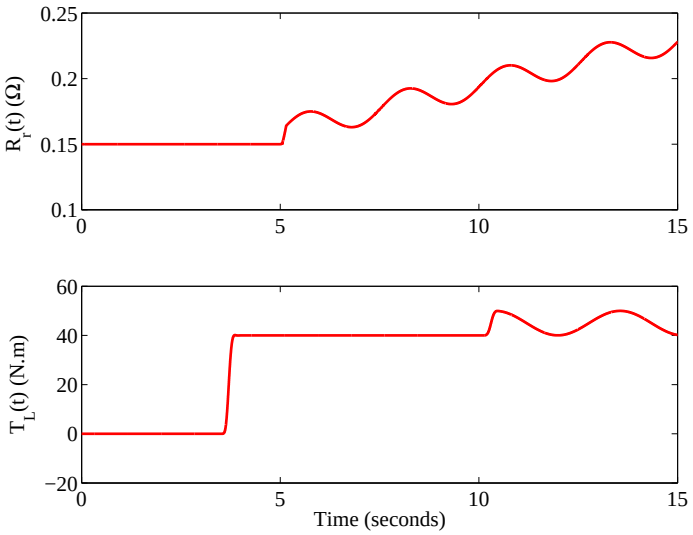


Figure 4.3: Time varying parameters with rotor resistance ($R_r(t)$) and load torque ($T_L(t)$) - HGPO

The unloaded induction motor reaches the speed $200rad/s$ at $t = 3.0s$ and rotor flux amplitude $|\psi| = 1.3Wb$ at $t = 1s$; then at $t = 5s$, speed reference increase to $300rad/s$ and return to $200rad/s$ at $t = 8s$; the flux reference

weakens to $0.8Wb$ at $t = 5s$ and return back to $1.3Wb$ at $t = 8s$. The relative details can be found in Figure 4.4 and Figure 4.5. These reference signals are shown in the dash line. All reference signals are smoothed via a low pass filter.

The parameters of linear control (4.3.10) are chosen as $k_{i1} = -900$, $k_{i2} = -60$, $i = 1, 2$ to assign the poles at $-30$. The same parameters are used in [51]. Parameters of HGPO (4.3.14), $\alpha_{i1} = -2500$, and $\alpha_{i2} = -100$, are chosen to assign poles of $A_i$ in the system (4.3.16) at $-50$, $\epsilon_i = 0.01$, $i = 1, 2$. Control $(u_a, u_b)$ is saturated with bounds $\pm 500$.

### 4.4.1 State Feedback with HGPO

The track response of the proposed control (4.3.10),(4.3.11), and (4.3.17) are shown in Figures 4.4 and 4.5 for speed response and flux amplitude response.

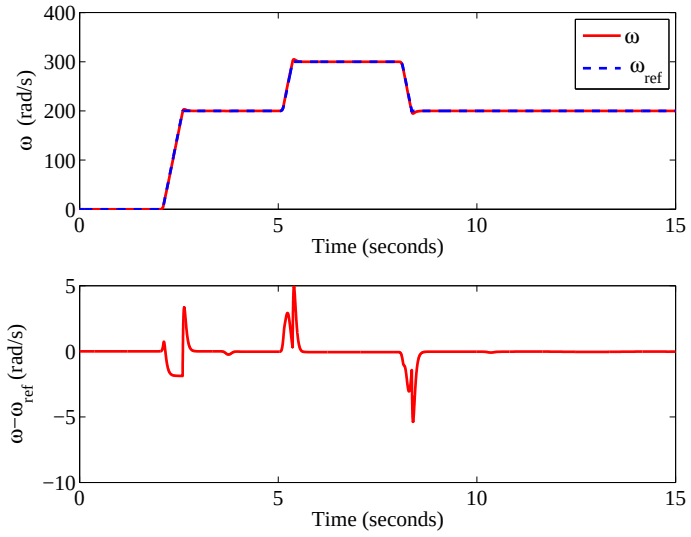


Figure 4.4: Track speed response ($\omega$) of state feedback - HGPO

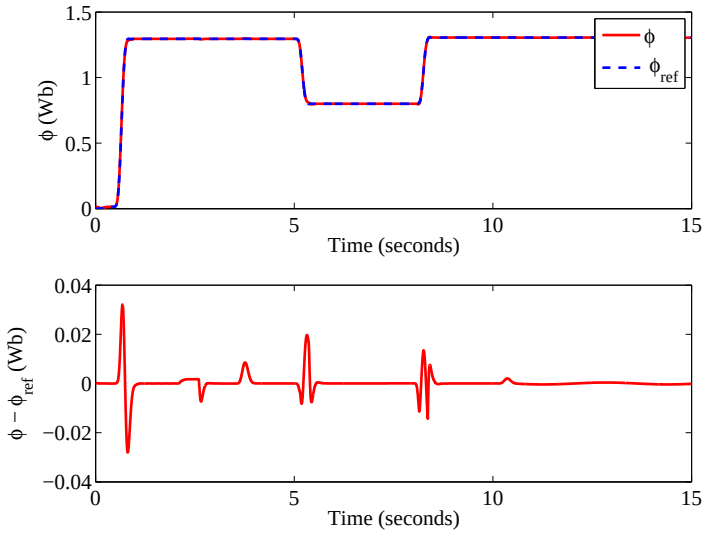


Figure 4.5: Track flux amplitude response ($\phi$) of state feedback - HGPO

It shows that the dynamic of speed and flux are totally decoupled and with the fast track dynamic when the reference signals change (at $t = 5s$ and $t = 8s$), excellent robustness with parameters uncertainties. Such as unknown load torque at $t = 3.5s$ and time-varying load torque after $t = 10s$. Consequently, up to 50% of the time-varying rotor resistance occurs after $t = 5s$. Figures 4.6 and 4.7 show the fast and accurate estimation of perturbation terms. From these figures, the relative error which is the difference between $\Psi_i - \hat{\Psi}_i$, are quite small. That can be mean that these two perturbation observers can obtain the results as good performance. The input control signals $u_a$ and $u_b$ are shown in Figure 4.8, note that these two signals are the input of the induction motor system, however, they are output of the state feedback nonlinear adaptive controller.

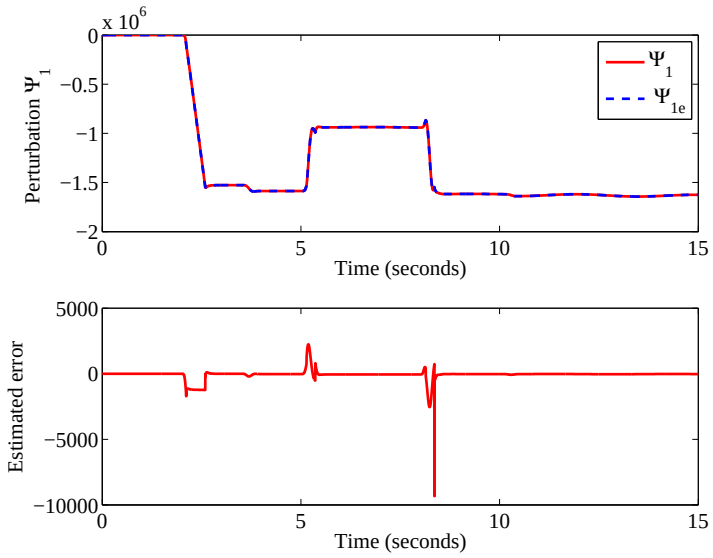


Figure 4.6: Estimate of defined perturbation ($\Psi_1$) - HGPO

## 4.5 Summary

This chapter has investigated and discussed a novel robust adaptive control approach to induction motors, based on perturbation estimation and input-output linearisation. Estimates of perturbation are employed to achieve robust and adaptive FLC. The detailed model of the induction motor is not required and a simple control law is obtained. The simulation results have shown a better performance obtained by the proposed algorithm against uncertainties and time-varying unknown load torque disturbances, in comparison to the classical VC and FLC based on the accurate system model.

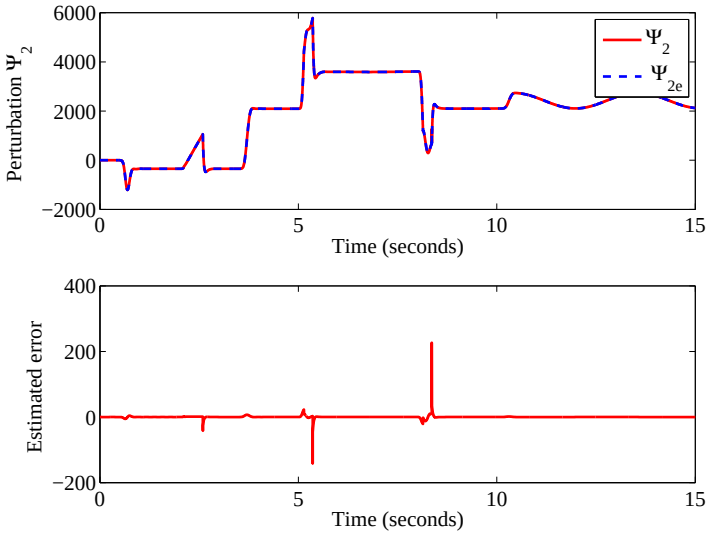


Figure 4.7: Estimate of defined perturbation ($\Psi_2$) - HGPO

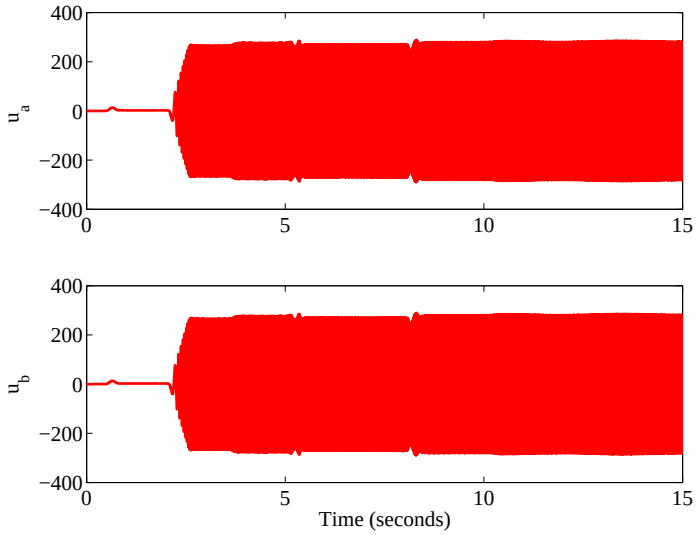


Figure 4.8: Input voltage control signals of $u_a$ and $u_b$ -HGPO-

# Chapter 5

# Nonlinear Adaptive Control of Induction Motor: Output Feedback

In this chapter, an output feedback nonlinear adaptive controller is proposed for the induction motor. Assuming only the rotor speed is measured, a state and high-gain perturbation observer is designed for estimating the derivative of the speed and the corresponding perturbation. Further, a fourth-order sliding mode flux observer is designed to estimate the rotor flux variables. Based on the estimated states and perturbation terms, output feedback nonlinear adaptive controllers are designed for the speed and flux subsystems. The stability of the overall closed-loop system, including the flux observer, state observer, perturbation observer, NAC and the induction motor, are also investigated. Finally, a simulation based on the MATLAB/Simulink is presented.

## 5.1 Introduction

One challenge surrounding the control of induction motors relates to the rotor currents and rotor flux, as they cannot be measured directly. The rotor flux detection is performed by means of a rotor flux estimator or observer [131]. Based on the model of an induction motor, many algorithms have been developed for this purpose. These observers require the accurate system model and their performance is dependent on the parameter uncertainties. To cope with this problem, a sliding mode flux observer [132][133] is used in this chapter to obtain the estimate of rotor flux.

This chapter also investigates the nonlinear adaptive control of the induction motor based on output feedback. A sliding mode flux observer [134]-[136] is designed to estimate the rotor flux. Furthermore, two third-order high gain state and perturbation observers (HGSPO) are designed based on the measurement of the rotor speed and the estimated rotor flux. Other parts of the proposed NAC consists of the same parts as proposed in Chapter Four. Measurement noise has also been introduced to test the sensitivity of the high gain observer.

## 5.2 Nonlinear Output Feedback Adaptive Control Methodology

The methodology of an output feedback nonlinear adaptive control proposed in [108] will be recalled briefly.

### 5.2.1 High Gain State and Perturbation Observer (HGSPO)

The system output $y = x_1$, is available for measurement, then a $(n+1)$th-order state observer is designed to estimate all other system states and perturbation.

A $(n+1)$th order states and perturbation observer is designed as the system (4.2.8) is obtained. Using the observer as follows:

$$\dot{\hat{x}}_e = A_1\hat{x}_e + B_3u + H(y - C_1\hat{x}_e). \tag{5.2.1}$$

where $\hat{x}_e$ is the estimated of $x_e$, all other parameters are defined as the same as system (4.2.8). The observer gain $H$ is chosen as:

$$H = \begin{bmatrix} \alpha_1/\epsilon \\ \alpha_2/\epsilon^2 \\ \vdots \\ \alpha_n/\epsilon^n \\ \alpha_{n+1}/\epsilon^{n+1} \end{bmatrix}, \tag{5.2.2}$$

where $\epsilon$ is a positive constant, $0 < \epsilon < 1$, to be specified and the positive constants $\alpha_i$, $i = 1, 2, \cdots, n+1$, are chosen such that the roots of

$$s^{n+1} + \alpha_1 s^n + \cdots + \alpha_n s + \alpha_{n+1} = 0$$

are in the open left-half complex plan, where $s$ is the Laplace operator.

Defining the estimation error as $\tilde{x}_e = x_e - \hat{x}_e$, substituting the equations (4.2.8) by equation (5.2.1), the error dynamics of observer (5.2.1) can be obtained as:

$$\dot{\tilde{x}}_e = (A_1 - HC_1)\tilde{x}_e + B_1\dot{\Psi}(\cdot). \tag{5.2.3}$$

For the purpose of analysis, the observer error dynamics can be replaced by the equivalent dynamics of the scaled estimation error as:

$$\eta_i = \frac{\tilde{x}_i}{\epsilon^{n+1-i}}, \qquad 1 \le i \le n+1.$$

Thus,

$$\begin{aligned} \hat{x}_e &= x_e - D(\epsilon)\eta \\ \eta &= [\eta_1, \eta_2, \cdots, \eta_{n+1}]^T, \\ D(\epsilon) &= \text{diag}[\epsilon^{n+1}, \cdots, 1]_{(n+1)\times(n+1)}. \end{aligned} \tag{5.2.4}$$

and the error dynamics of observer (5.2.3) can be represented in the singular perturbation form as:

$$\begin{aligned} \dot{\eta} &= D^{-1}(\epsilon)(A_1 - HC_1)D(\epsilon)\eta + D^{-1}(\eta)B_1\dot{\Psi}(\cdot) \\ &= \tfrac{1}{\epsilon}A_{10}\eta + B_1\dot{\Psi}(\cdot), \end{aligned} \tag{5.2.5}$$

where

$$A_{10} = \begin{bmatrix} -\alpha_1 & 1 & \cdots & \cdots & 0 \\ -\alpha_2 & 0 & 1 & \cdots & 0 \\ \vdots & & & & \vdots \\ -\alpha_n & 0 & 0 & \cdots & 1 \\ -\alpha_{n+1} & 0 & 0 & \cdots & 0 \end{bmatrix}$$

is Hurwitzian.

### 5.2.2 Closed-Loop Stability Analysis

To achieve fast enough tracking of the system states and perturbation, the observer gains can be chosen such that the estimation error $\tilde{x}_e$ will converge exponentially to a small neighbourhood which is arbitrarily close to origin. The analysis result is summarized as the following theorem [108].

**Theorem 5.1.** *Consider system (4.2.7), design a high gain state and perturbation observer (5.2.1) and choose the gain $H$ as described in equation (5.2.2). If assumptions A2.1 and A2.2 hold, then given any positive constant $\delta_{\text{spo}} > 0$, there exits a positive constant $\epsilon^*_{\text{spo}}$, such that $\forall\epsilon$, $0 < \epsilon < \epsilon^*_{\text{spo}}$, the observer error $\tilde{x}_e$, from any initial value $\tilde{x}_e(0)$, converges exponentially to the neighborhood*

$$\|\tilde{x}_e\| \leq \delta_{\text{spo}}.$$

Based on the estimates of states and perturbation, an output feedback linearization control law can be obtained for the nonlinear system (4.2.1), which is designed as the same as equations (4.2.15) and (4.2.16), except that the true

states are replaced with the estimated states. In the linear control $v$:

$$u = v/b_0 - \hat{x}_{n+1}/b_0, \tag{5.2.6}$$

$$v = -K\hat{x}, \tag{5.2.7}$$

where $K = [k_1, k_2, \cdots, k_n]^T$ are the linear feedback controller gains, which makes matrix $A_0 = A - BK$ Hurwitzian.

Represent that $\hat{x} = x - D'(\eta)\eta'$, and $\hat{x}_{n+1} = x_{n+1} - \eta_{n+1}$, where

$$D'(\epsilon) = \text{diag}[\epsilon^{n+1}, \cdots, \epsilon]_{(n)\times(n)},$$

and

$$\eta' = [\eta_1, \eta_2, \cdots, \eta_n]^T.$$

Control (5.2.6) can be represented as:

$$u = \frac{1}{b_0}(-x_{n+1} - Kx - K_1 D(\epsilon)\eta), \tag{5.2.8}$$

where $K_1 = [K, 1]^T$.

Applying control (5.2.8) to system (4.2.7), the closed-loop system can be represented by

$$\dot{x} = A_0 x + BK_1 D(\epsilon)\eta \tag{5.2.9}$$

$$\epsilon\dot{\eta} = A_{10}\eta + \epsilon B_4 \dot{\Psi}(x, D(\epsilon)\eta). \tag{5.2.10}$$

System (5.2.9) and (5.2.10) is a standard singular perturbed system, and $\eta = 0$ is the unique solution of system (5.2.10) when $\epsilon = 0$. The reduced system, obtained by substituting $\eta = 0$ in system (5.2.9), is obtained as follows:

$$\dot{x} = A_0 x. \tag{5.2.11}$$

The boundary-layer system, obtained by applying the change of time variable $\tau = t/\epsilon$ to (5.2.10) and then setting $\epsilon = 0$, is given by

$$\frac{d\eta}{d\tau} = A_{10}\eta. \tag{5.2.12}$$

The stability of the closed-loop system (5.2.9) and (5.2.10) are proofed by the following theorem [108].

**Theorem 5.2.** *Consider system (4.2.8) and high gain state and perturbation observer (5.2.1), choose the observer gain as described in equation (5.2.2), and let assumptions A*2.1 *and A*2.2 *hold; then,* $\exists \epsilon_2^*$, $\epsilon_2^* > 0$ *such that,* $\forall \epsilon$, $0 < \epsilon < \epsilon_2^*$, *the origin of system (5.2.9) and (5.2.10) is exponentially stable.*

**Remark 4.** *The designed state and perturbation observer can be regarded as a functional estimation method, in contrast to the parameter estimation method used in most nonlinear adaptive control. It can deal with fast varying unknown parameters, unknown nonlinear dynamics and external disturbances. When there does not exist uncertainties and external disturbances and the exact system nonlinearities are obtainable, such a controller provides almost the same performance as the state exact feedback linearization controller, when there exists uncertainties, such controller performs much better.*

**Remark 5.** *The proposed controller uses the estimates of states and perturbation to realize the whole controller, it needs only one measurable output and can be easily implemented in practice.*

## 5.3 Output Feedback Based on Nonlinear Adaptive Control for Induction Motor via High Gain State and Perturbation Observer

### 5.3.1 Design of Output Feedback Based on Nonlinear Adaptive Control for Induction Motor

When the rotor speed $y_1 = z_{11}$ and rotor flux modulus $y_2 = z_{21}$ are available to measure. Two third-order high-gain observers, called high gain state and perturbation observers, are designed to estimate the system states and perturbation. Estimates of states and perturbations are employed to design a robust

adaptive output-feedback linearising control law. Note that the rotor flux is still a required measurement. Output feedback based on rotor speed and stator currents will be included in future work.

Using $y_1 = z_{11}$ and $y_2 = z_{21}$ as available measurements, two third-order high gain state and perturbation observers are designed as:

$$\begin{cases} \dot{\hat{z}}_{i1} &= \hat{z}_{i2} + h_{i1}\tilde{z}_{i1} \\ \dot{\hat{z}}_{i2} &= \hat{z}_{i3} + h_{i2}\tilde{z}_{i1} + D_{i1}u_a + D_{i2}u_b \\ \dot{\hat{z}}_{i3} &= h_{i3}\tilde{z}_{i1}, \end{cases} \tag{5.3.1}$$

From system (4.3.8) and (5.3.1), the error dynamics of (5.3.1) becomes:

$$\begin{cases} \dot{\tilde{z}}_{i1} &= \tilde{z}_{i2} - h_{i1}\tilde{z}_{i1} \\ \dot{\tilde{z}}_{i2} &= \tilde{z}_{i3} - h_{i2}\tilde{z}_{i1} \\ \dot{\tilde{z}}_{i3} &= -h_{i3}\tilde{z}_{i1} + \dot{\Psi}_i \end{cases} \tag{5.3.2}$$

After defining the scaled observer gain and estimation errors, the observer error equation can be represented in a singularly perturbed form as:

$$\dot{\eta}_i = \tfrac{1}{\epsilon_i} A_{i1}\eta_i + B_{i1}\dot{\Psi}_i(\cdot), \tag{5.3.3}$$

where $\eta_i$,$A_{i1}$,$B_{i1}$ have similar structure as in (4.3.16), but with different dimensions.

Using the estimate of perturbation $\hat{z}_{i3}$ to cancel the system perturbation. The estimate of system states $\hat{z}_{i1}$, $\hat{z}_{i2}$ replace the real states. The robust and adaptive control law is obtained as:

$$\begin{pmatrix} u_a \\ u_b \end{pmatrix} = D^{-1}(x)\left[\begin{pmatrix} -\hat{z}_{13} \\ -\hat{z}_{23} \end{pmatrix} + \begin{pmatrix} v_a \\ v_b \end{pmatrix}\right] \tag{5.3.4}$$

$$v_a = -k_{11}\hat{z}_{11} - k_{12}\hat{z}_{12} + v_{a_{ref}} \tag{5.3.5}$$

$$v_b = -k_{21}\hat{z}_{11} - k_{22}\hat{z}_{12} + v_{b_{ref}} \tag{5.3.6}$$

where $v_{a_{ref}}$ and $v_{b_{ref}}$ are reference control defined in equation (4.3.11). The detailed block diagrams of output feedback approach is represented in Figure 5.1 and 5.2.

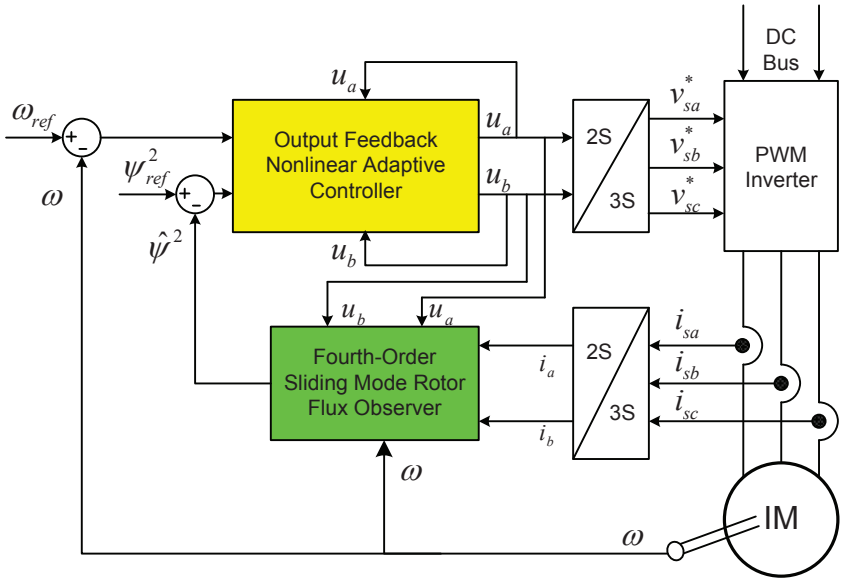


Figure 5.1: Diagram of proposed output feedback nonlinear adaptive control of induction motor by using sliding mode rotor flux observer

Substituting the control in (5.3.4), (5.3.5), and (5.3.6) into the system model (4.3.8), the track error dynamics is given by:

$$\dot{e}_i \quad = \quad A_{i0}e_i + B_iK_iT_i(\epsilon_i)\eta_i \tag{5.3.7}$$

where $K_i = [k_{i1}, k_{i2}, 1]$, and $T_i(\epsilon_i) = \text{diag}[\epsilon_i^2, \epsilon_i, 1]_{3\times 3}$.

The closed-loop system, including the controller/observer, is given by the systems in (5.3.3) and (5.3.7). Its stability can be investigated in similar way as in the state feedback.

## 5.4 Output Feedback with Sliding Mode Flux Observer

This subsection develops a fourth-order observer based on sliding mode ideas [98]. This sliding mode flux observer design methodology proposed in [104] should be briefly discussed at first. The diagram containing the sliding mode

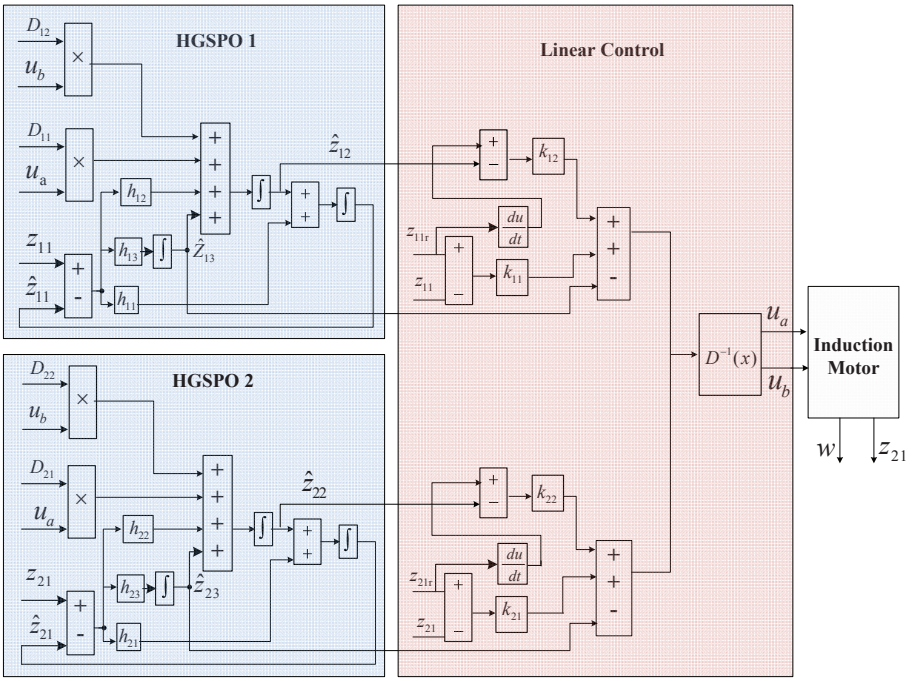


Figure 5.2: Detailed diagram of output feedback nonlinear adaptive controller

rotor flux observer is shown in Figure 5.1. The sliding mode approach generally depends on the specification of a surface (or manifold) $S$ in the state space considers the trajectories of the dynamical system, if they are forced to remain on S, the resulting reduced order motion is stable. The reduced order motion is termed the sliding motion and is specified by the choice of $S$. In accord with the observer design, the manifold is usually defined in the error states, by using this way, when the error states lie on the surface, the observer output is equal to the plant output.

Consideration the first four equations of the induction motor model, thus

the fifth-order system of induction motor can be simplified by equation (5.4.1):

$$\begin{aligned}
\dot{x_1} &= -a_1 x_1 + a_3 x_4 x_5 + a_2 x_3 + b u_a \\
\dot{x_2} &= -a_1 x_2 - a_3 x_3 x_5 + a_2 x_4 + b u_b \\
\dot{x_3} &= -a_5 x_3 - a_6 x_4 x_5 + a_4 x_1 \\
\dot{x_4} &= -a_5 x_4 + a_6 x_3 x_5 + a_4 x_2 \\
\dot{x_5} &= a_7 (x_2 x_3 - x_1 x_4) - a_8 - a_9 x_5 - a_{10} x_5^2
\end{aligned} \tag{5.4.1}$$

where the state vector which include five state variables:

$$X = [x_1, x_2, x_3, x_4, x_5]^T = [i_a, i_b, \psi_a, \psi_b, \omega_r]^T$$

and stator voltage U, is the control vector:

$$U = [u_a, u_b]^T$$

and the output vector Y is given by:

$$Y = [i_a, i_b, \omega_r]^T$$

Note that it does not require the rotor flux due to the rotor flux observer. The parameters are defined as Table 5.1.

Table 5.1: State Variable Parameters of the Fifth-Order Induction Motor Model

| | | |
|---|---|---|
| $a_1 = \gamma$ | $a_2 = K/T_r$ | $a_3 = pK$ |
| $a_4 = L_m/T_r$ | $a_5 = 1/T_r$ | $a_6 = p$ |
| $a_7 = pL_m/JL_r$ | $a_8 = T_1/J$ | $a_9 = (f + a_{11})/J$ |
| $a_{10} = a_{12}/J$ | | |

And $\gamma = R_s/\sigma L_s + R_r L_m^2/\sigma L_s L_r^2$, $K = L_m/\sigma L_s L_r$, $T_r = L_r/R_r$, where $R_s$ and $R_r$ are stator and rotor resistances, $L_s$ and $L_r$ are the stator and rotor inductances, $L_m$ is the mutual inductance, $p$ is the number of pole pairs, $f$ is

the friction coefficient, $J$ is the moment of inertia, $T_1$ is the constant term of load torque $T_L$, thus, the load torque can be obtained as follows:

$$T_L = T_1 + a_{11}x_5 + a_{12}x_5^2 \tag{5.4.2}$$

where $a_{11}a_{12}$ are a constant terms. Note that $i_a$ and $i_b$ are the stator currents, $\psi_a$ and $\psi_b$ are the rotor flux, and $\omega_r$ is rotor speed. In the following explanations, the speed $x_5$ in equation (5.4.1) will be considered as a varying parameter. The symbol $\omega_r$ will be replaced by $x_5$ in order to remove any confusion between the states and parameters. The proposed observer aims to estimate the unmeasured flux components of $x_3$ and $x_4$. The observer is given by the following system (5.4.3):

$$\begin{aligned}
\dot{\hat{x_1}} &= -a_1\hat{x_1} + a_3\hat{x_4}\omega_r + a_2\hat{x_3} + bu_a + \Lambda_1 \\
\dot{\hat{x_2}} &= -a_1\hat{x_2} - a_3\hat{x_3}\omega_r + a_2\hat{x_4} + bu_b + \Lambda_2 \\
\dot{\hat{x_3}} &= -a_5\hat{x_3} - a_6\hat{x_4}\omega_r + a_4\hat{x_1} + \Lambda_3 \\
\dot{\hat{x_4}} &= -a_5\hat{x_4} + a_6\hat{x_3}\omega_r + a_4\hat{x_2} + \Lambda_4
\end{aligned} \tag{5.4.3}$$

where the labels $\Lambda_1$, $\Lambda_2$, $\Lambda_3$, $\Lambda_4$ are observer output error dependent gains. The error components $e_i = x_i - \hat{x_i}$, and the error dynamics are stated by the following equations (5.4.4):

$$\begin{aligned}
\dot{e_1} &= -a_1e_1 + a_3\omega_re_4 + a_2e_3 + \Lambda_1 \\
\dot{e_2} &= -a_1e_2 - a_3\omega_re_3 + a_2e_4 + \Lambda_2 \\
\dot{e_3} &= -a_5e_3 - a_6\omega_re_4 + a_4e_1 + \Lambda_3 \\
\dot{e_4} &= -a_5e_4 + a_6\omega_re_3 + a_4e_2 + \Lambda_4
\end{aligned} \tag{5.4.4}$$

where the first two switching gains $\Lambda_1$ and $\Lambda_2$ have the following structure:

$$\begin{aligned}
\Lambda_1 &= -\rho_1\text{sign}(e_1) \\
\Lambda_2 &= -\rho_2\text{sign}(e_2)
\end{aligned} \tag{5.4.5}$$

The observer switching function is given by (5.4.6):

$$S_{obs} = \begin{bmatrix} s_1 \\ s_2 \end{bmatrix} = \begin{bmatrix} e_1 \\ e_2 \end{bmatrix} \tag{5.4.6}$$

and the sliding surface is given by $S_{obs}$=0. The stability analysis consists of determining $\Lambda_1$ and $\Lambda_2$ using the so-called reaching condition, which is given by the equation $S_{obs}^T \dot{S}_{obs} < 0$. A sufficient condition for this to be satisfied is that both $s_1\dot{s}_1 < 0$ and $s_2\dot{s}_2 < 0$. This condition guarantees that in a finite time $S_{obs} = 0$ and the states remain on the switching surface. And afterwards, $\Lambda_3$ and $\Lambda_4$ are determined, using the reduced-order system obtained when $S_{obs} = \dot{S}_{obs} = 0$ is stable. The time derivative of the switching function is given by the following equation:

$$\dot{S}_{obs} = \begin{bmatrix} \dot{s}_1 \\ \dot{s}_2 \end{bmatrix} = \begin{bmatrix} -a_1 & 0 \\ 0 & -a_1 \end{bmatrix} \begin{bmatrix} e_1 \\ e_2 \end{bmatrix} + \begin{bmatrix} a_2 & a_3\omega_r \\ -a_3\omega_r & a_2 \end{bmatrix} \begin{bmatrix} e_3 \\ e_4 \end{bmatrix} + \begin{bmatrix} -\rho_1 \text{sign}(e_1) \\ -\rho_2 \text{sign}(e_2) \end{bmatrix} \tag{5.4.7}$$

From the above equation, the equivalent output error injection necessary to ensure $\dot{S}_{obs} = 0$ is given by:

$$\begin{bmatrix} \Lambda_{1eq} \\ \Lambda_{2eq} \end{bmatrix} = - \begin{bmatrix} a_2 & a_3\omega_r \\ -a_3\omega_r & a_2 \end{bmatrix} \begin{bmatrix} e_3 \\ e_4 \end{bmatrix} \triangleq -\Gamma \begin{bmatrix} e_3 \\ e_4 \end{bmatrix} \tag{5.4.8}$$

Suppose that

$$\begin{bmatrix} \Lambda_3 \\ \Lambda_4 \end{bmatrix} = \Lambda \begin{bmatrix} \Lambda_1 \\ \Lambda_2 \end{bmatrix} \tag{5.4.9}$$

where $\Lambda \in \mathbb{R}^{2\times 2}$. When sliding is happening at:

$$\begin{bmatrix} \Lambda_3 \\ \Lambda_4 \end{bmatrix} = \Lambda \begin{bmatrix} \Lambda_{1eq} \\ \Lambda_{2eq} \end{bmatrix} = -\Lambda \begin{bmatrix} a_2 & a_3\omega_r \\ -a_3\omega_r & a_2 \end{bmatrix} \begin{bmatrix} e_3 \\ e_4 \end{bmatrix} = -\Lambda\Gamma \begin{bmatrix} e_3 \\ e_4 \end{bmatrix} \tag{5.4.10}$$

the equation $\Lambda = \Delta\Gamma^{-1}$ can be chose, where

$$\Delta = \begin{bmatrix} \delta_1 & -a_6\omega_r \\ a_6\omega_r & \delta_2 \end{bmatrix} \tag{5.4.11}$$

where $\delta_1$ and $\delta_2$ are positive design constants. Note that $det(\Gamma(\omega_r)) \neq 0$ for all $\omega_r$, Therefore, the inverse always exists. Consider now the second sub-system concerning the flux error dynamics given by (5.4.12):

$$\begin{aligned} \dot{e}_3 &= -a_5 e_3 - a_6 \omega_r e_4 + a_4 e_1 + \Lambda_3 \\ \dot{e}_4 &= -a_5 e_4 - a_6 \omega_r e_3 + a_4 e_2 + \Lambda_4 \end{aligned} \tag{5.4.12}$$

When sliding takes place, substituting from equation (5.4.10), the following equation can be obtained:

$$\begin{bmatrix} \dot{e}_3 \\ \dot{e}_4 \end{bmatrix} = \left[ \begin{bmatrix} -a_5 & a_6\omega_r \\ a_6\omega_r & -a_5 \end{bmatrix} - \Delta\Gamma^{-1}\Gamma \right] \begin{bmatrix} e_3 \\ e_4 \end{bmatrix} \tag{5.4.13}$$

and then we have

$$\begin{bmatrix} \dot{e}_3 \\ \dot{e}_4 \end{bmatrix} = \begin{bmatrix} -a_5 - \delta_1 & 0 \\ 0 & -a_5 - \delta_2 \end{bmatrix} \begin{bmatrix} e_3 \\ e_4 \end{bmatrix} \tag{5.4.14}$$

The flux errors $e_3$ and $e_4$ converge exponentially to zero.

## 5.5 Simulation and Analysis

The proposed control scheme is investigated by simulations, under similar conditions described in Chapter Four. The parameters of linear control (4.3.10) are chosen as $k_{i1} = -900$, $k_{i2} = -60$, $i = 1, 2$ and the poles are assigned at $-30$, and the same parameters used as in [51]. The parameters of HGSPO (5.3.1), which use $\alpha_{i1} = -30$, $\alpha_{i2} = -300$,$\alpha_{i3} = -1000$ to set poles of $A_{i1}$ in the system (4.3.16) at $-10$ and $\epsilon_i = 0.01$, $i = 1, 2$. The control $(u_a, u_b)$ is saturated with bounds $\pm 500$ (same conditions as previous). The time varying $T_L$ and $R_r$ has been referred to in Figure 5.3.

### 5.5.1 Output Feedback with HGSPO

The track response of the proposed control (5.3.4) and (5.3.5) and (5.3.6) are shown in Figures 5.4 and 5.5 for speed response and flux amplitude response.

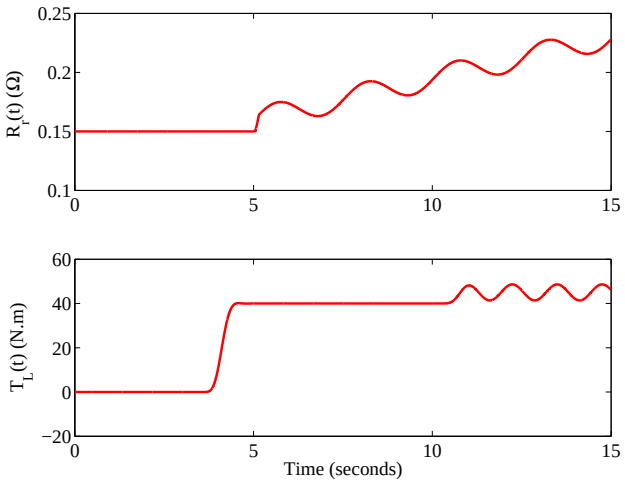


Figure 5.3: Time varying parameters with rotor resistance ($R_r(t)$) and load torque ($T_L(t)$) - HGSPO with noise and sliding mode flux observer

Those output feedback responses are in comparison with state feedback ones. However, a bigger track error is caused due to the estimation error of state variables, note that even though the state variables are not known, the estimation error is not too big. Figures 5.6 and 5.7 have shown the fast and accurate estimation of perturbation terms. From those figures, the two estimated perturbation terms can follow the real value of the perturbation terms with small error. The input control signals of induction motor model $u_a$ and $u_b$ are shown in Figure 5.8, they are also the output signals of output feedback nonlinear adaptive controller. The estimated errors of states are shown in Figures 5.9 to 5.12. During these four states represented in the figures, the estimated values can track the real values well with small errors.

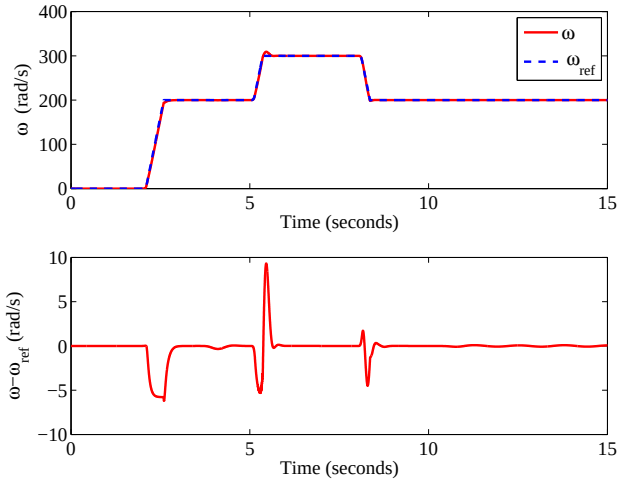


Figure 5.4: Track speed response ($\omega$) of output feedback control - HGSPO

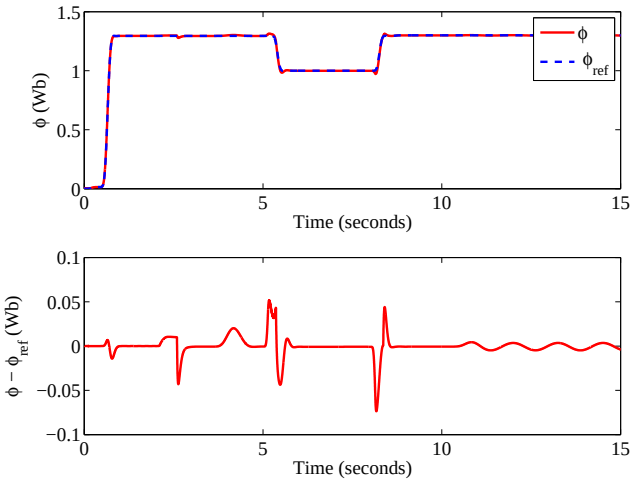


Figure 5.5: Track flux amplitude response ($\phi$) of output feedback control - HGSPO

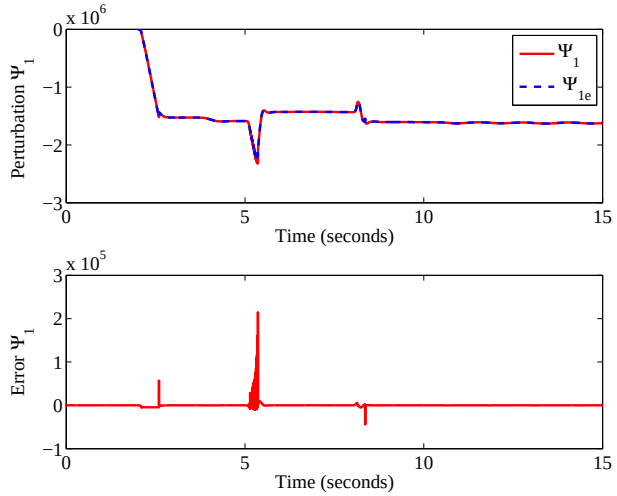


Figure 5.6: Estimate of defined perturbation ($\Psi_1$) - HGSPO

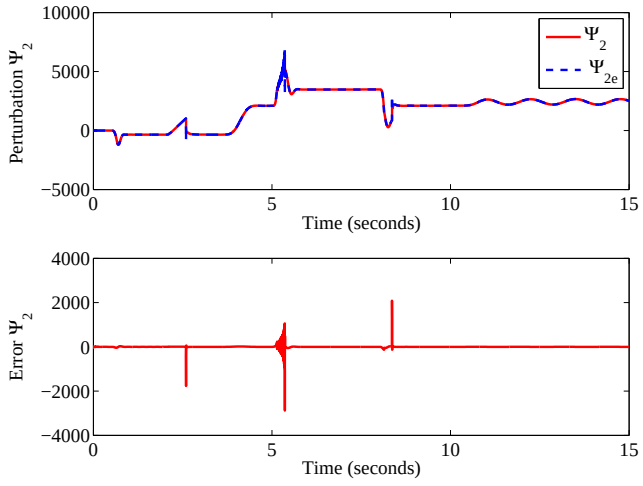


Figure 5.7: Estimate of defined perturbation ($\Psi_2$) - HGSPO

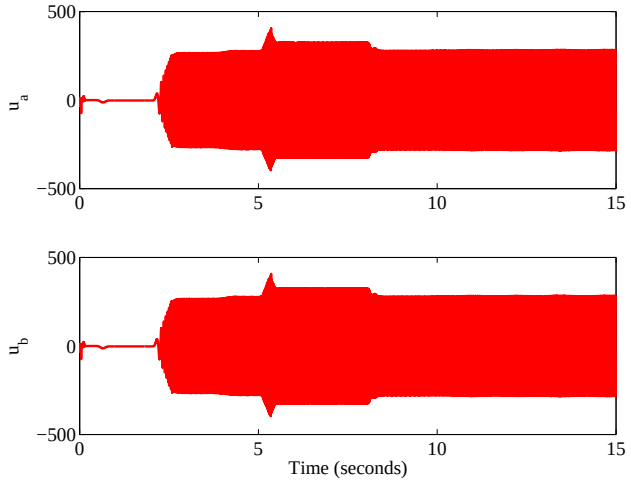


Figure 5.8: Input voltage control signals of $u_a$ and $u_b$ - HGSPO

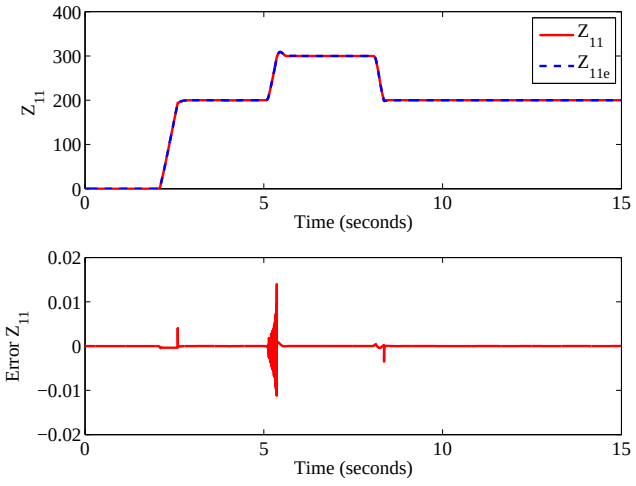


Figure 5.9: Responses of observer estimation error for rotor speed ($z_{11}$) - HGSPO

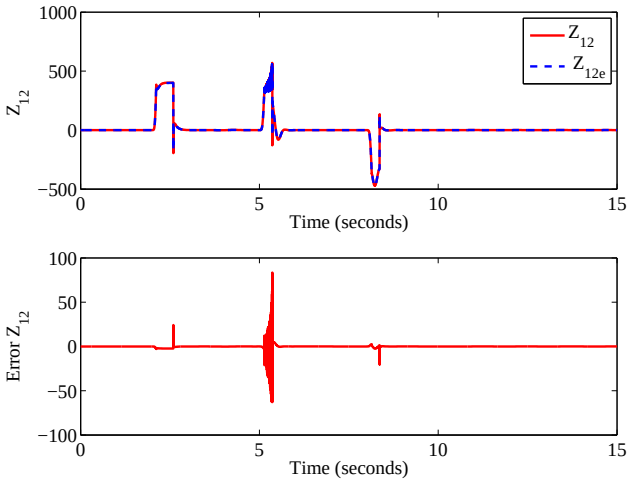


Figure 5.10: Responses of observer estimation error for the derivative of rotor speed ($z_{12}$) - HGSPO

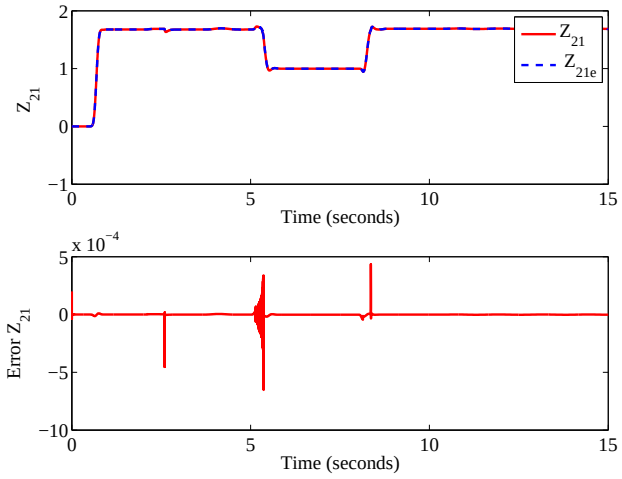


Figure 5.11: Responses of observer estimation error for rotor flux ($z_{21}$) - HGSPO

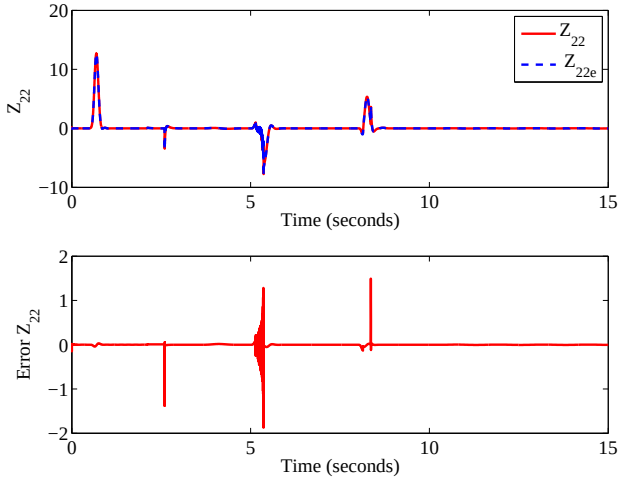


Figure 5.12: Responses of observer estimation error for the derivative of rotor flux ($z_{22}$) - HGSPO

### 5.5.2 Measurement Noise

The proposed controller (5.3.4), (5.3.5) and (5.3.6) is tested with measurement noise. The main purpose is to test the robustness of the high gain observer to the measurement noise. The measurement noise was taken as uniform random numbers between $\pm 0.2$ and added to $y_1 = \omega$ after $t = 2s$. The simulation model in SIMULINK used solver ode4 with a fixed step size $= 1e{-}4$. The speed response and flux track response are shown in Figures 5.13 and 5.14. From these two figures, the speed and flux have tracked the reference values with small errors.

After running the simulation, the degradation of both the speed and flux responses are not noticeable. This is because the proposed control scheme treats the introduced noise as part of the system perturbation and compensates this together with other uncertainties. The high gain observer can provide comparable results against other kinds of robust observers, such as the sliding mode observer [117] and nonlinear extended-state-observer [120], but with a

simpler structure. The estimated errors of states are shown in Figures 5.15 to 5.18. From these figures, it can be shown that the observers can provide accurate estimates of the system states, with a fast track without any phase delay.

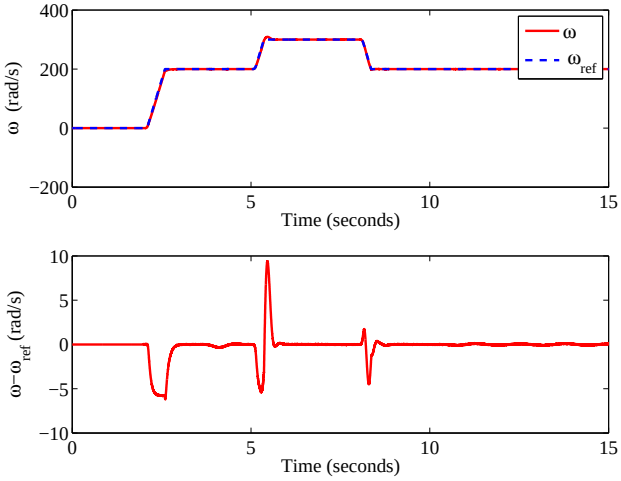


Figure 5.13: Track speed response ($\omega$) of output feedback control with noise

Figures 5.19 and 5.20 show the fast and accurate estimation of perturbation terms. These two observers can also obtain accurate estimates of system's perturbation. The input control signals $u_a$ and $u_b$ are shown in Figure 5.21.

### 5.5.3 Output Feedback with HGSPO and Sliding Mode Flux Observer

Simulation results of the proposed output feedback control (5.3.4) is simulated using the estimate of flux $\hat{\phi} = \hat{\psi}_a^2 + \hat{\psi}_b^2$ obtained from a four-order sliding mode flux observer which is taken from [104]. The time varying $T_L$ and $R_r$ has given in Figure 5.3.

Speed and flux responses, shown in Figures 5.22 and 5.23, are very close to those produced with the flux measurements with a bigger flux track error.

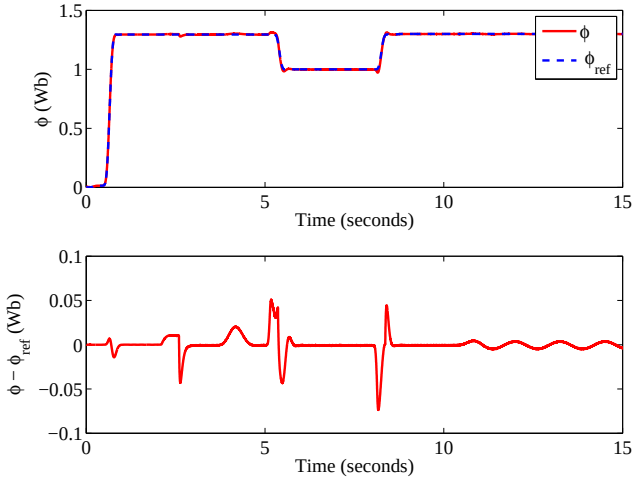


Figure 5.14: Track flux amplitude response ($\phi$) of output feedback control with noise

This is because the proposed control treats the introduced estimate rotor flux error $y_2 - \hat{y}_2$ as part of the system perturbation. Figures 5.24 and 5.25 show the fast and accurate estimation of perturbation terms. The input control signals $u_a$ and $u_b$ are shown in Figure 5.26. The estimated rotor flux errors of $\psi_a$ and $\psi_b$ are shown in Figures 5.27 and 5.28. They are represented that the estimated values of rotor fluxes are almost the same as the real values without too big errors. The estimated errors of states are shown in Figures 5.29 to 5.32, from these four figures, the results have shown that all the state variables can provide a satisfactory response, more details can be found in section 5.4.

Note that there is a noticeable track error of flux response after t=10s, when both $R_r(t)$ and $T_L(t)$ are time-varying.

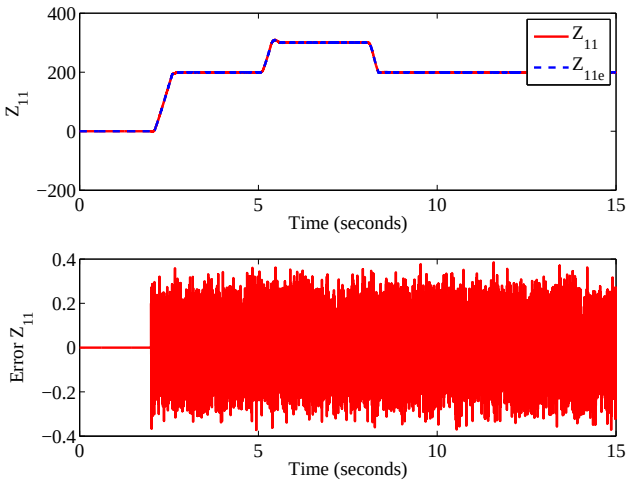


Figure 5.15: Estimation error response of rotor speed ($z_{11}$) by using designed observer - HGSPO with noise

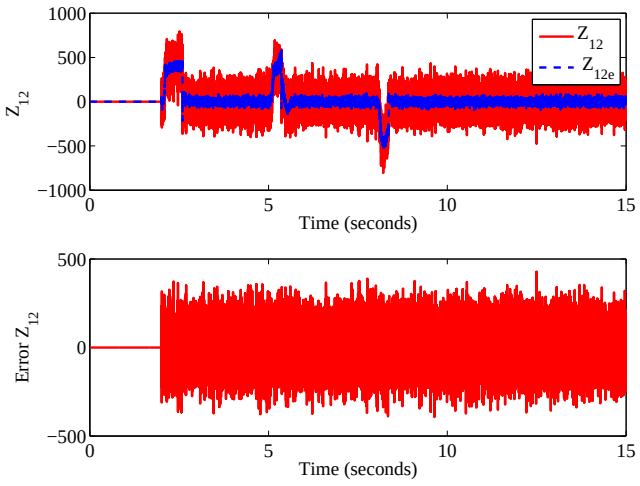


Figure 5.16: Estimation error response of the derivative of rotor speed ($z_{12}$) by using designed observer - HGSPO with noise

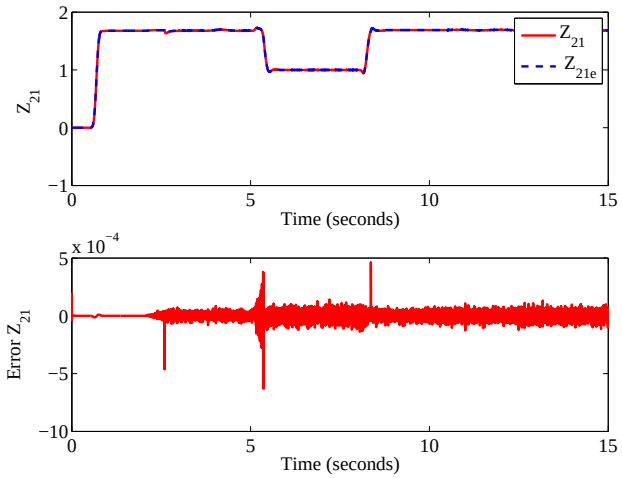


Figure 5.17: Estimation error response of flux ($z_{21}$) by using designed observer - HGSPO with noise

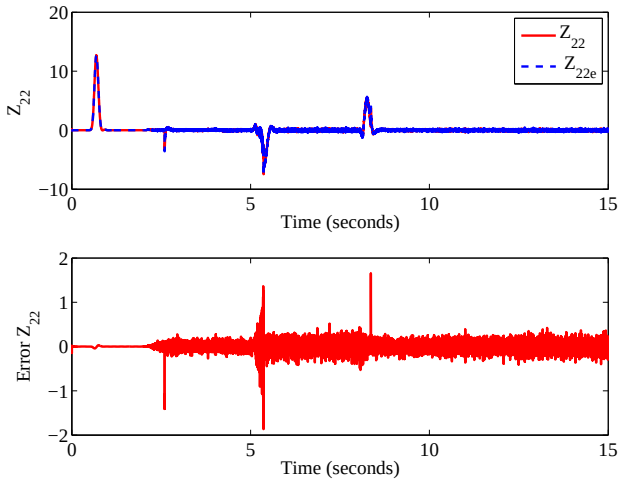


Figure 5.18: Estimation error response of the derivative of flux ($z_{22}$) - HGSPO with noise

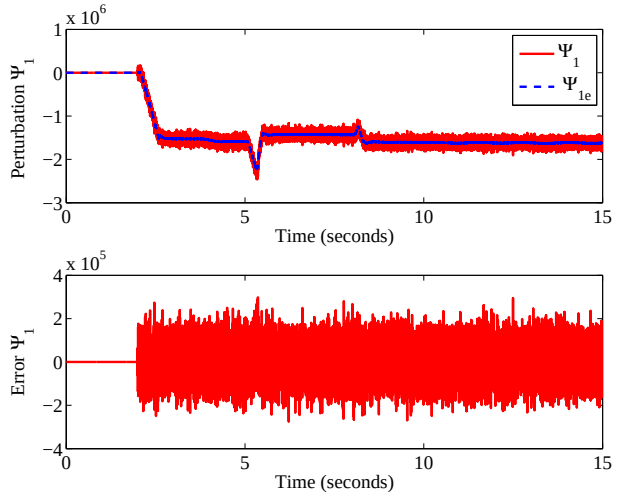


Figure 5.19: Estimate of defined perturbation ($\Psi_1$) - HGSPO with noise

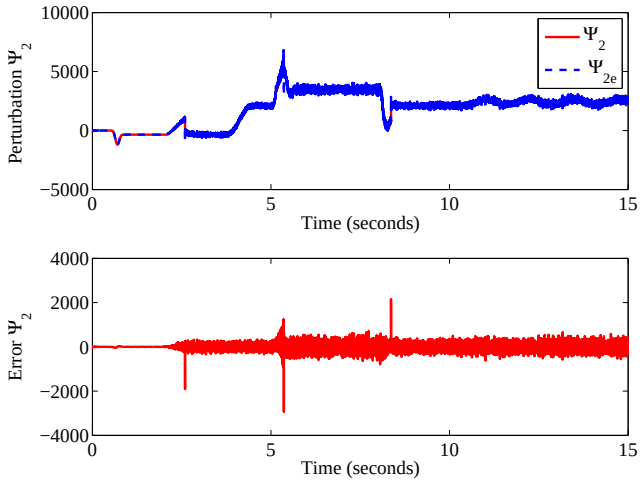


Figure 5.20: Estimate of defined perturbation ($\Psi_2$) - HGSPO with noise

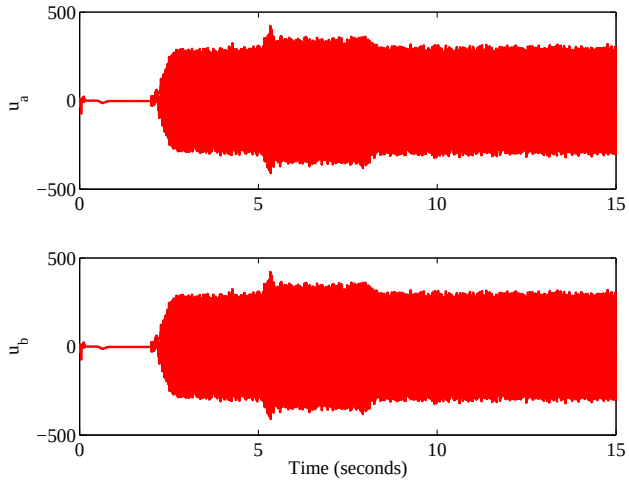


Figure 5.21: Input voltage control signals of $u_a$ and $u_b$ - HGSPO with noise

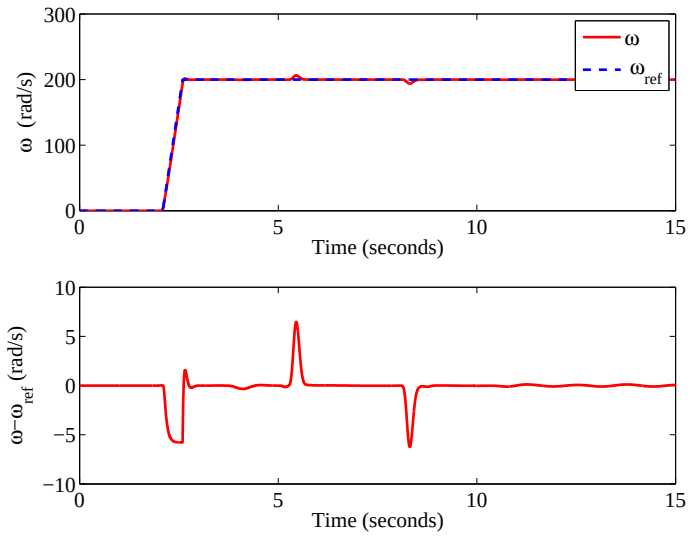


Figure 5.22: Track speed response ($\omega$) of output feedback control with flux observer

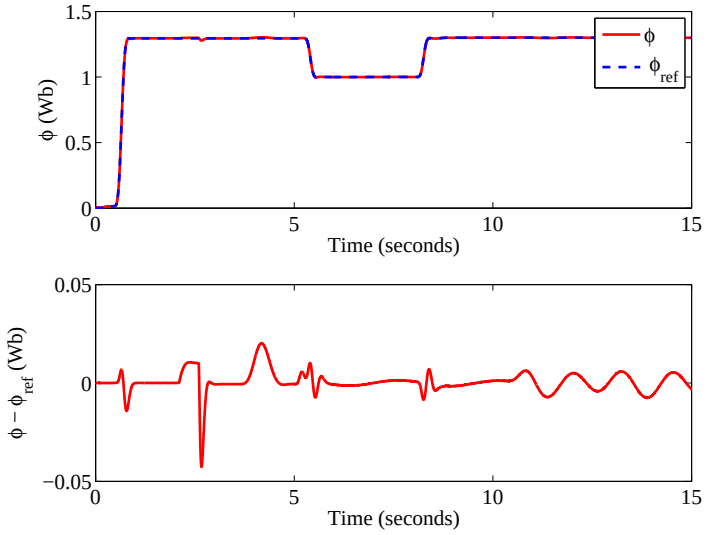


Figure 5.23: Track flux amplitude response ($\phi$) of output feedback control with flux observer

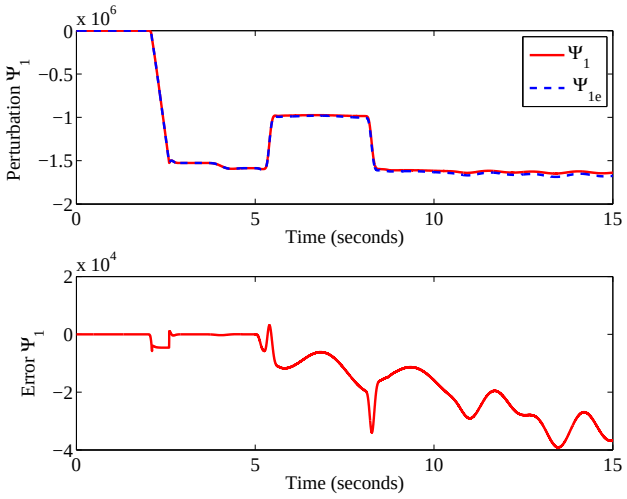


Figure 5.24: Estimate of defined perturbation ($\Psi_1$) - HGSPO with flux observer

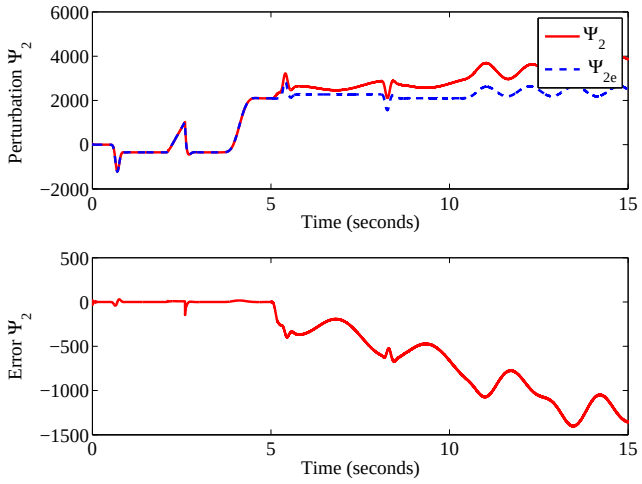


Figure 5.25: Estimate of defined perturbation ($\Psi_2$) - HGSPO with flux observer

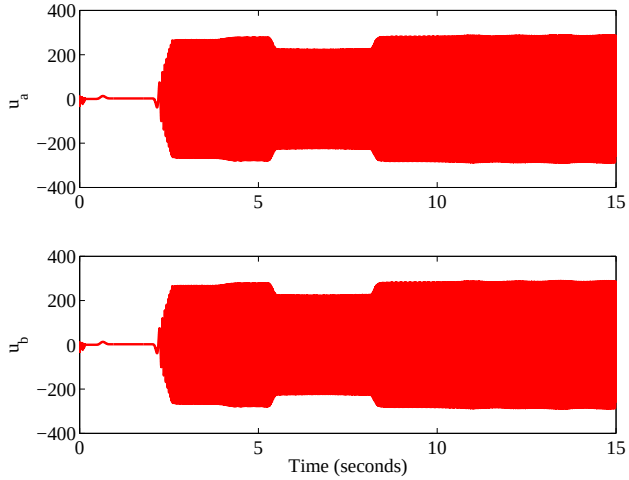


Figure 5.26: Input voltage control signals of $u_a$ and $u_b$ - HGSPO with flux observer

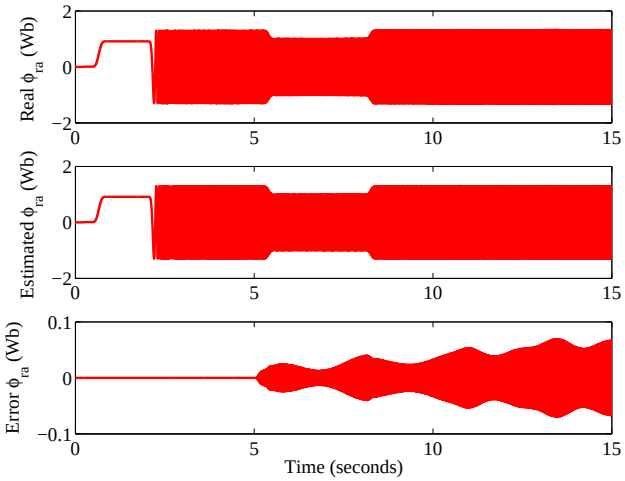


Figure 5.27: Estimated value and error of rotor flux ($\psi_{ra}$)

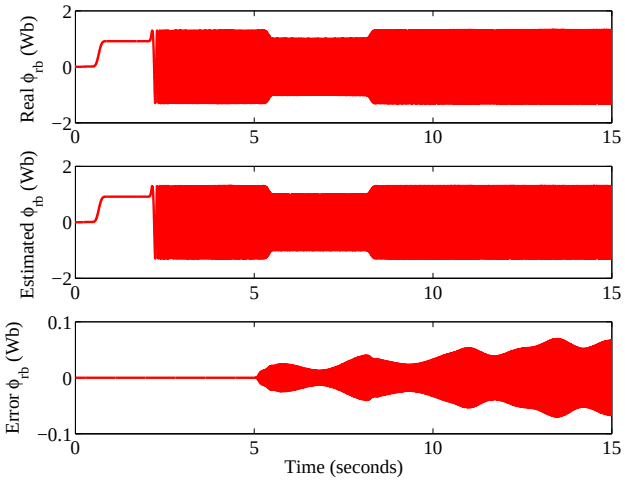


Figure 5.28: Estimated value and error of rotor flux ($\psi_{rb}$)

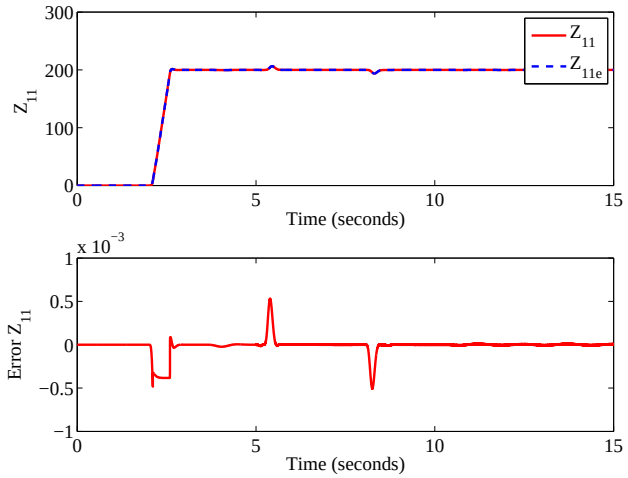


Figure 5.29: Estimation error response of rotor speed ($z_{11}$) by using proposed observer - HGSPO with flux observer

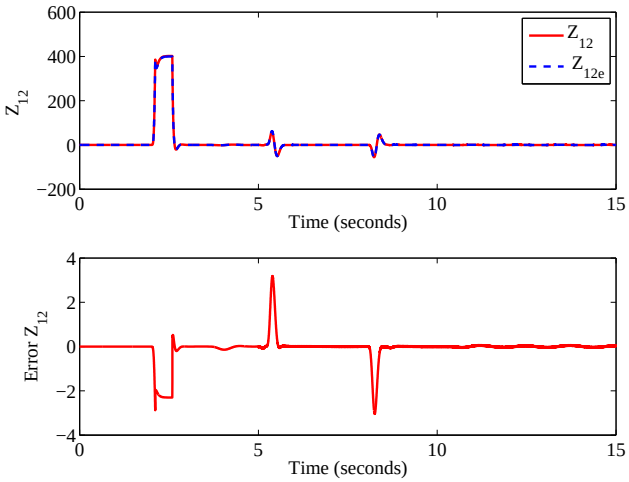


Figure 5.30: Estimation error response for the derivative of rotor speed ($z_{12}$) by using proposed observer - HGSPO with flux observer

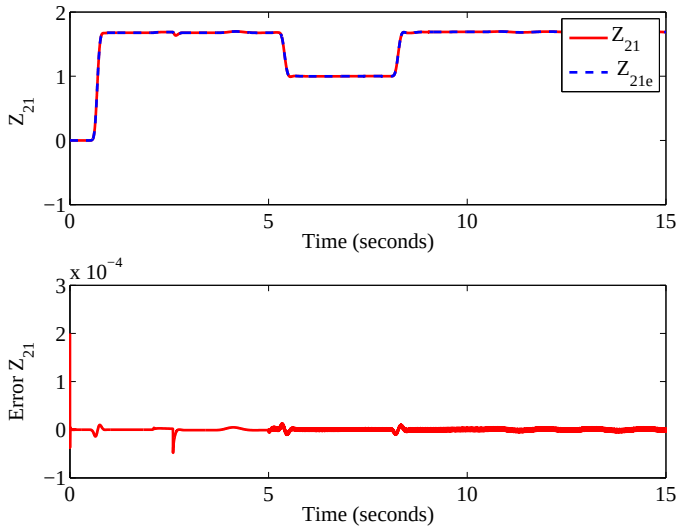


Figure 5.31: Estimation error response of flux ($z_{21}$) by using proposed observer - HGSPO with flux observer

## 5.6 Summary

This chapter has investigated an output feedback nonlinear adaptive control for an induction motor. A sliding mode flux observer is designed for the estimation of the rotor flux variables. Additionally, a state and perturbation observer is designed for the flux subsystem in order to obtain the corresponding state variables and perturbation. Moreover, assuming only the rotor speed is measured, a state and perturbation observer is designed for estimating the derivative of the speed and the corresponding perturbation. Based on the estimated states and perturbation terms, output feedback NACs are designed for the speed and flux subsystems. Stability of the overall closed-loop system, including the flux observer, state observer, perturbation observer, NAC and the induction motor, are investigated. Simulation results are verified the effectiveness of the proposed NACs.

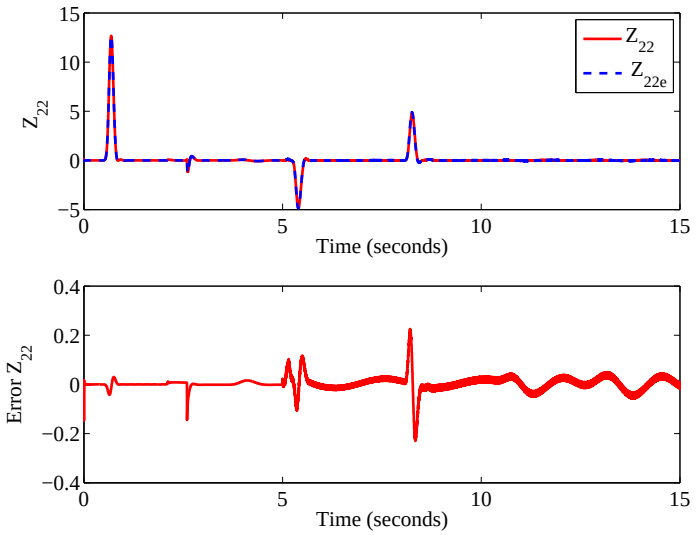


Figure 5.32: Estimation error response for the derivative of flux ($z_{22}$) by using proposed observer - HGSPO with flux observer

# Chapter 6

# Conclusion and Future Work

This chapter concludes the thesis. It has summarised the major work and achievements of the researcher, who works in the field of the control of the induction motor. A summary of the results obtained in this thesis are provided, and subsequent contributions highlighted. At the end of this chapter, possible suggestions for future investigations are also indicated.

## 6.1 Conclusion

At the beginning of the thesis, the background, control methodologies, motivations, objectives, and the contributions of this research work were presented. In order to improve the dynamic performance of the induction motor, this thesis has focused on the development of advanced control algorithms for the induction motor.

Initially, the modeling of an induction motor has been reviewed, which provides a basis for further controller design. This included a detailed nonlinear model of the induction motor derived from the original three-phase model. This was transferred from the three-phase induction motor into a two-phase stationary reference frame by Clark Transformation, and then to a two-phase $d^e - q^e$ rotating reference frame by Park Transformation. Vector control of the

induction motors has been discussed in Chapter Two as the classical method, which can achieve the decoupled control of speed and flux of induction motor.

Although vector control is the current industrial standard for the control of the induction motor, it still has some limitations which could be further improved. This is mainly because the induction motor is a nonlinear system with unmeasured state variables, time-varying parameters and also operates under unknown external disturbances. With the development of power electronics and microprocessor, the advanced control of the induction motor become feasible in terms of implementation. The vector control is in fact a partial linearisation control. A full input-output linearisation control of the induction motor has been designed in Chapter Three, where both the speed and the flux dynamic can be controlled simultaneously. Two cases were investigated to compare VC with FLC in Chapter Three. The first case involved decoupled dynamics without external disturbances. Simulation studies have verified the design and comparison against a conventional VC and IOLC are considered a success. In this case, FLC is a primer to VC. Under external disturbances, FLC can not obtain better results.

Nonlinear adaptive control, based on perturbation estimation and input-output linearisation, have been studied in Chapter Four. The perturbation terms, included parameter uncertainties, as all the system nonlinearities, are estimated by designing high-gain perturbation observers. The real time estimation of the system perturbation, which includes nonlinearities, time-varying parameters and external disturbances, is a functional estimation rather than a parameters estimation. A simple nonlinear adaptive control law has been obtained, as the accurate system model is not required for the controller design. This will result in a better controller compared to other complex nonlinear adaptive methods.

As the rotor flux cannot be measured directly, a sliding mode flux observer is designed in Chapter Five. Consequently, the definition of system perturbation

represents the combinatorial effect of the system nonlinearities, uncertainties, and external disturbances. Two state and perturbation observers are designed based on the speed measurement and the flux estimate. An output feedback nonlinear adaptive control schemes is developed. The estimation error of flux can be compensated for in the perturbation estimation together. Satisfactory regulation results have been achieved.

## 6.2 Recommendations for Future Work

Dependent on an understanding, which presented in this thesis, it is shown that the different control methodologies of induction motors are very important in its applications. As a result, a few of the related directions which include: deserve further investigation.

- an experimental test of the proposed control algorithms based on a small scale prototype. The input output linearisation control requires a detailed system model and lots of measurements, and the feasibility of the hardware to be implemented. Moreover, the nonlinear adaptive control design requires a dynamic observer to estimate the state and perturbation, in order to digitalise this dynamic controller such as the sampling rate, computation burden of observer, related PWM generation, should be verified via a real hardware based implementation;

- investigating the stability of the closed-loop system, including the nonlinear adaptive control, the state and perturbation observer, flux observer. Further, how will the parameter uncertainties, especially the variations of stator and rotor resistances, affect the accuracy of the flux estimation;

- examining the speed sensor-less control which removes the speed sensor and designs a speed observer to combine with the NAC and flux observer.

A complete output feedback control which does not require the speed sensor and rotor flux sensor will be developed; and

- the application of the proposed NAC for a wind power generation system based on the induction generator, where the full rate converter will be investigated.

# Bibliography


[1] J. J. Cathey. *Electric machines analysis and design applying MATLAB.* McGraw-Hill, Inc., New York, 2001.

[2] A. E. Fitzgerald, C. Kingsley, S. D. Umans. *Electric Machinery.* The McGraw-Hill Companies, Inc., New York, 2003.

[3] H. M. Mzungu, M. J. Manyage, M. A. Khan, P. Barendse, T. L. Mthombeni, P. Pillay. *Application of induction machine efficiency testing standards in south africa.* IEEE international conference, electric machines and drives, Miami, U.S.A., 2009, pp. 1455-1462.

[4] D. G. Taylor. *Nonlinear control of electric machines: an overview.* IEEE control system magzine, vol. 14, no. 6, 1994, pp. 41-51.

[5] B. K. Bose. *High performance control of induction motor drives.* IEEE industrial electronics society newsletter, vol. 45, no. 3, 1998, pp. 7-11.

[6] A. Smith, S. Gadoue, M. Armstrong, J. Finch. *Improved method for the scalar control of induction motor drives* IET electric power applications, vol. 7, no. 6, 2013, pp. 487-498.

[7] A. Oteafy, J. Chiasson. *A study of the Lyapunov stability of an open-loop induction machine* IEEE transactions, control systems technology, vol. 18, no. 6, 2010, pp. 1469-1476.

[8] A. Sayed-Ahmed, N. A. O. Demerdash. *Fault-tolerant operation of delta-connected scalar- and vector-controlled AC motor drives* IEEE transactions, power electronics, vol. 27, no. 6, 2012, pp. 3041-3049.

[9] A. Consoli, G. Scarcella, G. Scelba, M. Cacciato. *Energy efficient sensorless scalar control for full speed operating range IM drives* Proceedings of

the 14th European conference, power electronics and applications, 2011, pp. 1-10

[10] C. J. Francis, H. Z. De La Parra. *Stator resistance voltage-drop compensation for open-loop AC drives.* IEE proceedings, electric power applications, vol. 144, no. 1, 1997, pp. 21-26.

[11] H. Luo, Q. Y. Wang, X. Deng, S. Y. Wan. *A novel V/f scalar controlled induction motor drives with compensation based on decoupled stator current.* IEEE international conference industrial technology, 2006, pp. 1989-1994.

[12] A. M. Gajare, N. R. Bhasme. *A review on speed control techniques of single phase induction motor.* International journal of computer technology and electronics engineering, volume 2, no. 5, 2012.

[13] N. S. Nise. *Control systems engineering.* John Wiley and Sons (Asia) Pte Ltd, Asia, 2011.

[14] F. Blaschke. *A new method for the structural decoupling of A.C. induction machines.* Conference Rec. IFAC, Duesseldorf, Germany, 1971, pp. 1-15.

[15] T. Matsuo, T. A. Lipo. *A rotor parameter identification scheme for vector-controlled induction motor drives.* IEEE transactions, industry applications, vol. IA-21, no. 3, 1985, pp. 624-632.

[16] F. Mehazzem, A. Reama, Y. Hamam, H. Benalla. *Cascade sliding mode control of a field oriented induction motors with varying parameters.* International multi-conference, signals and devices, IEEE SSD, 2008, pp. 1-6.

[17] K. J. Hunt, et al. *Neural networks for control systems - survey.* Automatica, vol. 28, 1992, pp. 1083-1112.

[18] A. Savoia, C. M. Verrelli, M. Mengoni, A. Tani, D. Casadei. *Adaptive flux observer for induction machines with on-line estimation of stator and rotor resistances.* International power electronics and motion control conference, Novi Sad, 2012, pp. LS7b-1.3-1 - LS7b-1.3-6

[19] A. M. Trzynadlowski, S. Legowski. *Application of neural networks to the optimal control of three-phase voltage-controlled power inverters.* International conference, industrial electronics, control, instrumentation, and automation, vol. 1, San Diego, CA, 1992, pp. 524-529.

[20] Rashed. M., P.F.A. MacConnell, A.F. Stronach. *Nonlinear adaptive state-feedback speed control of a voltage-fed induction motor with varying parameters.* IEEE transactions, industry applications, vol. 42, no. 3, 2006.

[21] M. P. Kazmierkowski, D. Sobczuk. *Improved neural network current regulator for VC-PWM inverters* IEEE IECON conference, 1994, pp. 1237-1241.

[22] B. K. Bose. *Modern power electronics and ac drives.* Pearson-Hall, Inc, U.S.A., 2002.

[23] B. K. Bose. *Scalar decoupled control of induction motor.* IEEE transactions, industry applications, vol. IA-20, no. 1, 1984, pp. 216-225.

[24] F. Blaschke. *The principle of field orientation as applied to the new transvector closed-loop control system for rotating field machines.* Siemens-Review, vol. 34, 1972, pp. 217-220.

[25] L. J. Garces. *Parameter adaption for the speed controlled static ac drive with a squirrel cage induction motor.* IEEE transactions, industry applications, vol. IA-16, no. 2, 1980, pp. 173-178.

[26] P. P. Acarnley, J. W. Finch, D. J. Atkinson. *Field-orientation in ac drives: prospects.* IEE EMDA, London, 1987.

[27] Y. S. Ben, L. Sbita. *A Nonlinear State Feedback Control for Induction Motors.* Industrial technology, IEEE international conference, Mumbai, 2006, pp. 2067-2072.

[28] P. DeWit, R. Ortega, I. Mareels. *Indirect field-oriented control of induction motors is robustly globally stable.* Automatica, vol. 32, no. 10, 1996, pp. 1393-1402.

[29] I. Boldea, S. A. Nasar. *Vector Control of AC Drives.* Orlando, FL:CRC Press, 1992.

[30] T. Ohtani, N. Takada, K. Tanaka. *Vector control of induction motor without shaft encoder.* IEEE transactions, industry applications, vol. 28, no. 1, 1992, pp. 157-164.

[31] C. C. Gastaldini, R. P. Vieira, R. Z. Azzolin, H. A. Grundling. *An adaptive feedback linearization control for induction motor.* International conference, electrical machines, Rome, 2010, pp. 1-6.

[32] K. T. Boukas, T. G. Habetler. *High-performance induction motor speed control using exact feedback linearization with state and state derivative feedback* IEEE transactions, power electronics, vol. 19, no. 4, 2004, pp. 1022-1028.

[33] S. H. Kim, S. K. Sul. *Maximum torque control of an induction machine in the field weakening region.* IEEE transactions, industry applications, vol. 31, no. 4, 1995, pp. 784-794.

[34] S. Srilad, S. Tunyasrirut, T. Suksri. *Implementation of a scalar controlled induction motor drives.* SICE-ICASE International Joint conference, Busan, Korea, 2006, pp. 18-21.

[35] A. Behal, M. Feemster, D. Dawson. *An improved indirect field-oriented controller for the induction motor.* IEEE transactions, control systems technology, vol. 11, no. 2, 2003.

[36] L. Garces. *Parameter adaptation for the speed controlled AC drive with a squirrel-cage induction motor operated with variable frequency power supply.* IEEE transactions, vol. 16, IA, 1980, pp. 173-178.

[37] M. Bodson, J. Chiasson. *Differential-geometric methods for control of electric motors.* International journal of robust and nonlinear control, vol. 8, 1998, pp. 923-954.

[38] M. Depenbrock, A. Steimel. *High power traction drives and convertors.* Proceedings, electic drives symposium, Capri, 1990, pp. 1-9.

[39] A. H. O. Ahmed, M. O. Ajanguay, S. A. Mohamed, M. W. Dunnigan. *Combined sliding mode control with a feedback linearization for speed control of induction motor.* International conference, energ, power and control, Basrah, 2010, pp. 213-218.

[40] I. Takahashi, Y. Ohmori. *High-performance direct torque control of an induction motor*. IEEE transactions, industry applications, vol. 25, no. 2, 1989, pp. 257-264.

[41] D. Casadei, F. Profumo, G. Serra, A. Tani. *FOC and DTC: two viable schemes for induction motors torque control*. IEEE transactions, power electronics, vol. 17, no. 5, 2002.

[42] D. Casadei, G. Grandi, G. Serra. *Study and implementation of a simplified and efficient digital vector controller for induction motors*. International conference, electrical machines and drives, Oxford, U.K., 1993, pp. 196-201.

[43] D. Casadei, G. Grandi, G. Serra, A. Tani. *Effects of flux and torque hysteresis band amplitude in direct torque control of induction machines*. International conference, industrial electronics, control and instrumentation, Bologna, Italy, 1994, pp. 299-304.

[44] Y. Song, J. Ma, H. Zhang, N. He. *Digital implementation of neural network inverse control for induction motor based on DSP*. International conference, future computer and communication, vol. 1, 2010, pp. V1-174-V1-178.

[45] Y. Wang, Z. Mei, R. Wang. *The stability analysis of the position control system with disturbance observer for induction machine drive*. IEEE international symposium, industrial electronics, 2008, pp. 478-484.

[46] Y. Ben Salem, L. Sbita. *A Nonlinear State Feedback Control for Induction Motors*. IEEE international conference, industrial technology, 2006, pp. 2067-2072.

[47] N. Kabache, S. Moulahoum, K. Sebaa, H. Houassine. *Neural network based input output feedback control of induction motor*. International conference, optimization of electrical and electronic equipment, Brasov, 2012, pp. 578-583.

[48] P. Tiitinen, P. Pohkalainen, J. Lalu. *The next generation motor control method: Direct torque control (DTC)*. Proceedings of the 1996 international conference, power electronics, drives and energy systems for industrial growth, vol. 1, 1996, pp. 37-43.

[49] C. Lascu, I. Boldea, F. Blaabjerg. *A modified direct torque control (DTC) for induction motor sensorless drive.* Industry applications conference, vol. 1, 1998, pp. 415-422.

[50] D. Casadei, G. Serra, A. Tani, L. Zarri. *Theoretical and experimental analysis of an induction motor drive based on stator flux vector control.* Electromotion journal, vol. 6, no. 12, 1999, pp. 43-48.

[51] R. Marino, S. Peresada, P. Valigi. *Adaptive input-output linearizing control of induction motors.* IEEE transactions, automatic control, vol. 38, no. 2, 1993, pp. 208-221.

[52] D. Casadei, G. Serra, A. Tani. *Sensitivity investigation of a speed sensorless induction motor drive based on stator flux vector control.* Conference Rec. PESC97, St. Louis, MI, 1997, pp. 1055-1060.

[53] A. Isidori. *Nonlinear control systems.* Springer-Verlag, Berlin, Germany, 1995.

[54] A. Isidori. *Nonlinear control systems II.* Springer-Verlag, London, 1999.

[55] J. J. E. Slotine, W. P. Li. *Applied nonlinear control.* Prentice-Hall, Inc., London, 1991.

[56] H. K. Khalil. *Nonlinear systems.* Prentice-Hall, Inc., London, 1996.

[57] J. Chiasson. *Dynamic feedback linearization of the induction motor.* IEEE transactions, automatic control, vol. 38, no. 10, 1993, pp. 1588-1594.

[58] F. Chen, M. W. Dunnigan. *Sliding-mode torque and flux control of an induction machine.* IEE procedings, electric power applications, vol. 150, no. 2, 2003, pp. 227-236.

[59] Y. Zheng, H. A. Abdel Fattah, K. A. Loparo. *Non-linear adaptive sliding mode observer-controller scheme for induction motors.* International journal, adaptive control and signal processing, vol. 14, no. 2-3, 2000, pp. 245-273.

[60] R. B. Gardner, W. F. Shadwick. *The GS algorithm for exact linearization to Brunowsky normal form.* IEEE transactions, automation control, vol. 37, no. 2, 1992, pp. 224-230.

[61] J. J. E. Slotine, W. P. Li. *Applied Nonlinear Control.* Prentice-Hall, Eaglewood Cliffs, New Jersey, U.S.A. (in Chinese), 1991.

[62] I. Takahashi, T. Noguchi. *A new quick response and high efficiency control strategy of an induction motor.* IEEE transactions, industry applications, vol. IA-22, no. 5, 1986, pp. 820-827.

[63] G. Kim, I. J. Ha, M. S. Ko. *Control of indcution motors for both high dynamic performance and high power efficiency.* IEEE transactions, industrial electronics, vol. 39, no. 4, 1992, pp. 323-333.

[64] H. J. Marquez. *Nonlinear control systems analysis and design.* John Wiley & Sons, Inc., Hoboken, New Jersey, U.S.A., 2003.

[65] M. Krstić, I. Kanellakopoulos, P. V. Kokotović. *Nonlinear and adaptive control design.* John Wiley & Sons, Inc, New York, 1995.

[66] R. Ortega, C. Canudas, S. Seleme. *Nonlinear control of induction motor: Torque tracking with unknown load disturbance.* IEEE transactions, automatic control, vol. 38, no. 11, 1993, pp. 1675-1679.

[67] R. Ortega, P. J. Nicklasson, G. Espinosa-Perez. *On speed control of induction motors.* American control conference, vol. 5, 1996, pp. 3521-3525.

[68] P. J. Nicklasson, R. Ortega, G. Espinosa-Perez. *Passivity-based control of class of blondel-park transformable electric machines.* IEEE transactions, automatic control, vol. 42, no. 5, 1997, pp. 629-647.

[69] I. Kanellakopoulos, P. V. Kokotović, A. S. Morse. *Systematic design of adaptive controllers for feedback linearizable systems.* IEEE transactions, autonmatic control, vol. 36, no. 4, 1991, pp. 1241-1253.

[70] M. Rashed, F. Stronach, P. Vas. *A new stable MRAS-based speed and stator resistance estimators for sensorless vector control induction motor drive at low speeds.* Industry applications conference, vol. 2, 2003, pp. 1181-1188.

[71] L. Jiang, Q. H. Wu, G. Liu, D. Rees. *Robust adaptive control of induction motor based on perturbation estimation.* IEEE internation electric machines and drives conference, vol. 1, 2007, pp. 101-106.

[72] M. Krstić, I. Kanellakopoulos, P. V. Kokotović. *Adaptive nonlinear control without overparametrization.* Systems & Control Letters, vol. 19, 1995, pp. 177-185.

[73] S. S. Sastry, A. Isidori. *Adaptive control of linearizable systems.* IEEE transactions, autonmatic control, vol. 34, no. 11, 1989, pp. 1123-1131.

[74] J. B. Pomet, L. Praly. *Adaptive nonlinear regulation: estimation from the Lyapunov equation.* IEEE transactions, autonmatic control, vol. 37, no. 6, 1992, 729-740.

[75] R. Marino, P. Tomei. *Global adaptive output-feedback control of nonlinear systems, part i: linear parametrization.* IEEE transactions, automatic control, vol. 38, 1993, pp. 17-32.

[76] R. Marino, P. Tomei. *Global adaptive output-feedback control of nonlinear systems, part ii: nonlinear parametrization.* IEEE transactions, automatic control, vol. 38, 1993, pp. 32-48.

[77] I. Kanellakopoulos, P. V. Kokotović, A. S. Morse. *Adaptive nonlinear control with incomplete state information.* International journal, adaptive control and signal processing, vol. 6, 1992, pp. 367-394.

[78] A. R. Teel. *Adaptive tracking with robust stability.* Proceedings of the 32th IEEE conference , decision and control, San Antonio, TX, 1993, pp. 570-575.

[79] H. K. Khalil. *Adaptive output-feedback control of nonlinear systems represented by input-output models.* IEEE transactions, autonmatic control, vol. 41, no. 2, 1996, pp. 177-188.

[80] J. Hu, D. Dawson. *Adaptive control of induction motor systems despite rotor resistance uncertainty.* Automatica, vol. 32, no. 8, 1996, pp. 1127-1143.

[81] D. Dawson, J. Hu, T. Burg. *Nonlinear control of electric machinery.* Marcel Dekker, New York, 1998.

[82] R. Marino, S. Peresada, P. Tomei. *Global adaptive output feedback control of induction motors with uncertain rotor resistance.* IEEE transactions, Autom. Control, vol. 44, no. 5, 1999, pp. 967-983.

[83] R. Marino, S. Peresada, P. Tomei. *Adaptive output feedback control of current-fed induction motors with uncertain rotor resistance and load torque.* Automatica, vol. 34, no. 5, 1998, pp. 617-624.

[84] R. Marino, P. Tomei, C. Verrelli. *A nonlinear tracking control for sensorless induction motors.* Automatica, vol. 41, no. 6, 2005, pp. 1071-1077.

[85] M. Feemster, P. Aquino, D. Dawson, A. Behal. *Sensorless rotor velocity tracking control for induction motors.* IEEE transactions, control systems technology, vol. 9, no. 4, 2001, pp. 645-653.

[86] D. Karagiannis, A. Astolfi, R. Ortega, M. Hilairet. *A nonlinear tracking controller for voltage-fed induction motors with uncertain load torque.* IEEE transactions, control systems technology, vol. 17, no. 3, 2009.

[87] R. Ortega, A. van der Schaft, B. Maschke, G. Escobar. *Interconnection and damping assignment passivity-based control of port-controlled hamiltonian systems.* Automatica, vol. 38, no. 4, 2002, pp. 585-596.

[88] H. Kubota, K. Matsuse, T. Nakano. *DSP-based speed adaptive flux observer of induction motor.* IEEE transactions, industry applications, vol. 29, no. 2, 1993, pp. 344-348.

[89] R. Kim, S. K. Sul, M. H. Park. *Speed sensorless vector control of induction motor using extended Kalman filter.* IEEE transactions, industry applications, vol. 30, no. 5, 1994, pp. 1225-1233.

[90] H. Kubota, K. Matsuse. *Speed sensorless field oriented control of induction motor with rotor resistance adaptation.* IEEE transactions, industry applications, vol. 30, no. 5, 1994, pp. 1219-1224.

[91] C. Ilas, R. Magureanu. *An improved speed sensorless scheme for vector-controlled induction motor drives.* Electromotion, no. 3, 1996, pp. 67-71.

[92] S. Sangwongwanich, S. Doki, T. Yonemoto, T. Furu-hashi, S. Okuma *Design of sliding observers for robust estimation of rotor flux of induction motors.* Proceedings International power electronics conference, Tokyo, Japan, 1990, pp. 1235-1242.

[93] P. Vas. *Sensorless vector and direct torque control.* Oxford University Press, Oxford, U.K., 1998.

[94] M. Tsuji, E. Yamada, F. Parasiliti, M. Tursini. *A digital parameter identification for a vector controlled induction motor.* Proc. 7th european conference power electronics and applications (EPE97), vol. 4, Trondheim, Norway, 1997, pp. 603-608.

[95] F. Parasiliti, R. Petrella, M. Tursini. *Sensorless speed control of a PM synchronous motor by sliding mode observer.* Proceedings of IEEE international symposium, industrial electronics (ISIE97), vol. 3, Guimaraes, Portugal, 1997, pp. 1106-1111.

[96] M. Tursini, R. Petrella, F. Parasiliti. *Adaptive sliding-mode observer for speed-sensorless control of induction motors.* IEEE transactions, industry applications, vol. 36, no. 5, 2000, pp. 1380-1387.

[97] K. Jezernik, A. Hren, D. Dreversek. *Robust sliding-mode continuous control of an IM drive.* Conference record of IEEE/IAS annual meeting, 1995, pp. 335-342.

[98] V. I. Utkin. *Sliding mode control design principles and application to electric drives.* IEEE transactions, industrial electronics, vol. 40, no. 1, 1993, pp. 23-36.

[99] A. Benchaib, A. Rachid, E. Audrezet, M. Tadjine. *Real time sliding mode observer and control of an induction motor.* IEEE transactions, industrial electronics, vol. 46, no. 1, 1999, pp. 128-138.

[100] C. C. Chan, H. Q. Wang. *New scheme of sliding-mode control for high performance induction motor drives.* IEE proceedings electrical power applications, vol. 143, no. 3, 1996, pp. 177-185.

[101] L. G. Shiau, J. L. Lin. *Stability of sliding-mode current control for high performance induction motor position drives.* IEE Proceedings, electric power applications, vol. 148, no. 1, 2001.

[102] F. Barrero, A. Torralba, E. Galvn, L. G. Franquelo. *A switching fuzzy controller for induction motors with self-tuning capability.* IECON-95, Orlando, FL, 1995.

[103] F. Barrero, E. Galvn, A. Torralba, L. G. Franquelo. *Fuzzy selftuning system for induction motor controllers.* Europe power electronics conference, Seville, Spain, 1995.

[104] A. Benchaib, C. Edwards. *Nonlinear sliding mode control of an induction motor.* International journal, adaptive control and signal processing, vol. 14, no. 1, 2000, pp. 201-221.

[105] A. Benchaib, A. Rachid, E. Audrezet. *Sliding mode, input-output linearization and field orientation for real time control of induction motor.* IEEE transactions, power electronics, vol. 14, no. 1, 1999, pp. 3-13.

[106] F. Boudjema, A. Benchaib, A. Rachid. *Backstepping approach for nonlinear sliding mode control of an induction motor.* International journal, electro motion, vol. 5, no. 1, 1998, pp. 29-34.

[107] A. Deluca, G. Ulivi. *Design of exact nonlinear controller for induction motor.* IEEE transactions, automatic control, vol. 34, no. 12, 1989, pp. 1304-1307.

[108] L. Jiang. *Nonlinear adaptive control and applications in power systems.* The University of Liverpool PhD thesis, 2001.

[109] T. Raumer, J. M. Dion, L. Dugard, J. L. Thomas. *Applied nonlinear control of an induction motor using digital signal processing.* IEEE transactions, control systems technology, vol. 2, no. 4, 1994, pp. 327-335.

[110] M. Bodson, J. Chiasson, R. Novotnak. *High-performance induction motor control via input-output linearisation.* IEEE control system magazine, vol. 14, no. 4, 1994, pp. 25-33.

[111] K. Youcef-Toumi. *A time delay controller for systems with unknown dynamics.* Journal of dynamic system, measurement, and control, transactions of ASME, vol. 112, no. 1, 1990, pp. 133–142.

[112] K. Toumi, S. T. Wu, *Input/output linearization using time delay control.* Journal of dynamic system, measurement, and control, transactions of ASME, vol. 114, no. 1, 1992, pp. 10-19.

[113] V. J. Utkin. *Sliding mode control design principles and applications to electric drives.* IEEE transactions, Ind. Electr., vol.40, no.1, 1993, pp. 23-36.

[114] T. Tahar, H. Samir, M. Abdelkader, C. Tarek. *Robust speed control with rotor resistance estimation.* Canadian journal, electrical and computer engineering, vol. 36, no. 2, 2013, pp. 43-51

[115] B. Metidji, N. Taib, L. Baghli, T. Rekioua, S. Bacha. *Low-cost direct torque control algorithm for induction motor without AC phase current sensors.* IEEE transactions, power electronics, vol. 27, no. 9, 2012, pp. 4132-4139.

[116] J. Alvarez-Gallegos, R. J. Herrera-Alfonsin. *Sliding mode control of induction motors using singular perturbation techniques.* IEEE conference, control applications, vol. 2, Dayton, OH, 1992, pp. 922-927.

[117] L. Jiang, Q. H. Wu. *Nonlinear adaptive control via sliding mode state and perturbation observer.* IEE proceedings: control theory and applications, vol. 149, no. 4, 2002, pp. 269-277.

[118] L. Jiang, Q. H. Wu, J. Y. Wen. *Decentralized nonlinear adaptive control for multi-machine power systems via high gain perturbation observer.* IEEE transactions, circuits and systems C I: fundamental theory and applications, vol. 51, no. 10, 2004, pp. 2052-2059.

[119] Q. H. Wu, L. Jiang, J. Y. Wen. *Decentralised adaptive control of nonlinear systems using high gain observer.* International journal of control, vol. 77, no. 8, 2004, pp. 703-712.

[120] J. Q. Han. *Disturbance auto-rejection controller and its application.* Control and decision, vol. 12, no. 2, 1997, pp. 12-17. (in Chinese)

[121] R. Pupadubsin, N. Chayopitak, D. G. Taylor, N. Nulek, S. Kachapornkul, P. Jitkreeyarn, P. Somsiri, K. Tungpimolrut. *Adaptive integral sliding-mode position control of a coupled-phase linear variable reluctance motor for high-precision applications.* IEEE transactions, industry applications, vol. 48, no. 4, 2012, pp. 1353-1363.

[122] W. Sung, J. Shin, Y. Jeong. *Energy-efficient and robust control for high-performance induction motor drive with an application in electric vehicles.* IEEE transactions, vehicular technology, vol. 61, no. 8, 2012, pp. 3394-3405.

[123] Q. H. Wu, L. Jiang. *Nonlinear control theory and its applications in power systems: a survey.* Automation of electric power systems, vol. 25, no. 3, 2001, pp. 1-10.

[124] O. Chee-Mun *Dynamic simulation of electric machinery using Matlab/SIMULINK.* Prentice-Hall, Inc., U.S.A. 1998.

[125] S. Kwon, W. Chung. *Perturbation compensator based robust tracking control and state estimation of mechnical systems.* Lecture notes: control and information sciences, 307, Editor M. homa, M. Morari, London: Springer-Verlag, 2005.

[126] G. Marian, D. Cristi , N. Viorel , B. Razvan , P. Ion. *Optimal control implementation of the three-phase induction machine based on adaptive drive system.* International symposium, advanced topics in electrical engineering (ATEE), Bucharest, Romania, 2013, pp. 1-4.

[127] G. Feng, Y. F. Liu, L. P. Huang. *A new robust algorithm to improve the dynamic performance on the speed control of induction motor drive.* IEEE transactions, power electronics, vol. 19, no. 6, 2004, pp. 1614-1627.

[128] H. K. Khalil. *Nonlinear Systems.* 3rd Edition, Pearson Eduation Ltd., London, 2000.

[129] O. Barambones, P. Alkorta, J. M. Gonzalez de Durana, E. Kremers. *A robust position control for induction motors using a load torque observer.* Mediterranean conference, control and automation, Barcelona, 2012, pp. 278-283.

[130] Chin-I Huang, Kou-Cheng Hsu , Hsin-Han Chiang , Kuang-Yang Kou , Tsu-Tian Lee. *Adaptive fuzzy sliding mode control of linear induction motors with unknown end effect consideration.* International conference, advanced mechatronic systems, Tokyo, 2012, pp. 626-631.

[131] Y. Feng, M. H. Zhou, H. Y. Shi, X. H. Yu. *Flux estimation of induction motors using high-order terminal sliding-mode observer.* World congress, intelligent control and automation, Beijing, China, 2012, pp. 1860-1863.

[132] D. P. Thinh, B. T. Luan, K. H. Kyeong, K. S. Bong. *Sliding-mode observer design for sensorless vector control of AC induction motor.* 9th Asian control conference (ASCC), Istanbul, Turkey, 2013, pp. 1-5.

[133] H. Abu-Rub, H. Shehadeh, J. Guzinski. *Robust flux observer system with sliding mode and fuzzy logic control of induction motors.* IECON, annual conference of IEEE, industrial electronics, Oriando, FL, 2008, pp. 1349-1354.

[134] Z. Sutnar, Z. Peroutka, M. Rodič. *Sliding mode flux observer and rotor speed estimation for DTC-controlled induction motor drive.* 13th European conference, power electronics and applications, Barcelona, 2009, pp. 1-10.

[135] H. Y. Shi, Y. Feng. *A hybrid sliding mode flux observer for induction motor drive.* Chinese control conference (CCC), Yantai, China, 2011, pp. 762-767.

[136] D. Sobczuk, M. Malinowski. *Feedback linearization control of inverter fed induction motor - with sliding mode speed and flux observers.* IECON - 32nd annual conference, IEEE industrial electronics, Paris, 2006, pp. 1299-1304.